WATERBOUWKUNDIG LABORATORIUM ANTWERPEN

Analysis of tidal current velocities at the harbour of Zeebrugge using a physical scale model

Bachelor Thesis

De Waard, Sander

22-7-2013

UNIVERSITEIT TWENTE.

A research project to investigate the current velocities in and around the harbour of Zeebrugge by applying different scenarios on a physical scale model and analysing the results.

Preface

Before you lies my bachelor thesis report, within the details of my research can be found. I started my research at 21-5-2013 at Waterbouwkundig Laboratorium (WL) in Antwerp. My internship at WL in Antwerp and this report will serve as final research project to finish my bachelor Civil Engineering at the University of Twente. I would like to thank my supervisor at WL dr. ir. Wael Hassan, who provided me with help regarding the technical part of my research. Furthermore, I would like to thank Glen Heyvaert, the model operator of Zeebrugge who helped me collecting data and ir. Marc Willems, the project leader of Zeebrugge who always came with good insights of possible solutions. Finally I would like to thank dr. ir. Pieter Roos for his help and guidance on my bachelor thesis.

Contents

1. Management Summary

At high tide strong current velocities occur at the entrance of the harbour of Zeebrugge. 8-10 hours a day the water level in the harbour is high enough to allow large ships (draught ±16m) to enter Zeebrugge. However, the strong current velocities occurring at high tide in front of the harbour reduce the window of opportunity for these ships to 4-6 hours a day. A physical scale model was constructed to study the effects of different design scenarios in front of the harbour. These scenarios should reduce the current velocity at the harbour entrance. After the calibration of the Zeebrugge model the situation at sea was optimized, however within the harbour itself the tidal currents did not show the desired eddy pattern and velocities. This study is done to optimize the tidal current behaviour inside the harbour of Zeebrugge without endangering the optimization of the tidal current in sea. This is done to make a reliable base model in which different design scenarios can be tested for further research.

To be able to ensure the legitimacy of the model, the model advantages/disadvantages, the hydraulic processes and the measurement equipment have been studied. The physical model of Zeebrugge is a geometrically distorted model. The absence of waves in the model takes away several negative effects of a distorted model. However it might have effect regarding the eddy duration in the harbour, this eddy duration is longer in the physical model compared to the natural data. A possible cause is the reduced effect of bottom roughness which a distorted model gives. The measuring equipment used in the model is accurate enough to ensure reliable data. The total uncertainty in the model is only 4.2%. The uncertainty of the natural data is unknown because of the many negative effects of weather, waves and shipping traffic during the data collection.

To achieve the goal of a reliable base model, six scenarios have been tested. These scenarios all included a change in bathymetry level or roughness. From the six scenarios only two showed an eddy pattern which matched the eddy pattern of the natural data. These two have been further examined and scenario 5 (an increase in roughness along the west dam and an increase in volume of the east head) appeared to be the scenario that came closest to the natural data according to several performance criteria. The match could be further improved by increasing the roughness on the west dam of the harbour entrance. However this is not advised because it might have a negative effect on the current velocity conditions in front of the harbour.

The reason the current is not behaving the correct way in the harbour is because the speed of the tidal current in front of the harbour builds up too fast. The applied roughness reduces this negative effect and is only effective if the entrance location of the harbour is not changed. If a design scenario is tested which includes a repositioning of the harbour entrance, it should be kept in mind that the alternations of scenario 5 might not suffice anymore for a reliable pattern inside the harbour because the applied roughness is specific for this point in the model.

2. Introduction

2.1 Context

Zeebrugge is the seaport of Brugge and is situated to the north of Brugge close to the Dutch border (figure 1). Zeebrugge is the second largest port in Belgium after Antwerp and has a direct and open connection with the North Sea. The port is not only used for the transportation of cargo but also as fishing and recreational port. The port of Zeebrugge is currently Europe's fastest growing port. Annually the port of Zeebrugge transports 700.000 passengers and 50 tons of cargo. Zeebrugge is Europe's most important port regarding roll-on-roll-off traffic (rorotraffic) and the world's most important port for the import and export of new cars (Port of Zeebrugge, 2013).

2.1.1 Structure of the harbour

Figure 1: Location of the port of Zeebrugge (Google Maps, 2013)

The outer port

Figure 2: Outer harbour of Zeebrugge (Port of Zeebrugge, 2013)

The outer port of Zeebrugge (figure 2) lies completely in sea and is protected by two 4km long rubble mound breakwaters around it. These breakwaters stretch more than 3km out into sea (Troch, De Rouck, & Van Damme, 1998). Because of its relatively large depth of ±20 meters and open connection to the North Sea, this part of the harbour is ideal for rorotraffic and heavy container ships. This is also the place where ships with liquid gas unload their cargo. The ships that dock in the outer port do not need to pass any locks (Port of Zeebrugge, 2013).

The inner port

Figure 3: Inner port of Zeebrugge (Port of Zeebrugge, 2013)

Via the Pierre Vandamma lock (built in 1985) and the Visart lock (built in 1905) vessels can sail towards the inner port (figure 3). The inner port houses two large docks, the Northern Inlet dock and the Southern Canal dock. Around these docks several logistic centres are located for the handling, storing and distribution of new cars, bulk cargo or food products (Port of Zeebrugge, 2013).

The seaport of Brugge

Figure 4: The seaport of Brugge (Port of Zeebrugge, 2013)

Via the Baudouin canal ships sail to the seaport of Brugge (figure 4). In this port zone terminal activity is mainly focused on bulk and conventional cargoes (Port of Zeebrugge, 2013). In this study the seaport and the inner port of Zeebrugge will be left outside of the research scope. Only the outer port of Zeebrugge will be taken into account because this is the place where the design problems occur. These problems will be explained in section 2.2.

2.1.2 Characteristics of the study area.

In figure 5 the study area is shown, it is roughly 15 km alongshore and 6 km in cross-shore direction. The maximum depth in the study area is found in the maritime access way and in the harbour itself and is about 20 meters. The port of Zeebrugge is situated in the southern bight of the North Sea. This area of the North Sea is known for its high concentrations of silt (Fettweis & Van den Eynde, 2003). In figure 6 the silt concentration of the southern part of the North Sea is shown. It is clear to see that around the port of Zeebrugge a large concentration of silt is situated. In front of the port the silt concentration is as high as 75% of the soil. In reality this means that the silt layer in and around the port of Zeebrugge can be as high as 3 meters, which reduces the effective water depth to 17 meters.

Figure 5: Borders of the study area and the physical model (Willems et al, 2011)

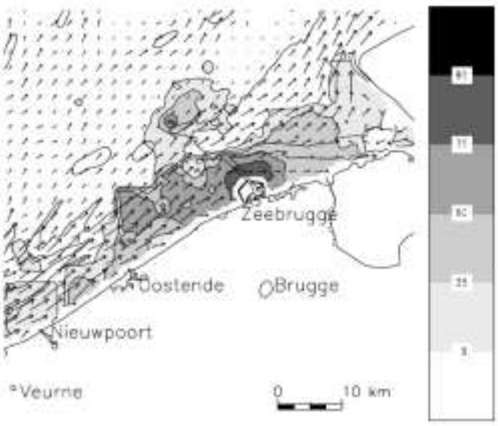

Figure 6: Silt concentration around Zeebrugge (Fettweis & Van den Eynde, 2003)

The average spring tidal range that has to be taken into consideration in the port of Zeebrugge is about 4.3 meters (Vlaamse Hydrografie, 2011). The average wave height around the port is about 130 cm (Vlaamse Overheid, 2013). In extreme conditions the wave height can reach values up to 454 cm, this is a height that occurs once every 10 years (Geysen, 2010).

2.2 Hosting organization

My internship started at Waterbouwkundig Laboratorium (WL) in Antwerpen (Belgium). WL is a department of the Technical Supportive Services of the Ministry of Mobility and Public Works of the Flemish Government (figure 7). WL counts more than 140 employees and has three main goals (Waterbouwkundig Laboratorium, 2013):


Figure 7: Waterbouwkundig Labaratorium (Waterbouwkundig Laboratorium, 2013)

1. Optimization of hydraulic structures as harbours, dikes, locks etc.
2. Guaranteeing a safe and fast manoeuvrability of ships in the Flemish harbours and inland waterways.
3. Efficient management of water levels in Flemish waterways and formulating goal orientated arrangements to avoid water shortage and floods.

2.2.1 Research Facilities

To be able to reach the goals stated above (section 2.2) WL has a wide variety of research tools. They do not only have access to advanced software programs to simulate different hydraulic effects (like DELFT3D, SWAN, LITPACK, etc.); But also to several physical installations and models (like a towing tank, a multifunction test basin, a current flume, etc.), multiple ship simulators (SIM 360+, SIM 225 and LARA) and a sediment laboratory (Waterbouwkundig Laboratorium, 2013).

The most interesting tool for my research is the physical model of Zeebrugge, which is the largest model at WL. This model is situated in one of the research halls of WL (figure 8) next to the wave flume, the wave basin and the silt test tank. This model is about 70 meters long and about 40 meters wide (Willems et al, 2011). The construction of the model took about 3 years and calibration of the model took about 1 year.

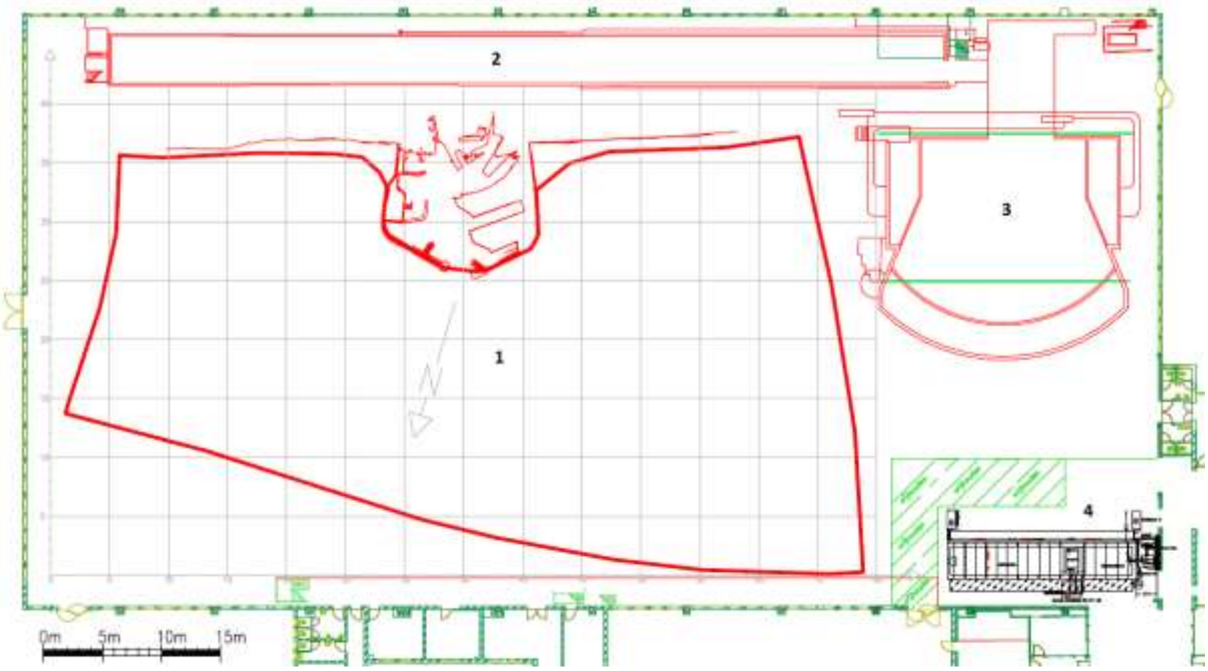

Figure 8: Layout of laboratory hall 3 at WL. With the Zeebrugge model (1) the wave flume (2), the wave basin (3) and the silt test tank (4) (Willems et al, 2011)

2.3 Problem Definition

In previous years the Flemish government invested a lot in dredging of the maritime entrance of Zeebrugge. This resulted in the current situation where ships with a draught of 15.5 - 16 meters should be able to enter the harbour within a window of 8-10 hours a day during high tide. However during high tide a strong alongshore current in front of the harbour occurs. This current has a velocity of 2.1 m/s during high tide and 1.5 m/s during low tide. These values are the depth-averaged velocities of the upper 10 meters of water (IVA Maritieme Dienstverlening en Kust, 2011). Because of this high velocity current at the entrance of the harbour, ships can only enter the harbour 4-6 hours a day for safety reasons.

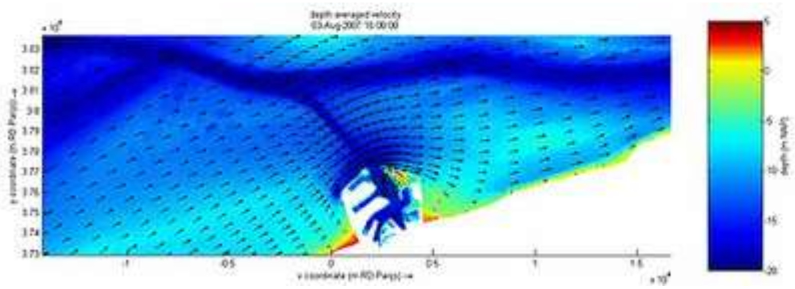

Figure 9: Streamlines and depths around the port of Zeebrugge during high tide (Waterbouwkundig Laboratorium, 2013)

Since the expansion of the port in 1985 a layer of silt began to form in the maritime access way of the harbour and within the outer part of the harbour (Fettweis & Van den Eynde, 2003). This layer of silt makes it difficult to guarantee the depth of the whole waterway and the whole outer harbour during any given time. The Under Keel Clearance (UKC) of a ship needs to be at least 10% of the ships draught in harbours and harbours. This can increase to 20-30% depending on different aspects of the ship like speed, squat, angle of list, etc. (Thompson Clarke, 2007). In the harbour of Zeebrugge this is a problem because a ship with a draught of 16 meters needs a minimum UKC of 1.6 meters and if the depth in the harbour is only 17 meters because of the silt intrusion there will not be enough depth to guarantee safe conduct (figure 9). Next to regular dredging, the Flemish government is trying to find practical and cost efficient ways to maintain a sufficient water depth.

2.4 Study purpose and research goals

The department of Maritime Access Ways of the Flemish government, responsible for the accessibility of the port of Zeebrugge, asked WL in Antwerp to research the causes of the problems stated above and to find a solution. WL stated the following research goals (Waterbouwkundig Laboratorium, 2013):

- Find a way to guarantee the accessibility of the port of Zeebrugge through infrastructural improvements at the entrance to the harbour
- Find a way to reduce the silt intrusion of the harbour to reduce the cost of maintenance dredging.

The research at WL will only consider the current velocities in and around the harbour and will exclude the silt intrusion. The problem of the silt intrusion is examined by another company. In my research I will focus specifically on the physical model of Zeebrugge. The calibration phase of the model is finished, but only regarding the current velocities in sea and in front of the harbour. Inside the harbour the physical scale model is not showing the desired effects. The current that comes into the harbour has a different direction than in reality. This results in an eddy pattern which circulates clockwise within the model of the harbour, while in reality the current circulates counter-clockwise. Regarding the problem occurring within the harbour I will state my main research goals as following:

1. Analyse the different hydraulic processes which occur in the harbour by using data from the model and from the field measurements
2. Find a way to implement the different hydraulic processes that occur in nature into the physical scale model
3. Find a reliable base model in which different design scenarios to reduce tidal current velocity can be compared.

2.5 Research Questions

Specific research questions will be presented in this section, these research questions will aid in answering the research goals as numbered above (Section 2.4).

1. What are the possibilities and limitations of a physical scale model?
2. What are the different measurement instrument used to calculate the current velocity and direction and what are the uncertainties in them?
3. What are the tidal influences on the hydraulic system at the harbour entrance?
4. What is the cause of the differences between the physical model and the reality and is it possible to reduce these differences?

2.6 Research Methodology

In this section the different tools and methods are described which will be used during the research and the steps to reach my research goals are shown.

2.6.1 Research Tools

In this subsection the two main tools used during my research will be discussed.

The physical scale model:

The main research tool which has been used during my research is the physical scale model of the harbour of Zeebrugge (figure 10). In figure 11 a detailed picture of the port itself is shown.

Figure 10: Physical scale model of Zeebrugge (Willems et al, 2011)

Figure 11: Physical scale model of Zeebrugge, detailed port (Willems et al, 2011)

With this model, data regarding the current velocities in and around the harbour were collected. The different scenarios were implemented in the model and their effects are studied. A detailed description of the model and its characteristics are introduced chapter 4.

To be able to know exactly what the flow patterns and velocities are within the physical scale model, measurement techniques have been used. The two measurement techniques used are 'Electromagnetic Speed monitors' (EMS) instruments and video recordings.

EMS instrument data are collected by an electromagnetic device placed underwater inside the physical scale model. It registers the two components of the current velocity (U and V) of the water at a fixed point. With these components the direction and the velocity of the current can be calculated (see chapter 5).

The advantage of this method is its accuracy. It is an accurate way to measure the current velocity and direction of the current during the whole tidal simulation within the model. The disadvantage is that it is only possible to measure at one fixed point within the model, what happens around this point cannot be registered by a single EMS instrument.

With the video recordings it is possible to get a global view of the current velocity in a large area of the physical model. When video footage of a great area of the model is needed the water will be filled with little floating balls. From a top of the model a camera can register the balls and trace their path within the water. This way the current velocities can be made visible and a large area of the model can be examined. The advantage of this method is its large examination area. The disadvantage is that it is less accurate then the EMS method because it only shows the flows on the surface and not underneath.

Literature study

To find information on the subject of physical modelling in harbours a literature study is done. This literature study covers several subjects like: Limitations and possibilities of physical modelling, hydraulic processes and harbours with similar problems.

How the physical model and the literature study will be used to answer the research questions will be presented in the next subsection 2.6.2.

2.6.2 Research Design

In this subsection the different research questions and steps are shown. Also the methods which were used to answer them are discussed.

1. What are the possibilities and limitations of a physical scale model?

To answer this question a literature study was done on the subject of physical scale models. This way answer could be found to several questions: What is the advantage of physical scale models? What are the limitations of physical scale models? Why would we use physical scale models instead of numerical models? Next to the literature study, the model of Zeebrugge also needs to be examined. What are the characteristics of the model? How are data processed and interpreted? And what are the parameters that can be changed to improve the outcome of the model? These are important questions that will need to be answered by examining the model.

2. What are the different measuring instruments used to measure the current velocity and direction and what are the uncertainties in them?

To analyse the physical model data and compare them with the field data, the uncertainty of the measuring instruments of the model need to be examined. These instruments include the EMS equipment and video footage. To make a good analysis the right data needs to be extracted from the model. If the uncertainties of these methods are known than the influences of these uncertainties in the data collected by the model is known. These uncertainties need to be taken into account when conclusions are drawn from the data.

3. What are the tidal influences on the hydraulic system in the harbour entrance?

To answer this question a literature study is needed on the subject of hydraulic engineering. Different books like “Introduction to Fluid Mechanics”, ”Coastal Engineering” and “Hydrology in Practice” can be of good use (Fox et al, 2010) (Reeve et al, 2004) (Shaw et al, 2011). With this literature study the hydraulic processes that occur in front of the harbour are examined. The goal is to find out which hydraulic effects are responsible for the current velocities in front of the harbour and the inflow direction into the harbour. When these effects are known it is possible to identify the influence of different parameters within the model that will affect the speed and flow direction of the current.

4. What is the cause of the differences between the model and the reality and how can they be minimized?

When the knowledge of the measuring equipment is acquired in combination with the knowledge of the hydraulic effects occurring at the harbour entrance, the reason why certain model outcomes might vary with the reality can be explained. With the knowledge of the hydraulic effects in the area different scenarios can be designed to improve the model and make a better match with the reality. Then the physical model will be used to implement these alternations and test the results. By analysing the data from the model a comparison between different scenarios and the reality can be made. Then the results from the data analysis and their influences in the current at the harbour will be explained.

2.7 Report Structure

In this bachelor thesis the following subjects will be presented: First an insight in the principles of physical modelling will be presented (chapter 3). Second a description of the physical model of Zeebrugge and a clarification of its operating systems will be given (chapter 4). Third an insight of the different measurement equipment used in the model and in nature will be given and a discussion about the uncertainties in them will follow (chapter 5). Fourth a description of the natural data collected from Zeebrugge (chapter 6) and the physical model data collected from the model (chapter 7) will be given. And finally a discussion (chapter 8) and a chapter with conclusions and recommendations will be presented (chapter 9).

3. Principles of physical scale modelling

This chapter provides an insight in the principles of physical scale modelling. The purpose of this chapter is to give the reader a basic understanding of the physical model theory. The advantages and disadvantages of physical modelling will also be discussed in this chapter.

3.1 Principles of similarity

The basis of all physical models is that they should behave similar to the prototype (real world situation) they represent. Thus, a properly validated physical model can be used to predict the way the prototype will behave in certain conditions. However it is impossible to make a perfect simulation of reality due to scale effects and laboratory conditions. The role of the physical model engineer is to minimize these imperfections through careful model operation (Hughes et al, 2010).

According to Hughes et al (2010) there are three forms of similarity which need to be met in order to have a proper free-surface flow physical model.

1. **Geometric similarity** exists between two objects or systems if the ratios of all corresponding linear dimensions are equal (Warnock, 1950). Physical models which have the same horizontal and vertical axis scale are undistorted models. The physical scale model of Zeebrugge is an example of a distorted model. The effects of this distortion will be explained in section 3.2.
2. **Kinematic similarity** is the similarity in motions between the particles in the model and the prototype. Kinematic similarity is achieved when all the vectorial motions of the model have the same ratio compared to the prototype for every given particle at any given time (Hudson et al, 1979). This similarity assures the right direction and velocity of the tidal current within the model.
3. **Dynamic similarity** between two geometrically and kinematically similar systems requires that the ratios of all vectorial forces in the two systems are the same (Warnock, 1950). In other words, the ratios of all the masses and forces within the system need to be equal.

3.2 Distorted physical models

As stated above (section 3.1) the physical model of Zeebrugge is a geometrically distorted model. The distortion factor of this model is three. This means that the horizontal axis scale is a factor 3 smaller than the vertical axis scale. Normally this will mean that the criteria for a proper physical model as stated above are (section 3.1) are not met. However in some specific situations the distortion effects can be minimized so the model will be reliable enough to simulate the prototype. For instance: if the vertical velocities and accelerations are very small compared to the horizontal velocities and accelerations (Hughes, 1993).

The main advantage of a geographically distorted model is that it is possible to scale the horizontal axis in a way that the model fits in the available space, without having the negative effects of a vertical axis which is scaled too small. If the vertical axis is scaled to small, other problems will occur. Like an unnatural high percentage of bottom friction and surface tension (Hughes et al, 2010). A distorted model allows larger water depths to prevent these unwanted effects and makes it possible to measure the effects which occur in the vertical axis more accurately.

Of course there are also disadvantages of a distorted model which need to be taken into consideration. The biggest problem is that it is not possible to simulate short waves (wind waves) in addition to long waves (Hughes et al, 2010). In the model of Zeebrugge, however, this will not be a problem since no waves are generated in this model, only tidal currents. The other disadvantage does need to be taken into account: The boundary slopes in the model are steeper than in the prototype (Hughes et al, 2010). This could have an influence on the flows within the physical model.

3.3 Advantages of a physical model

Physical models are still important to solve hydraulic problems. The upcoming numerical models are not always able to simulate certain effects. When we try to find solutions to problems that are beyond our theoretical understanding or problems which are too complicated, a numerical model might not suffice. These problems are often studied with data collected from well calibrated and validated physical models. According to Hughes (1993) these are the main advantages of physical models:

1. Physical models incorporate the fully nonlinear conservation laws of the modelled process without simplifying assumptions.
2. Complex boundaries and bathymetry can be included without difficulty.
3. The controlled laboratory conditions of the model permits easy data collection
4. Similitude requirements for many problems are well understood and easily implemented.
5. Visual feedback from a physical model often reveals aspects of the physical process that had not been considered previously. Observation also helps us to understand the differences that arise from changing the forcing conditions, and they often stimulate new ideas or alternative solutions.
6. Engineering solutions can be optimized in a physical model to achieve project functionality at minimum expense.

3.4 Disadvantages of a physical model

Of course there are not only advantages to the use of physical models, also several disadvantages occur. These negative effects need to be taken into account to be able to make a reliable physical model. The disadvantages according to Hughes (1993) are stated below:

1. The prototype needs to be modelled in a limited amount of space. Therefore model boundaries need to be created where in reality no boundaries exist. At these boundaries flow will need to be introduced or removed, this requires knowledge about the flow rate at these boundary locations and a complicated system to simulate these effects correctly.
2. The total discharge of the boundary is not the only problem. The cross-channel discharge distribution also needs to be taken into account. This can vary in time and is a process which is difficult to model. However if the boundaries of the model are far enough from the point of interest, and the total boundary discharge is accurate, the cross-channel discharge distribution should naturally adjust to a correct distribution downstream.
3. Not every aspect of a tidal sequence can be simulated. Selections in this simulation need to be made. This often results in a tidal sequence which is modelled as a sinusoidal sequence. This results in an incomplete result which will not be able to reproduce all the different aspects of spring-neap tidal differences.

4. Slopes in a geometrically distorted model are steeper than in the prototype, this should not be a problem for the mean flow condition within the model. Hughes and Pizzo (2003) conclude there is some distortion near the bottom of the model when the boundary objects get steeper. However this effect is small and reduces with the height of the flow, on the surface hardly any distortion is noted. What does need to be taken into account is that a steeper slope will impact the three-dimensional structure of large eddies (Hughes et al, 2010) (Hughes & Pizzo, 2003)
5. Because of the rotation of the earth the Coriolis force occurs. The Coriolis force influences the tidal sequence in great waters like the North Sea (Ducrotoy et al, 2000). Because of the reduced size of the model and the scaled time frame, it will not be possible to simulate the Coriolis force properly. This could result in differences between the data collected from the prototype and the model.

4. Technical design of the physical model

In this chapter the characteristics of the physical model of Zeebrugge are presented. This will include the definition of the model boundaries, the scale and the operating system.

4.1 Model boundaries

The model boundaries, as shown in figure 5 and again in figure 12, are chosen according to the expected area of influence of the different design scenarios (Ides et al, 2009). In figure 12 an estimated area of influence of a floodable dam on the west side of the harbour entrance. This area of effect has been calculated with a numerical model of the harbour. The model boundaries are chosen in a way that the main flow of the tidal current flows straight through the east and west boundaries and parallel to the sea boundary. This is chosen because it makes the water inflow and outflow in the scale model easier to operate.

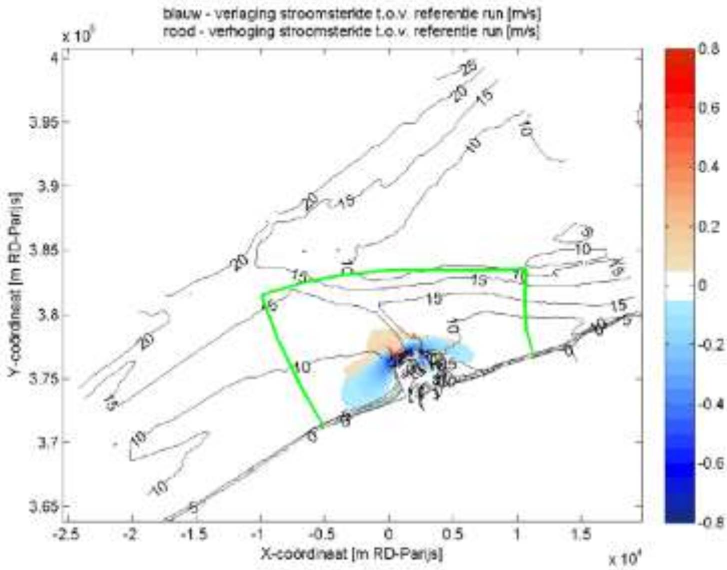

Figure 12: study area, including physical model boundaries. (Ides et al, 2009)

4.2 Scale

The physical scale model has a scale of 1:300 on the horizontal axis and a scale of 1:100 on the vertical axis (Willems et al, 2011). This means that the size of the harbour is 300 times smaller in the model than in the prototype but the depth of the harbour is only 100 times smaller in the model than in the prototype. The horizontal axis scale is chosen with a scale of 1:300 so the model would be able to fit in one of the research halls at WL. The vertical axis scale is chosen for practical reasons (ensuring the accuracy of the measurement instruments and making it easier to get accurate water level readings during the calibration phase) (Willems et al, 2011). A disadvantage of this is that there will be a distortion within the model. The influences of this distortion have already been discussed in section 3.2. A summary of all the scales within the model is given below (Willems et al, 2011):

- Horizontal scale 1:300
- Vertical scale 1:100
- Flow speed scale 1:10
- Time scale 1:30
- Flow rate 1:300.000

The reference point of the model is at low tide and equals 0 TAW. TAW is the “Tweede Algemene Waterpassing”. This is the water level of an averaged low tide at Oostende (Belgium). All the water level values within the model are expressed in meters from TAW.

4.3 Operating system

The model has three boundaries where water can flow in and out of the model: The west side, the east side and the north side. To be able to make a good simulation of the tidal current these boundaries need to allow water to flow into the system at certain points in time and make outflow possible at other times. The amount of inflow and outflow in each border strongly affects the current direction and velocity within the model.

East and west sides

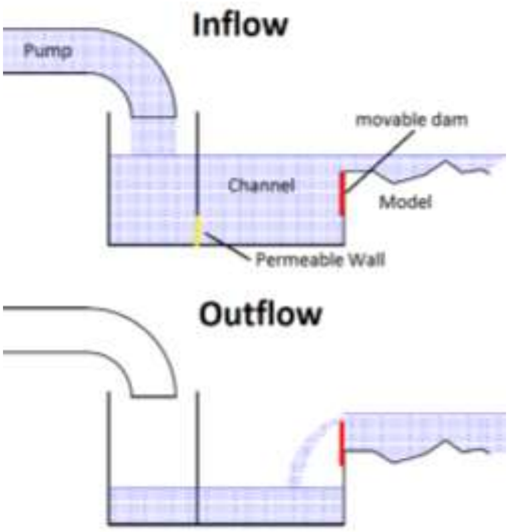

Figure 13: Pump system east and west sides

In figure 13 a schematization of the operating system of the east and west side is shown. On the east and the west side pumps are situated. These pumps fuel a channel on the edge of the model. There are 2 pumps on each side and these pumps deliver a maximum flow rate of 250 L/s each. At the moment of inflow this is more than required to fill the model, the excessive amount of water is let out of the channel back into the water reservoir beneath the model by using two butterfly valves. At the moment of outflow these valves are also used to extract the water from the model (Willems et al, 2011).

From the channels on each side the model is filled through 7 movable dams on the east side and 11 on the west side. The length of these dams is 2.9 meters and the height is computerized and variable over time. By adjusting the height of these dams the water flow over them can be controlled, this way the right amount of water can be brought into the model from the side channel or be extracted out of the model. It is also possible to vary the place of inflow. This will affect the flow direction within the model (Willems et al, 2011). These movable dams have an error of roughly 1 mm (or 1%).

The channel has two compartments (see figure 13). This is only because the water coming out of the pumps is very turbulent and has to calm down before it can flow into the model. Via the submerged permeable wall the water will flow to the actual model access channel.

North side

The inflow and outflow from the seaside is realized by a sunken channel along the north side (figure 14). From numerical model explorations it is shown that the inflow and outflow from the north side is constant within time. This makes it possible to use a similar system as for the east side and west side, but without the movable dams to vary the inflow over time. Between the channel and the model there is a permeable wall to ensure a calm inflow into the model.

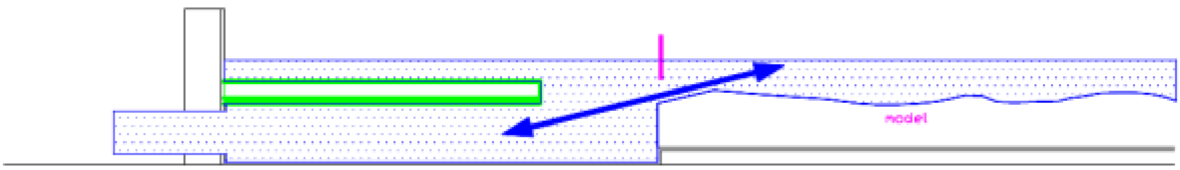

Figure 14: Pump system north side (Willems et al, 2011)

5. Measurement techniques

Within this chapter the several measuring equipment which are used within the physical model of Zeebrugge are shown and the associated uncertainties are discussed.

5.1 Physical model data collection

Flow rate indicator

The flow indicators are situated on the pipes feeding the model and on the pipes which allow the water to flow back into the reservoir under the model. The flow meters are situated outside the pipe and work with sound waves. It sends out sound waves upstream and downstream and because sound travels faster downstream than upstream the velocity of the water in the pipe can be found from the difference in the speed of sound. With the velocity known and the diameter of the pipe constant the flow rate can be calculated. The uncertainty in these flow rate indicators are ±1% of the measured value (Krohne, 2013).

Water level indicator

Ten ultrasonic water level indicators are available on the physical model of Zeebrugge. These water level indicators measure the water levels in the model with high frequency sound waves. These sound waves are reflected by the water surface and the time it takes them to travel indicates how far the water level is away from the measurement instrument. This is an accurate way to measure the water level in the model. The uncertainty in this measuring system is 1-2mm (or 0.5-1%) depending on the frequency of the device (Banner, 2013).

EMS

The Electromagnetic Speed monitor (EMS) is one of the most important ways to measure flow velocities within the model. EMS data is collected by an electromagnetic device placed in the water of the physical scale model. It records the horizontal and vertical components of the current velocity at a fixed point (Willems et al, 2011). The velocity is calculated with equation 1 with U the horizontal component of the velocity, V the vertical component and C_V the magnitude of the current velocity.

Equation (1): $C_V{}^2 = U^2 + V^2$

The direction of the current can be calculated with equation 2 where α is the angle of the current with the U axis.

Equation (2): $\tan(\alpha) = \frac{V}{U}$

The measuring location of the EMS is directly below the electrodes of the probe (ellipsoid 11 x 33 mm). The measuring volume is 5 mm thick and has a diameter of 50 mm. There are 6 of these EMS instruments available for the model of Zeebrugge. These can be placed at any point in the model.

The EMS used can measure up to 2.5 m/s and with an uncertainty as little as 1% of the measured value. The measurement point of the EMS is -2 TAW (2 cm below low tide in the model). This point is chosen because it is far enough under water to measure during low tide. In figure 15 the velocity profile from the model is shown, with on the horizontal axes the speed in m/s and on the vertical axis the depth of the EMS measurement instrument. From this figure the conclusion can be drawn that the velocity of the current does not decrease significantly with the depth in the first few meters.

Therefore the velocity measured by the EMS instruments on -2 TAW can be compared with the surface velocity measured by the PTV-analysis.

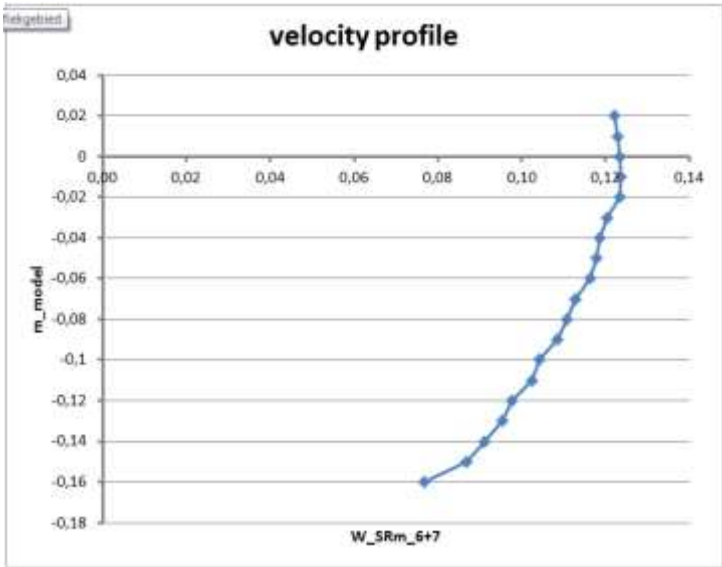

Figure 15: Velocity Profile of a stationary flow, with on the horizontal axis the speed in m/s and on the vertical axis the water depth (Heyvaert, 2012)

An advantage of the EMS method is that it is accurate. It is a reliable way to measure the current velocity and direction of the current during the whole tidal simulation within the model. The disadvantage is that it is only possible to measure one fixed point within the model, what happens around this point is unknown.

Surface PTV-analysis

A surface Particle Tracing Velocimetry (PTV)-analysis is a relative easy and reliable way to show current behaviour in shallow water like coastal zones and rivers where the two-dimensional force in the water current is dominant (Weibrecht et al, 2002). In contrast with standard Particle Image Velocimetry (PIV) applications where measurements are carried out within the water body using a laser to illuminate the particles in the water (Rockwell et al, 1993) (Sheridan et al, 1997), surface PTV measurement requires no lasers. It is a straight forward method which registers particles on the surface which are illuminated by regular lighting. The PTV software used to trace the particles in the model of Zeebrugge is Streams. Streams analyses the camera footage and takes certain steps in time and compares the location of the particles within this time step. This way it records the movement of the particles over this time step. From these movements the software makes a vector field so the speed and the direction of the displacement on a certain point in time can be shown. In figure 16 the basic principle of surface PTV-analysis is shown.

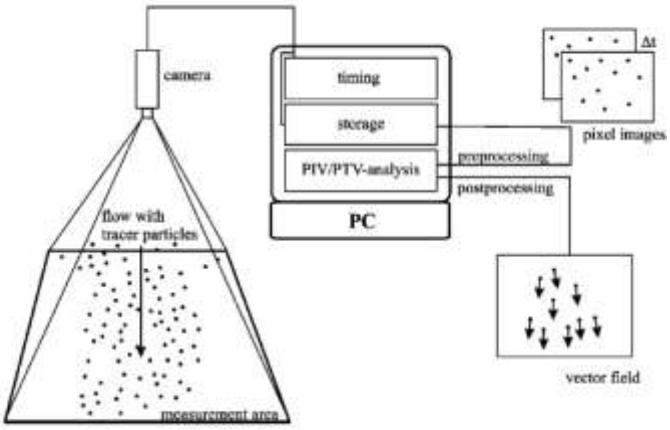

Figure 16: PTV-analysis system (Weibrecht et al, 2002)

An advantage of this method is its large examination section. A disadvantage is that it is less accurate than the EMS results because it only shows the flows on the surface and not underneath. As concluded in the section above with figure 15 the velocity measured by the PTV-analysis will be roughly the same as the velocity measured with the EMS instruments so this disadvantage is negligible. Another disadvantage is that the software can only trace the tracer particles in the water. When the particles stick together (as surface particles often do) or if the boarders are not fed properly, gaps can arise in the measurement area where no data can be collected. It is important to avoid this problem by making sure there are enough people assisting with the analysis to feed the measurement area with tracer particles and to prevent gaps.

5.2 Natural data collection

To collect natural data from the harbour of Zeebrugge several ships equipped with different measurement equipment have been dispatched. These ships have roamed the water of the harbour from November 2010 till May 2011. Several days and tides where measured to gain a reliable set of data. The main instrument used was the Acoustic Doppler Current Profiler (ADCP). This instrument is a sort of sonar which is used to measure the velocities and directions of the tidal currents beneath a ship. It is even capable of distinguishing differences in velocities and directions over the whole water depth (Eurosense & Aqua Vision, 2011). The exact uncertainty of this system is unknown. The model measurements are done under controlled conditions. This is not possible in the prototype. In reality a lot of obstruction occurred while doing the measurements. For example extreme weather conditions make unexpected waves and currents in harbour which do not match the overall pattern, these data need to be corrected or removed. Another example: Through commercial shipping in the harbour it is impossible for the measurement vessels to keep their correct course all the time so it was not possible to get the data of specific courses during the whole tidal sequence. In some places the quality of the data collected was so poor that after corrections no valid data remained, for these points an interpolation was done of the speeds and directions in the surrounding points to reconstruct the data (Eurosense & Aqua Vision, 2011).

5.3 Uncertainty

In section 5.1 the different measuring equipment and their uncertainty where discussed. To test the actual uncertainty in the model a test was run with 9 equal tidal sequences. During this test data of the water level and the velocity of the tide was collected and is shown in figure 17.

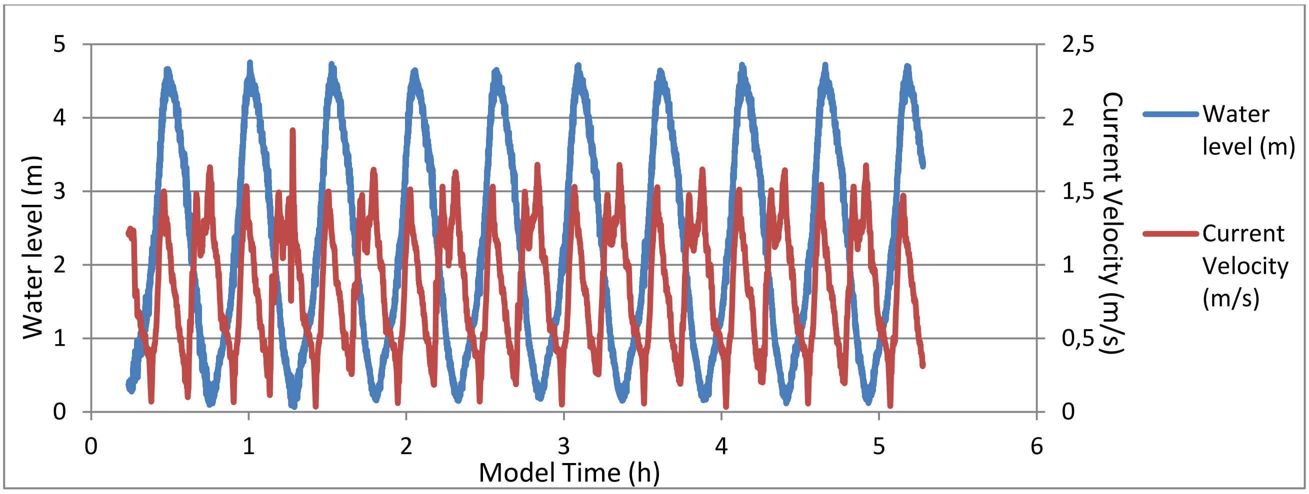

Figure 17: Water level (m) and Current velocity (m/s) at PO6

If the 9 tidal sequences are inspected more closely it is seen that in the velocity of the second sequence is much higher than the other sequences. This could be because someone accidentally touched the EMS instrument during the test. To be sure this sequence does not have a negative effect on the other results it is removed and the other 8 sequences have been compared to determine an average sequence and the Rooted Mean Square Error (Willmott & Matsuura, 2005).

Equation (3): $RMSE = \sqrt{\frac{1}{n} * \sum(V_i - V_{mean})^2}$

The RMSE value of the test should be close to 0. The RMSE value of the velocity test is 0.037 m/s, with an average of 0.87 m/s this means that the average uncertainty is 4.2%. For such a large model this is a relatively low level of uncertainty. Therefore the model of Zeebrugge is a reliable model to collect data from.

As described above (section 5.2) the natural data are less certain then the physical model data and the authors of the “stroomatlas” (IVA Maritieme Dienstverlening en Kust, 2011)(appendix A) warn for the uncertainties which it could contain. However the natural data is the only data available of the prototype to compare the physical model with. Therefore it is not possible to be too critical about this set of data. With the help of several experts the data which seemed incorrect where removed from the dataset and interpolation calculations where used to restore these data sets (Eurosense & Aqua Vision, 2011). Therefore we can say that the natural data are reliable enough to compare to the physical model.

6. Tidal flow process

In this chapter the most important hydraulic processes which occur at the entrance of the harbour of Zeebrugge will be described. These are processes which have been observed in nature. To be able to reproduce these processes in the physical model we need to understand as much as possible of the cause of these processes.

As described in section 2.3 the problem occurring at the harbour of Zeebrugge is caused by the high flow velocities at the entrance of the harbour. To be able to get a good impression of the problem a “stroomatlas” of the harbour of Zeebrugge is made (IVA Maritieme Dienstverlening en Kust, 2011). In this atlas the velocities of the tidal currents at the harbour are shown. The atlas makes steps in time of 20 minutes and the times are referred to as minutes and hours before and after high water. In figure 18 an example of one of these steps is shown, this is the moment at 1 hour and 40 minutes before high water where the inflow into the harbour begins. In appendix A the full charts are shown during at part of the high tide sequence, 2 hours before high water and 2 hours and 20 minutes after high water. The velocities shown in this stroomatlas are the average velocities measured over the top 10 meters of water.

The velocities given by this stroomatlas will be the velocities used to compare with the data from the physical model. These natural data give a decent insight in the main currents at the harbour. In the next section these natural data will be compared to the data from the physical model.

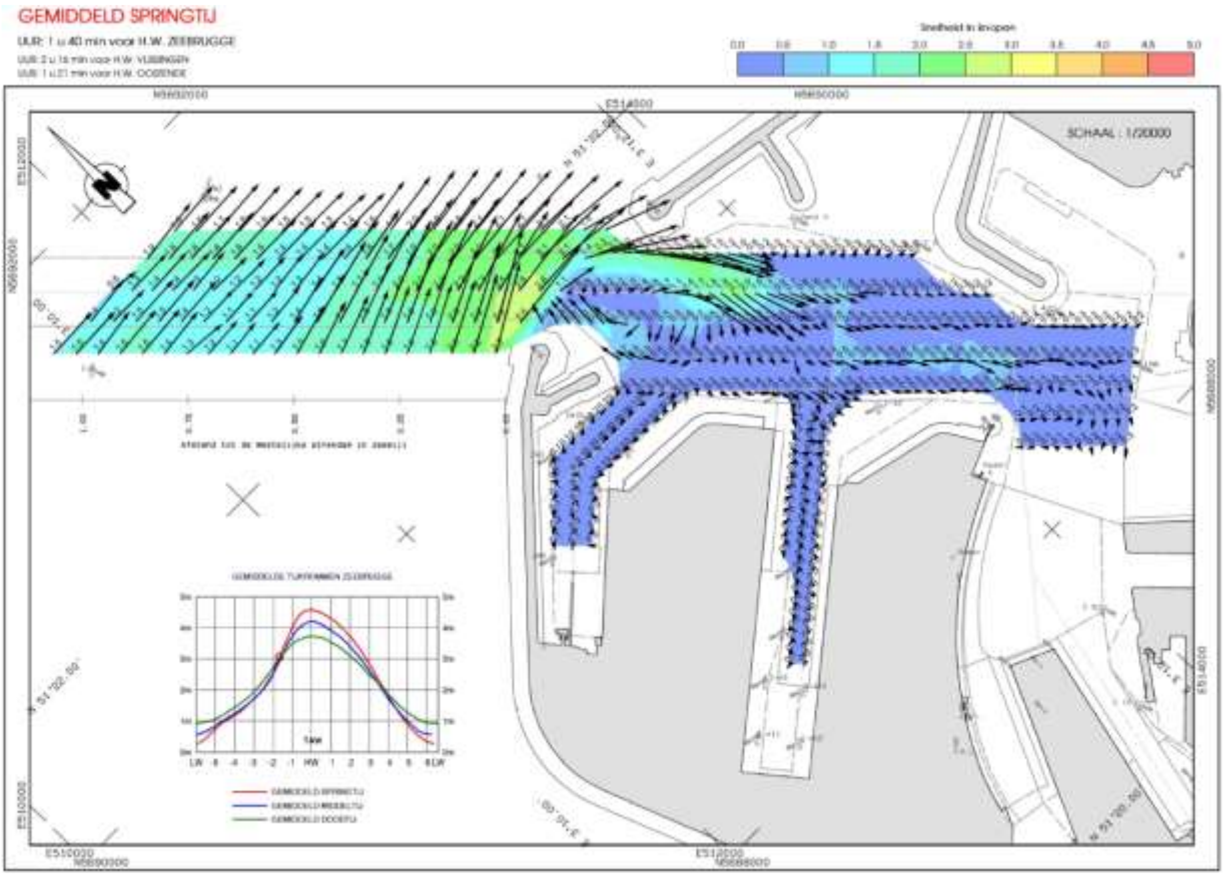

Figure 18: Velocity field of natural data at 1 hour and 40 minutes before high water during an average springtide (IVA Maritieme Dienstverlening en Kust, 2011)

6.1 Tide

The inflow of water into the harbour of Zeebrugge is the most important hydraulic process occurring. Due to the tidal sequence, the water level of the North Sea rises during high tide and falls during low tide. Not only the water level rises and falls, but the flow direction past the harbour changes as well. During high tide the water flows from west to east and during low tide the water flows from east to west. The actual inflow in the harbour strongly depends on the velocities and directions of the flows in front of the harbour and differs over time. To be able to study the properties of the inflow the scope will be set to 2 hours before high water until 2 hours and 20 minutes after high water. This is the moment when most interesting hydraulic processes occur. In figure 18 a velocity field is shown of the moment in time where the flow starts entering the harbour. This image comes from the stroomatlas and is made from the measured natural data and represents the flows occurring at 1 hour and 40 minutes before high water during a spring tide sequence (IVA Maritieme Dienstverlening en Kust, 2011).

The velocity of the inflow is a combination of the strength of the tidal current, the roughness on the bottom and the water depth in the area. The direction of the inflow depends on the point where the current separates from the west entrance and the shape of the east entrance where the current deflects and changes course. The velocity of the inflow at the harbour also has an effect on the inflow direction (section 6.2).

6.2 Eddy formation

A schematic overview of the processes occurring at a harbour entrance along a river with stationary current is show in figure 19. From the figure it is shown that the inflow during high tide is a result of the difference in velocity between the harbour and the river (Langendoen, 1992). The mixing layer consists of water from the river and from the harbour and increases its width as it travels downstream. Downstream it will meet the side wall of the harbour and a stagnation point will separate the flow going into the harbour and the flow going past the harbour. Because of the curvature in the inflow of the harbour an eddy occurs in the harbour entrance. The strength of this eddy is dependent on different factors like the velocity outside the harbour, the geometry and the orientation of the harbour and the harbour entrance (Langendoen, 1992).

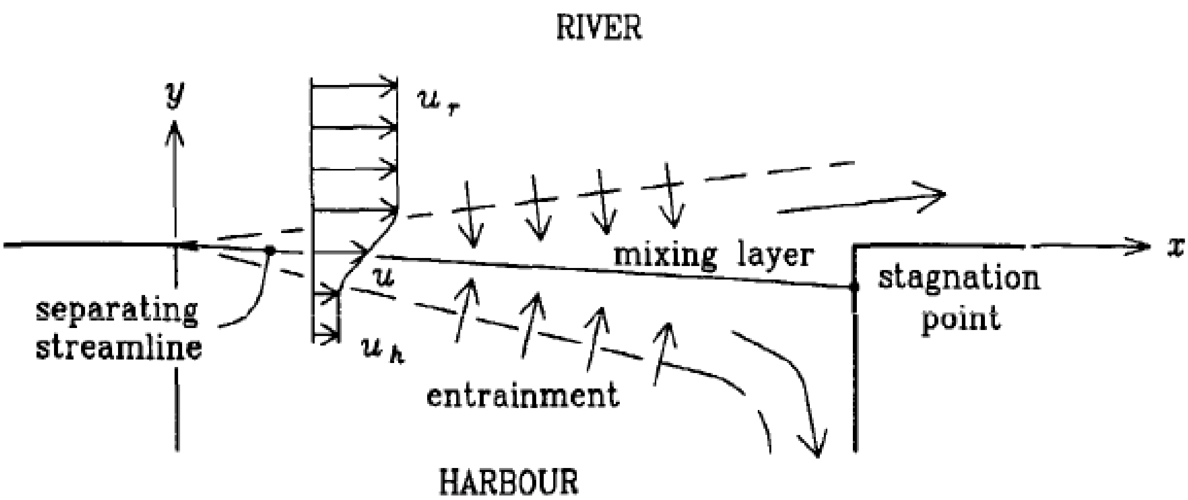

Figure 19: Mixing layer between a river and a harbour (Langendoen, 1992)

For a tidal harbour the principle of the mixing layer is the same. There is only a small difference because of the tidal sequence. The variation is that the currents in front of a tidal harbour change direction over time and the currents in front of a river harbour do not. According to Booij (1989) an eddy in a tidal harbour only occurs during high tide. The high tide strengthens the formation of the eddy and the low tide decreases the strength of the eddy. Because of the existence of the eddy in the harbour during high tide, the inflow area is less than the outflow area. This will result in stronger inflow velocities compared to the outflow velocities (see figure 20) (Christiansens, 1987).

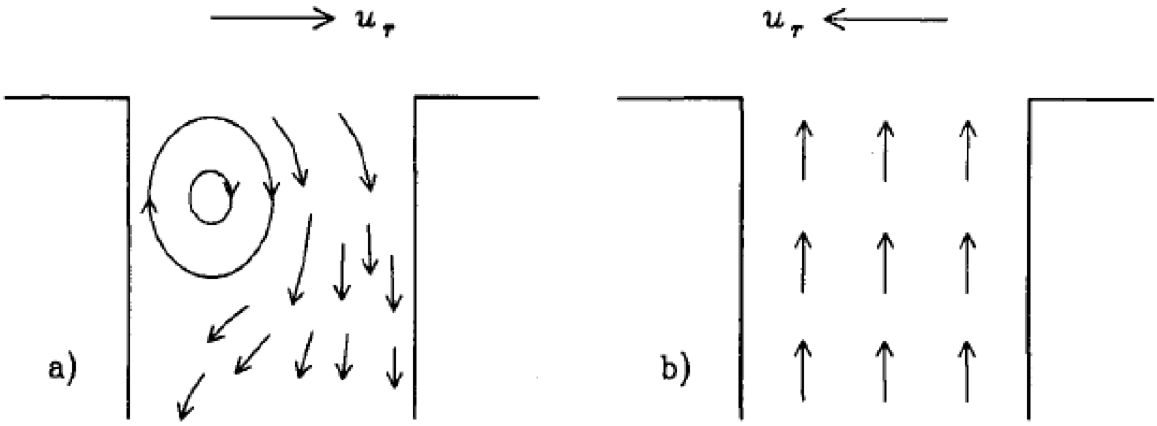

Figure 20: Inflow and outflow of a tidal harbour (Christiansens, 1987)

7. Physical model data

In this chapter the physical model data of the starting situation is shown. This is the situation without any roughness inside the harbour. This starting situation will be compared with the velocity fields of the natural data and the differences and their probable causes will be discussed.

7.1 Harbour without extra roughness

The situation without extra roughness of the physical model is the situation right after the calibration of the sea. As described in section 2.3 the natural data does not match the physical model data. The main stream inside of the model is clockwise and in the natural data this is counter-clockwise. In figure 21 a vector field made from the natural data is shown. This vector field is compared with the vector field made from the physical model data at the same time (1 hour and 40 minutes before high water). It is clearly shown that there are several differences in these data. The differences and their possible causes are stated in the next section.

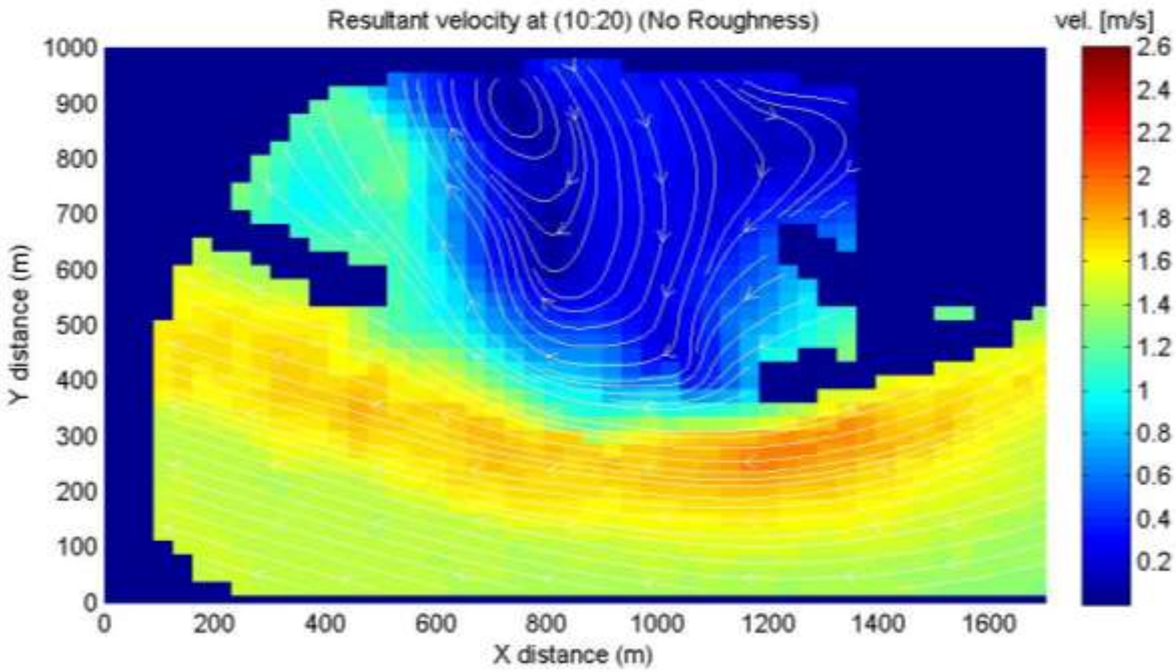

Figure 21: Velocity field of physical model data at 1 hour and 40 minutes before high water during an average springtide.

7.2 Comparison with natural data

First of all some interesting differences can be observed regarding the inflow of the harbour at 1 hour and 40 minutes before high water. If we compare the natural data of figure 18 and the physical model data of figure 21 the first thing noticeable is the difference in direction of inflow. In the natural data it is clearly seen that the current which is coming from the west side deflects of the east head of the harbour and then crosses over to the other side of the harbour. This way two separate eddies are formed, a small one at the harbour entrance which circulates clockwise and a larger one in the back of the harbour which circulates counter-clockwise. If we compare this to the physical model velocity field of figure 21 it is seen that the current does not properly deflect from the east wall but rushes past it instead. This way one large eddy is generated which circulates clockwise in over the whole length of the harbour. This eddy pattern in undesired and needs to be changed in order to simulate the prototype better. There are several probable causes of this difference already described in chapter 6. The probable cause is that the stagnation point of the mixing layer (as explained in section 6.2) is located too far towards the harbour entrance. This can have two different causes: The streamlines are not pushed out far enough so the separation point from the west head is too far towards the harbour entrance. Or the velocity of the tidal current outside of the harbour is too strong.

Since the model is on scale it is unlikely that the separation point is in this situation is too far towards the harbour entrance, therefore the focus is on the velocities. If we look at the velocities at this point it is seen that in the natural data the maximum velocity in front of the harbour is about 1.3 m/s and in the physical model this is about 1.9 m/s. This is a remarkable difference and could well be the cause of the problem of the inflow error and the eddy pattern. However if we look at the maximum velocity occurring at 1 hour before high water it is seen that this velocity is about 2.1 m/s in both the natural data and 2.2 m/s the physical model data. A solution to higher the stagnation point of the mixing layer would be to reduce the velocity of the harbour entrance by applying extra roughness. However if the velocity at 1 hour and 40 minutes before high water would be reduced from 1.9 m/s to 1.3 m/s to make the inflow direction better, the maximum velocity would be slowed as well by the extra roughness. This must to be prevented because the match of the maximum velocity with the prototype is more important. This velocity is the main problem occurring in the harbour and the reason the scale model of Zeebrugge was build was to reduce this flow velocity. It is not possible to change the boundary conditions of the model. If we change the boundary conditions to reduce the speed at this moment in time, the risk is high that the situation at sea gets worse.

Another way to get the stagnation point of the mixing layer to the right position needs to be explored. A possible option is to press the streamlines more sea inward to allow a higher separation point and this may result in a proper stagnation point of the mixing layer so the current in the harbour can be improved without affecting the conditions in front of the harbour too much. The results of the test scenarios used to improve the inflow direction and the eddy pattern is presented in the next section.

7.3 Results

In this chapter different roughness scenarios will be evaluated. These scenarios contain measures to alter the currents in the physical model and make them more in alignment with the natural data. The effect of these measures is stated below.

7.3.1 Scenario Description

During the research 6 different scenarios were tried to influence the tidal currents inside the harbour and at the harbour entrance. All these scenarios include a local change in the roughness or bed level of the model. In figures 22, 23 and 24 pictures of the applied roughness are shown. The exact location of the scenarios can be found in appendix B.

Figure 22: Roughness on the west head

Figure 23: Roughness on the east head

Figure 24: Roughness on the west dam

Scenario 1 was described in section 7.1. In this scenario no extra roughness was applied. This scenario was analysed to get a good idea of the differences occurring between the physical model velocity field and the natural data velocity field.

Scenarios 2 and 4 feature two different ways to push the streamlines of the model more sea inward: Roughness on the west head with a maximum height of 0 TAW and roughness alongthe west dam with a maximum height of -1 TAW. These scenarios should push the separation point of the mixing layer more sea inward, with a higher stagnation point of the mixing layer on the east head as goal. This should improve the deflection direction of the east head, so that the desired eddy pattern within the harbour would occur.

Scenario 3 is an increased amount of roughness on the east head. This roughness was not intended to slow the inflow down at this point but to raise the bathymetry level of this area to create a larger east head. This way it should be easier to get the stagnation point of the mixing layer on to this enlarged east head. This is done to improve the deflection direction into the harbour to create the desired eddy pattern.

Scenarios 5 and 6 are combinations of the scenarios mentioned above. Scenario 5 has roughness on the west dam and on the east head. And scenario 6 has roughness on the west head and on the east head (scenario 6).

7.3.2 PTV-Analysis

In appendix C the PTV-analysis of the harbour entrance is shown for the 6 different scenarios. The point in time chosen to show here (figure 25) is 10.20 (or 1 hour and 40 minutes before high water). This is done because at this time the inflow into the harbour has just started and it is easy to see how the inflow behaves. If we look back at figure 18 we can there see the natural data during this period in time. The differences will be discussed below.

In the natural data it is seen that the inflow deflects from the east head of the harbour and then goes straight forward with a small curvature back to the west side of the harbour. This was concluded in section 7.2. As was shown in figure 21 and again in the top left corner of figure 25 the flow did not deflect and went past the east head to make one big eddy in the harbour. We can see by comparing this situation with the other scenarios, that in scenario 4 with only the west dam (figure 25 bottom left corner) has the same inflow pattern as the scenario without roughness. The only difference is its increased velocity. From observation it was seen that the eddy pattern with this scenario was the same as in the scenario without roughness. So this scenario did not improve the eddy pattern inside the harbour.

In the scenario with the west head (figure 25 top right picture) two things stand out. The first is its increased velocity at the harbour entrance. As discussed in section 7.2 the overall velocity in front of the harbour at 10.20 hours was too high. But in the scenario with the west head this velocity has increased even further to 2.1 m/s. The second is the dark blue spot behind the east head. This indicates that the current does not pass the east head completely anymore like in the scenarios before, but actually meets the east head and is showing a little deflection so a little improvement in the inflow direction is seen, however this improvement was not enough to create the desired eddy pattern.

When applying the roughness on the east head the velocity field of the centre top picture of figure 25 is generated. There we see the same as with the roughness on the west head, a blue spot behind the east head. This indicates the same as was just discussed, the deflection seems right but for some unknown reason the current goes east again after it meets the enlarged east head. Again this scenario only creates one eddy and does not meet the desired eddy pattern.

Only by combining the scenarios as mentioned above the desired eddy patterns emerge. When applying scenario 6 (figure 25 bottom right picture) with the west head and the east head a clear difference with the other scenarios is seen. The inflow current has a larger velocity and actually deflects correctly compared to the natural data. The current goes straight forward with a little curvature towards the west side of the harbour.

If we look at scenario 5 (figure 25 bottom centre picture) we do not see much difference between this scenario and scenario 3 with the roughness on the east head. Only the velocity of inflow is a little higher and after meeting the east head the current does not flow back to the east side but continues through the middle. During the inflow this might not seem like a big difference for the flow pattern, but inside of the harbour it has a big difference. In the case with the east head the eddy pattern is one large eddy as with the scenario without roughness but when the west dam is added as well the pattern changes in the desired two eddy pattern. From the scenarios 5 and 6 an extra PTV-analysis is made to inspect them in greater detail because these are the only two scenarios that show the desired eddy pattern.

The extra PTV-analysis is seen in figure 26, here the same time is shown as in figure 25 (10.20 hours or 1 hour and 40 minutes before high water). It is clearly seen in this figure that the inflow current goes straight through the middle of the harbour and creates two eddies inside of the harbour. In this figure little difference is shown with the natural data only the current velocity of both scenarios is higher and the west head creates a higher velocity then the west dam in front of the harbour. How the current develops over time is seen in appendix D and can be compared with the natural data at the same times of appendix A. The second major difference in physical model data and the natural data occurs around 11.40 hours. In the natural data it is seen that during this point in time the first eddy stops whirling around and is replaced by an area of still water. In the physical model data it is seen that at this point the first eddy is still visible. And this first eddy will stay visible until 13.00 for the west head and about 13.10 for the west dam. This is a difference of 1.20-1.30 hours in time. In figure 27 the last traces of the first eddy are still seen. The reason that this eddy keeps existing so long is unknown. Probably the distortion of the model makes the current less sensitive to roughness on the model bed. Applying roughness at the area of the small eddy was successful in slowing it down, however it was not possible to slow it down enough to match the natural data completely.

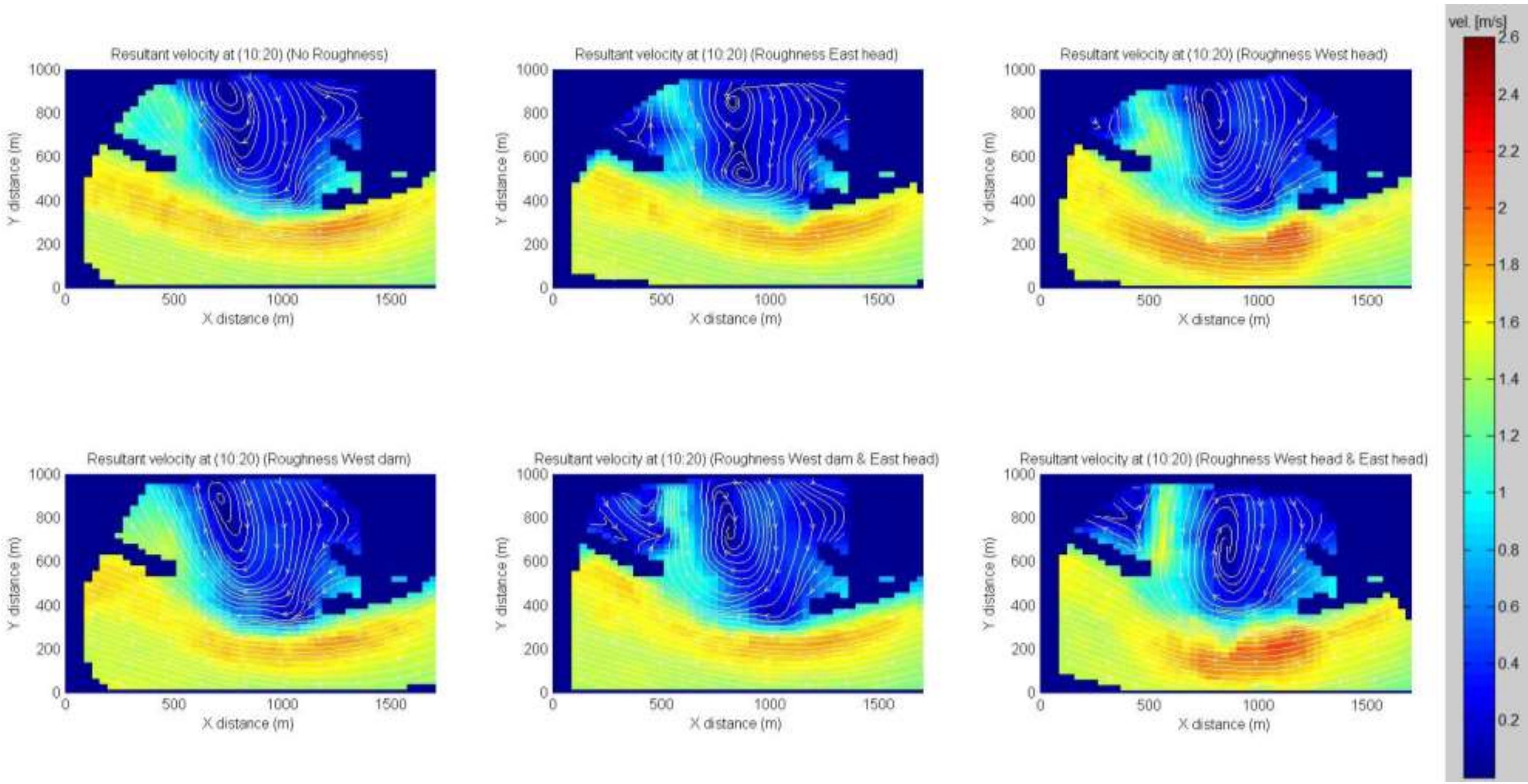

Figure 25: Velocity fields of the six different scenarios: Top left is scenario 1, top centre scenario 3, top right scenario 2, bottom left scenario 4, bottom centre scenario 5 and bottom left scenario 6

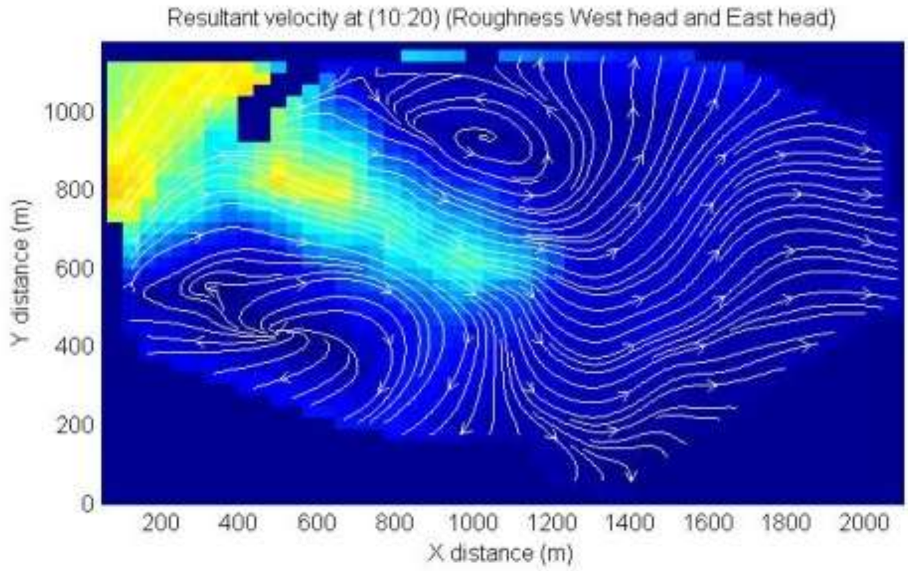

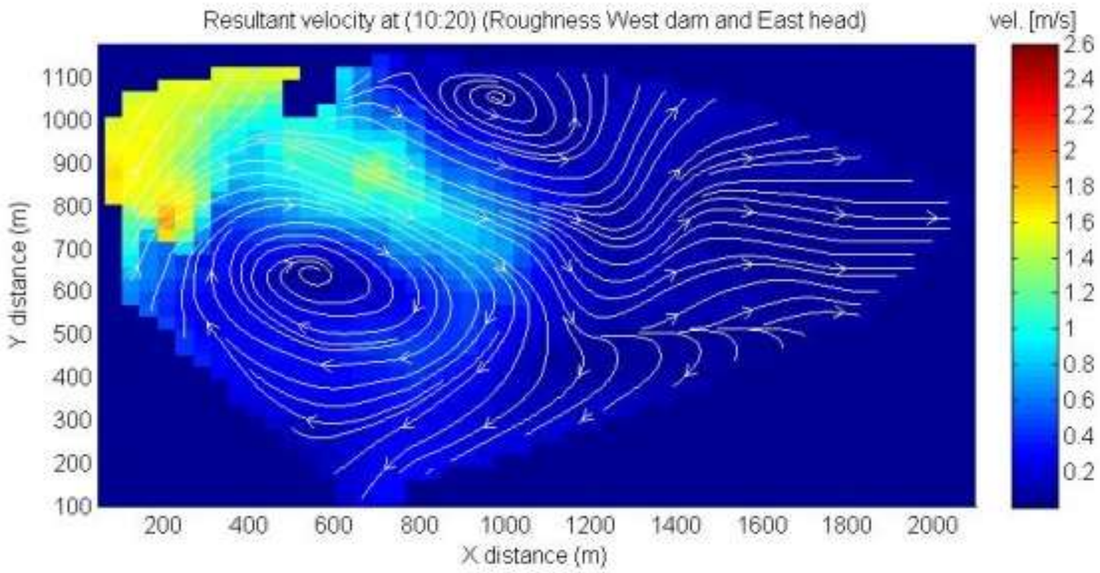

Figure 26: Velocity field inside the harbour of scenario 5 and 6 at 1 hour and 40 minutes before high water

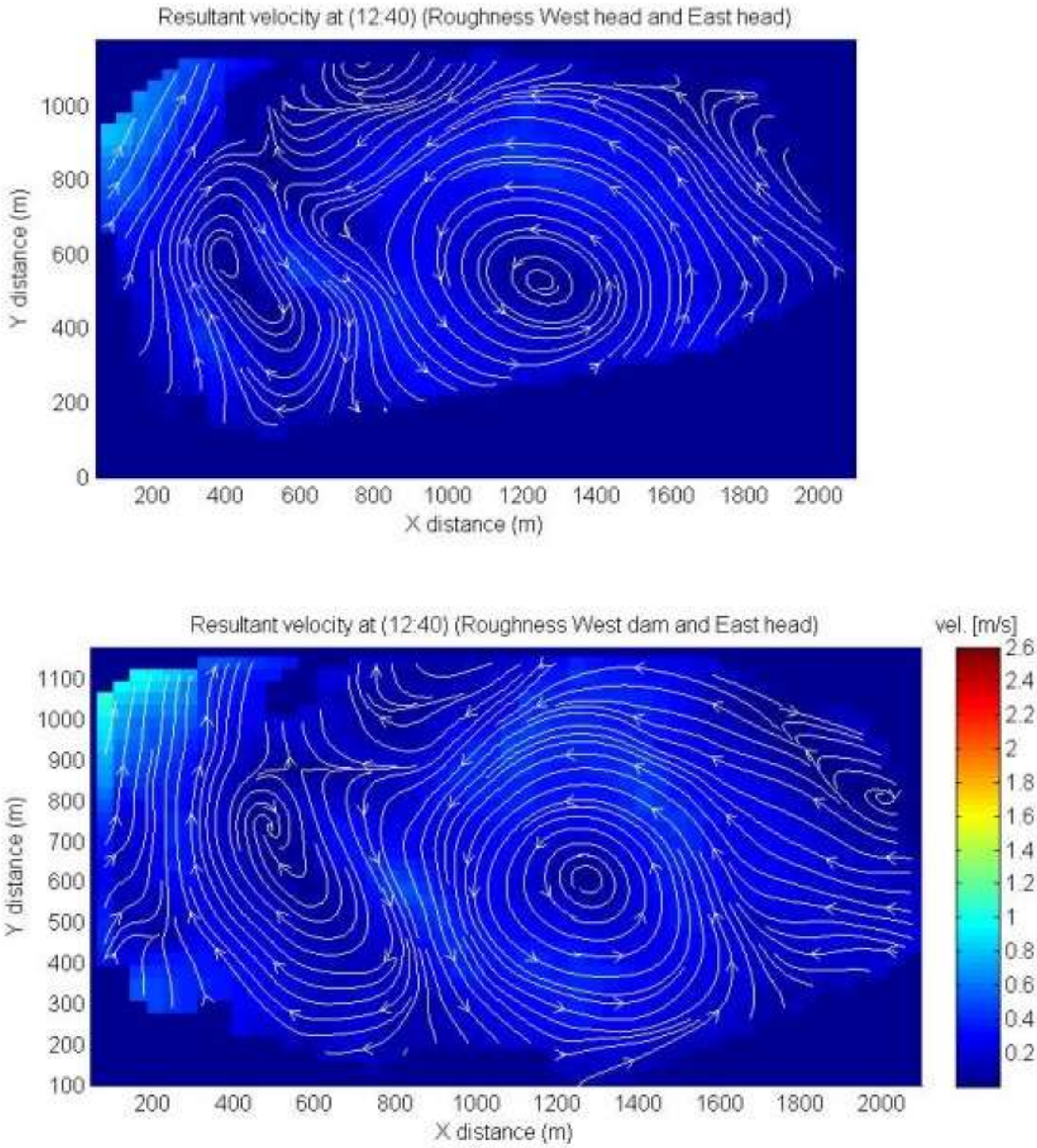

Figure 27: Velocity field inside the harbour at 40 minutes after high water

7.3.3 EMS Analysis

For the EMS measurements three points in the model are important because they are most likely to be influenced by the scenarios. These are points RPA-P06, RPA-P07 and RPA-P08. In figure 28 a grid is shown of the harbour and the locations of several measuring instruments. Points RPA-P06, RPA-P07 and RPA-P08 are found in the maritime access way close to the harbour entrance.

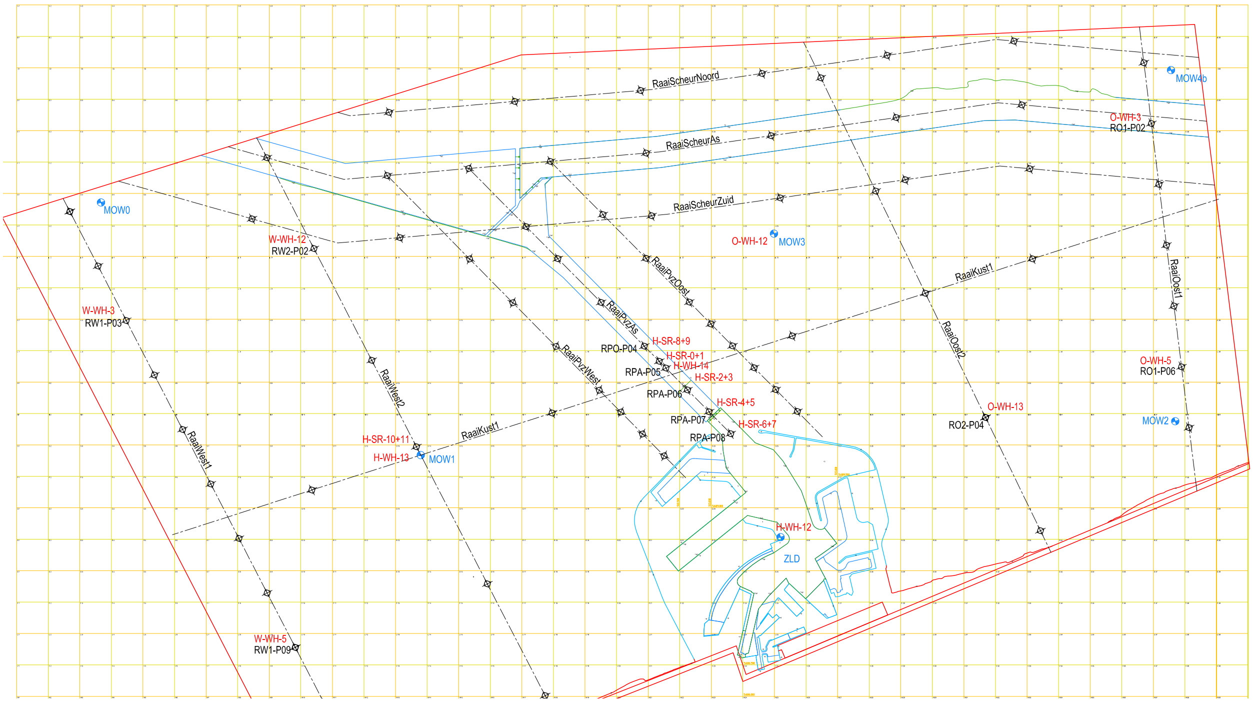

Figure 28: Instrumentation plan of the physical model of Zeebrugge

An example of the data collected by the EMS instruments is shown in figure 29, the other graphs used can be found in appendix E. Within figure 29 the velocity (V) and the water level (WH) of point RPA-P06 under the conditions of scenario 1 is shown. This graph shows the velocities and water level of an average spring tide constructed from at least 4 similar tidal sequences in the model. The natural data for the water level and the velocity are added in this figure to be able to easily compare the data from the prototype with the data from the model.

In figure 30 the horizontal and vertical components of the EMS data of point RPA-P06 are shown. This figure is constructed from the same data set as figure 29. Also here the natural data have been added to the graph to make a good comparison. To be able to see which scenario has the closest fit with reality different performance criteria are used. These performance criteria are described below.

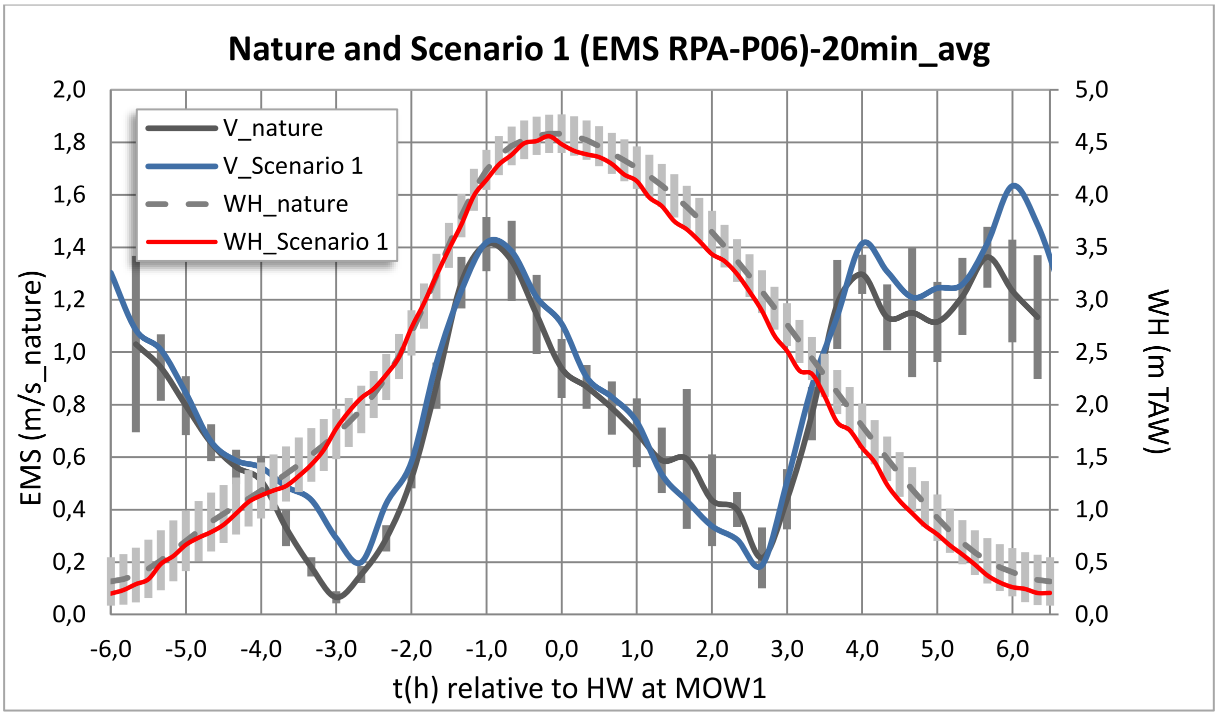

Figure 29: The Velocity (V) and Water Level (WH) of point RPA-P06 under the conditions of scenario 1

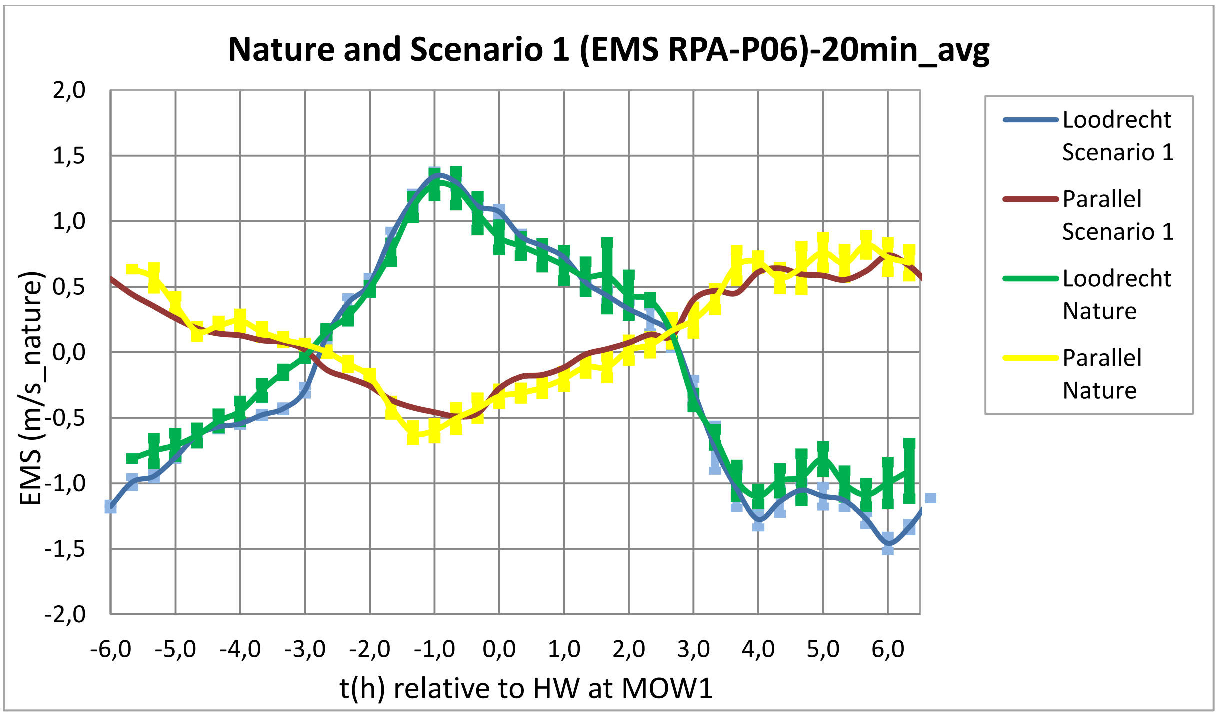

Figure 30: Horizontal (Parallel to the access channel) and Vertical (Loodrecht on the access channel) components of the EMS analysis at point P06 in scenario 1

Root of the Mean Squared Error (RMSE)

The RMSE was already introduced in section 5.3 and is obtained by taking the mean of the total squared error (MSE) and then use the square root over the MSE. The optimal value of the RMSE should be around zero. The formula of the RMSE was already in equation 3.

Mean Average Error (MAE)

The MAE is the mean of the absolute difference between the model values and the natural values. In equation 4 the MAE is found. The ideal value of the MAE is the value closest to zero

Equation (4): $MAE = \frac{1}{n}\sum_{i=1}^{n}(abs(V_{mod} - V_{nat}))$

Mean Bias Error (MBE)

The MBA is found in equation 5. It is usually used to indicate the average model bias. This is the average over- or underestimation. The ideal value of the MBE is zero.

Equation (5): $MBE = \frac{1}{n}\sum(V_{mod} - V_{nat})$

In table 1 the results from the performance criteria have been summarized. It is only possible to make conclusions regarding scenario 1 and 6 at this moment. Scenario 5 was measured several weeks later. During the tests done with scenario 5 an error in the EMS instruments was discovered. After several tidal sequences the starting value of the EMS changed significantly. Recalibration of the EMS instruments did not solve the problem. The reason for the problem is unknown, even the mechanics from the company who delivered these EMS instruments did not know the cause of the problem. The EMS instruments where returned for repairs.

The values given in table 1 are the differences between the natural data and the physical model data. If we inspect the number more closely it is seen that the changes in the water level do not change much. This is as expected because the applied roughness of the scenarios is not supposed to have influence on the water level.

If the values of P06 are inspected, it is seen that scenario 6 has a negative effect on point P06. The values of the velocity, the horizontal (parallel) and the vertical (loodrecht) EMS components differ more from the natural data then in scenario 1.

If we look at P07 at the same points, it is seen that scenario 6 has a positive effect on point P07. The values of the velocity, the horizontal and the vertical EMS components are more in alignment with the natural data.

In point P08 little difference is seen between scenario 1 and 6. This is probably because all the values of point P08 lay close together. If we look at the graph of P08 (appendix E) it is seen that this point is quite indifferent. There is no clear pattern shown because of the low velocities and the continuing change of flow direction. Therefore point P08 is an unreliable point to base any conclusions on.

		Scenario 1	Scenario 5	Scenario 6
Water level (m)	MAE	0.12	0.11	0.13
	MBE	-0.1	-0.09	-0.12
	RMSE	0.14	0.13	0.16
Velocity P06 (m/s)	MAE	0.1	0.11	0.17
	MBE	0.07	0.09	0.11
	RMSE	0.13	0.13	0.21
Velocity P07 (m/s)	MAE	0.24	0.32	0.17
	MBE	0.04	0.06	0.01
	RMSE	0.29	0.38	0.22
Velocity P08 (m/s)	MAE	0.1	0.22	0.09
	MBE	-0.03	0.19	-0.01
	RMSE	0.13	0.24	0.12
Loodrecht P06 (m/s)	MAE	0.13	0.14	0.15
	MBE	-0.08	0.01	-0.13
	RMSE	0.17	0.16	0.19
Loodrecht P07 (m/s)	MAE	0.22	0.39	0.16
	MBE	-0.21	-0.39	-0.05
	RMSE	0.28	0.46	0.22
Loodrecht P08 (m/s)	MAE	0.12	0.1	0.11
	MBE	-0.07	-0.09	0.06
	RMSE	0.15	0.14	0.14
Parallel P06 (m/s)	MAE	0.1	0.09	0.18
	MBE	-0.02	-0.02	0.17
	RMSE	0.11	0.11	0.22
Parallel P07 (m/s)	MAE	0.13	0.13	0.11
	MBE	0.07	-0.1	0.03
	RMSE	0.16	0.17	0.14
Parallel P08 (m/s)	MAE	0.11	0.26	0.09
	MBE	-0.05	0.26	-0.03
	RMSE	0.14	0.29	0.12

Table 1: Errors MAE, MBE and RMSE of scenario 1, 5 and 6 compared to the natural data

8. Discussion

As stated in section 2.4 the goal of the research was to produce a reliable base model to test future infrastructural design scenarios in. When applying infrastructural design scenarios to reduce the velocity at the harbour entrance, it is good to keep in mind that the velocity in the physical model builds up too fast. At one hour and 40 minutes before high water a current velocity of 1.9 m/s was measured between points P08 and P07. The current velocity at this point should be 1.3 m/s according to the natural data. Because of the increased velocity, the stagnation point of the mixing layer will be positioned further harbour inward in the physical model compared to its location in reality. This could result in a different eddy pattern. This effect can be reduced by the applied roughness but when infrastructural design scenarios are tested which includes a change in the harbour entrance location, this could become an issue again and must be considered when evaluating the results.

A good calibration is needed to ensure a reduction in error between the physical model and the natural data by adjusting different physical model parameters. Only when the physical model is correctly calibrated inside and outside the harbour it can be used to extract reliable data for further research. With the small errors at the key points P07 and P06 and the applied roughness causing a desired eddy pattern, it can be said that the calibration phase of the physical model has been successfully completed. Two aspects of the model are still not completely in line with the natural data, these are the velocity in front of the harbour which builds up too fast and the small eddy at the harbour entrance which exists too long. For both problems the best situation has been chosen in the limited time of the calibration process.

It must be noted that the current physical model of Zeebrugge is only calibrated. To make a truly reliable model it needs to be validated with another set of data. Currently there is no other set of data available. This makes validation in this point in time impossible.

The accuracy of the measured EMS values is currently done with the RMSE method. This is the most common method of calculating errors. However some literature studies like Willmott & Matsuura (2005) state that the MAE is a more accurate way to calculate the uncertainty. Of the PTV-analysis no uncertainty analysis is done because there was only one test analysed twice with the PTV-analysis and this is not enough to base an uncertainty analysis on. The uncertainty analysis of the PTV-analysis should have been done to get a completer overview of the uncertainty of the measuring equipment.

In the figures 29 and 30 it is seen that during the 2 hours before high water and the 2 hours after high water the physical model data matches the natural data well. These are the important hours in reality because within these hours the problems occur regarding the high velocities. In the hours of low water some differences occur in the measured velocity and a larger error is seen. The performance criteria RMSE and MAE are measured over the whole tidal sequence. Therefore a higher average uncertainty is measured of the model then necessary. An uncertainty analysis could have been done with only the data from the 2 hours before high water and the 2 hours after high water to get an idea of the uncertainty of the measurements during the key period of the model.

In figure 29 it is seen that the velocity measured by the EMS instruments has a slight but consistent underestimation of the velocities compared to the natural data. The PTV-analysis shows a slight but consistent overestimation of the velocity in the physical model compared to the natural data. The cause of these differences is probably the assumption that the velocity measured on -2 TAW is the same as the velocity measured on the surface. There might be a slight error in this assumption and a scaling factor could have been calculated with the results from the velocity profile. This way the results from the two measuring systems would be more in alignment.

9. Conclusions and recommendations
Within this chapter the conclusions of my research will be presented and the recommendations for further research will be given.

9.1 Conclusions
In this chapter conclusions will be drawn from the research results and answers will be given to the research questions of section 2.5.

- *What are the possibilities and limitations of a physical scale model of Zeebrugge?*

The possibilities of a physical scale model are: It is capable of easy data collection under controlled laboratory conditions, complex bathymetry is easily implemented and complex conservation laws are implemented without simplifications. The limitations are mainly the distortion of the model and the incapability of simulating large scale hydraulic processes like the Coriolis force and several kind of waves.

- *What are the different measurement instrument used to calculate the current velocity and direction and what are the uncertainties in them?*

The different measurement instruments used to calculate the current velocity and the current direction are the PTV-analysis and the EMS instruments. The uncertainty of the PTV-analysis was not found, the average uncertainty of the EMS instruments is 0.037 m/s and this equals 4.2% of the measured value.

- *What are the tidal influences on the hydraulic system at the harbour entrance?*

The tide causes the inflow and the outflow of the harbour. During the inflow an eddy occurs at the harbour entrance, the strength and size of this eddy is dependent on tidal flow rate and the separation point of the mixing layer at the harbour entrance.

- *What is the cause of the differences between the physical model and the reality and is it possible to reduce these differences?*

In order to match the physical model data to the natural data inside the harbour, six different roughness scenarios have been tested. These scenarios where used in the calibration process of the harbour. The best scenario is the one that has the most correspondence with the natural data regarding current velocity, inflow direction, eddy pattern and eddy duration. From the six scenarios only two (5 and 6) had the desired inflow direction which resulted in the desired eddy pattern of two eddies, a small one rotating clockwise in the harbour entrance and a large one rotating counter-clockwise inside the harbour. Regarding the eddy duration it was seen that scenario 5 and 6 both had a primary eddy that existed too long.

Regarding the current velocity both had the right inflow speed. However scenario 6 had an increased velocity in front of the harbour entrance of 0.3 m/s. This is an unwanted side effect of the roughness on the west head. The points in front of the harbour entrance (mainly point P06 and P07) were key points during the calibration of the sea and every alternation in the model during this process was aimed on the improvement of these points in the model. Therefore the roughness alternations of this research could not have negative influence on the harbour entrance in the model.

With the EMS data the points P06, P07 and P08 in front of the harbour entrance have been examined. This was done to make sure that the roughness scenarios of scenario 5 and 6 would not have a negative influence on the direction and velocity of the tidal current. From the current EMS data it is not possible to state any clear conclusions because of the incorrect data of scenario 5. Scenario 6 improved the current direction of point P07 significantly. However, it made point P06 significantly worse.

Because of the indifferent results from the EMS data and the result from the PTV-analysis that showed the right eddy pattern of scenario 6 it can be said that scenario 6 a better scenario then the original scenario 1. Because of the missing data of the EMS analysis for scenario 5 no clear conclusion can be stated about this point. However, according to the PTV-analysis scenario 5 does not have the unwanted increase in velocity between the points P07 and P08. Therefore, it is expected that scenario 5 will be the best scenario. This expectation needs to be verified by gathering correct EMS data from scenario 5.

9.2 Recommendations

Many tests where done to see the effects of the roughness in the model. The eddy pattern was very sensitive to the placement of the roughness. For example, if the form of the roughness on the east head was changed only a little, it would result in a big difference in eddy pattern. Therefore it is not recommended to change any roughness on the east head. The same was true for the location of the roughness on the west head. The location of roughness in the form of a west head was the best in the location described by scenario 2. Therefore this scenario was tested and any other form of the west head should be avoided.

The eddy pattern in with the west head instead of the west dam is slightly better. The first eddy is gone 10 minutes earlier and is smaller than with the west dam. This is more in alignment with the natural data. It is possible to gain this same pattern with the west dam by applying more roughness on the west dam sea inward. This way the streamlines will be pushed more seaward and the separation and stagnation points of the mixing layers will be higher, which will result in a better eddy pattern. However there is already a lot of roughness on the west dam and when more roughness is applied it will probably have a greater negative effect on points P06 and P07. Therefore it is not recommended to increase the roughness of the west dam further to make a slight improvement in the eddy pattern at the cost of the velocity pattern in front of the harbour.

The physical model of Zeebrugge should be validated. The current physical model of Zeebrugge is only calibrated. This validation could be done by acquiring more data from the prototype or by combining the data from the numerical model of Zeebrugge with the physical model. Numerical models do not have the problem of distortion and have the possibility to implement the hydraulic processes on a larger scale like the Coriolis force. This way the numerical model and the physical model can be combined to find an ultimate solution.

The EMS instruments have a slight underestimation compared to the natural data, and the PTV-analysis has a slight overestimation of the natural data. Both measuring techniques should give the same output value. Therefore a correction factor should be calculated which eliminates the differences between the velocity on the surface and the velocities measured at -2 TAW.

11. References

Banner. (2013). *U-GAGE Q45UR Series—Analog*. Retrieved 06 18, 2013, from Banner Engineering: http://www.bannerengineering.com/en-US/products/sub/235

Brown, E., Colling, A., Park, D., Phillips, J., Rothery, D., & Wright, J. (1999). *Waves, Tides and Shallow-water Processes.* Burlington: Butterworth-Heinemann.

Christiansens, H. (1987). *New insights on mud formation and sedimentation processes in tidal harbours, Proc of Coastal and Port Eng in Developing Countries, Vol 2, Group D, pp1332-1340.*

Chubarenko, B. V., Wang, Y., Chubarenko, I. P., & Hutter, K. (2001). Wind-driven current simulations around the Island Mainau (Lake Constance). *Ecological Modelling*, 55-73.

de Kramer, J. (2002). *Waterbeweging in de Westerschelde, een literatuurstudie.* Middelburg: Rijkswaterstaat - Rijksinstituut voor Kest en Zee (RIKZ).

Deleforie, G., & Vantorre, M. E. (2005). Modelling navigation in muddy areas through captive model tests. *Journal of Marine Science and Technology*, 188-202.

Ducrotoy, J.-P., Elliott, M., & De Jonge, V. N. (2000). The North Sea. *Marine Pollution Bulletin Vol. 41*, 5-23.

Eurosense & Aqua Vision. (2011). *Verwerkingsrapport Stroming Meetcampanges Zeebrugge.* Antwerpen: Maritime Dienstverlening en Kust.

Fettweis, M., & Van den Eynde, D. (2003). The mud deposits and the high turbidity in the Belgian-Dutch coastal zone, southern bight of the North Sea. *Continental Shelf Research 23*, 669-691.

Fox, R. W., Pritchard, P. J., & McDonald, A. T. (2010). *Introduction to Fluid Mechanics Edition 7.* John Wiley & Sons, INC.

Geysen, B. (2010). *Toetsen van de frequentie van voorkomen van windsnelheid en golfhoogte tijdens stormperiodes.* Vlaamse Overheid.

Google Maps. (2013). *Google Maps*. Retrieved 2013, from Google: http://www.google.nl/maps

Grifoll, M., Fontán, A., Ferrer, L., Mader, J., González, M., & Espino, M. (2009). #D hydrodynamic charaterisation of a meso-tidal harbour: The case of Bilbao (northern Spain). *Coastal Engineering 56*, 907-918.

Heyvaert, G. (2012). *Memo, Velocity Profile.* Antwerpen: Waterbouwkundig Laboratorium.

Hudson, R., Herrmann, F., Sager, R., Whalin, R., Keulegan, G., Chatham, C., et al. (1979). *Coastal Hydrolic models.* Vicksburg: U.S. Army Engineer Waterways Experiment Station.

Hughes, S. A. (1993). *Physical models and laboratory techniques in coastal engineering.* Singapore: JBW Printers & Binders.

Hughes, S. A., & Pizzo, G.-M. (2003). *Flow Table Study of Cook Inlet, Alaska* . Vicksburg: U.S. Army Enigneer Research and Development Center.

Hughes, S. A., Cohen, J. A., & Acuff, H. F. (2010). *Physical Model of Knik Arm and the Port of Anchorage, Alaska.* Vicksburg: Coastal and Hydraulics Laboratory.

Ides, S. (2009). *Optimalisatie maritime toegangkelijkheid haven Zeebrugge.* Antwerpen: Waterbouwkundig Laboratorium.

Ides, S., De Mulder, T., & Mostaert, F. (2009). *Optimalisatie toegankelijkheid haven Zeebrugge - Onderzoeksplan, versie 13/02/2009.* Antwerpen : Waterbouwkundig Laboratorium.

IVA Maritieme Dienstverlening en Kust. (2011). *Stroomatlas, Haven van Zeebrugge.* Antwerpen: Ministerie van Mobiliteit en Openbare Werken.

Krohne. (2013). *Krohne Product Downloads - Optisonic 6x00.* Retrieved Juni 24, 2013, from Krohne.com: http://krohne.com/en/dlc/product-related-downloads/flowmeters/ultrasonic-flowmeters/optisonic-6x00/

Langendoen, E. (1992). *Flow patterns and transport of dissolved matter in tidal harbours.* Delft: TU Delft.

Nihoul, J. C., & Ronday, F. C. (1975). The influence of "Tidal stress" on the residual circulation, Application to the Southern Bight of the North Sea. *Tellus XXVII*, 484-490.

Port of Zeebrugge. (2013). *Port of Zeebrugge*. Retrieved May 14, 2013, from www.portofzeebrugge.be

Reeve, D., Chadwick, A., & Fleming, C. (2004). *Coastal Engineering.* London and New York: Spon Press.

Rockwell, D., Magness, C., Towfighi, J., Akin, O., & Corcoran, T. (1993). High-image-density particle image velocimetry using laser-scanning techniques. *Expts Fluids*, 181-192.

Shaw, E. M., Beven, K. J., Chappell, N. A., & Lamb, R. (2011). *Hydrology in Practice.* London and New York: Spon Press.

Sheridan, J., Lin, J., & Rockwell, D. (1997). Flow past a cylinder close to a free surface. *Journal of Fluid Mechanics 330*, 1-30.

Steehouder, M. (2006). *Leren communiceren.* Groningen: Noordhoff Uitgevers B.V.

Thompson Clarke. (2007). *Assistance with the implementation of an Under Keel Clearance System for Torres Strait.* Sydney: Australian Government, Australian Maritime Safety Authority.

Troch, P., De Rouck, J., & Van Damme, L. (1998). Instrumentation and prototype measurements at the Zeebrugge rubble mound breakwater. *Coastal Engineering 35*, 141-166.

University of Gent & Department of Mobility and Public Works. (2013). *Knowledge Centre Manouvring in Shallow and Confined Water*. Retrieved juni 3, 2013, from Shallow Water: http://www.shallowwater.be/

Vlaamse Hydrografie. (2011). *Overzicht van de tijwaarnemingen langs te Belgische kust.* Oostende: Agentschap Maritieme dienstverlening en kust.

Vlaamse Overheid. (2013). *Meetnet Vlaamse Banken*. Retrieved Mei 24, 2013, from www.meetnetvlaamsebanken.be: http://www.meetnetvlaamsebanken.be/Default.aspx?Page=Map&L=en

Warnock, J. (1950). Hydraulic similitude. *Engineering hydraulics*, 136-176.

Waterbouwkundig Laboratorium. (2011b). *Langdurige monitoring van zout/zoet-verdeling in de haven van Zeebrugge en monitoring van zoutconcentratie, slibconcentratie en hooggeconcentreerde slibsuspensies in de Belgische kustzone.* Antwerpen: Vlaamse Overheid, Departement Mobiliteit en Openbare werken.

Waterbouwkundig Laboratorium. (2013). *Organisatie van het Waterbouwkundig Laboratorium*. Retrieved Mei 14, 2013, from Waterbouwkundig Laboratorium: http://www.watlab.be/nl/organisatie

Waterbouwkunidg Laboratorium. (2011). *Jaarverslag 2011.* Antwerpen: Waterbouwkundig Laboratorium.

Willems, M., Van Dingen, B., Delgado, R., Verwaest, T., & Mostaert, F. (2011). *Nautische Toegankelijkheid haven Zeebrugge.* Antwerpen: Waterbouwkundig Laboratorium.

Willmott, C., & Matsuura, K. (2005). Advantages of the mean absolute error (MAE) over the root mean square error (RMSE) in assessing average model performance. *Climate research*, 79-82.

Appendix A: Natural data stroomatlas

In this appendix the stroomatlas is shown (IVA Maritieme Dienstverlening en Kust, 2011), this are the velocity fields made from the natural data between the 2 hours before and the 2 hours and 20 minutes after high water during an average springtide. At 2 hours before high water the inflow starts and the activity in the harbour stops at 2 hours and 20 minutes after high water.

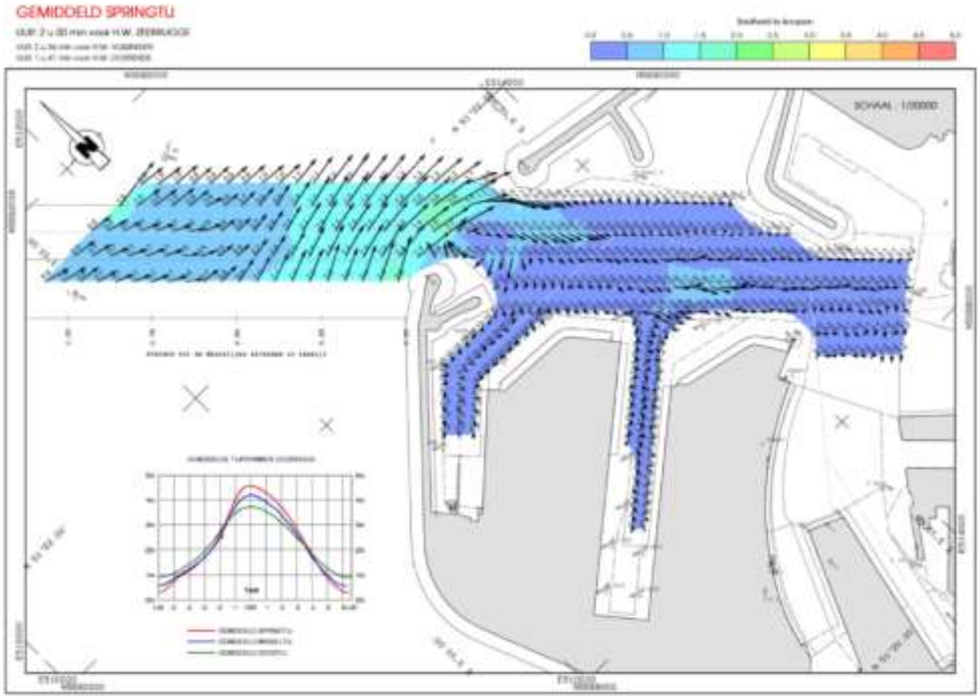

Figure 1: Velocity field of the harbour of Zeebrugge at 2 hours before high water (IVA Maritieme Dienstverlening en Kust, 2011)

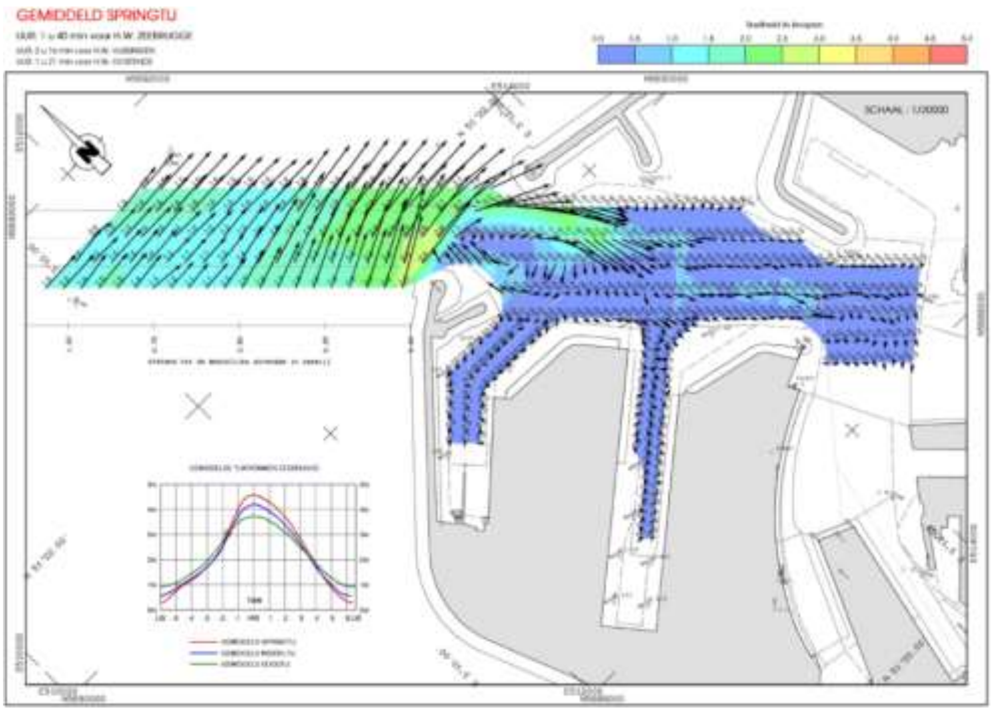

Figure 2: Velocity field of the harbour of Zeebrugge at 1 hour and 40 minutes before high water (IVA Maritieme Dienstverlening en Kust, 2011)

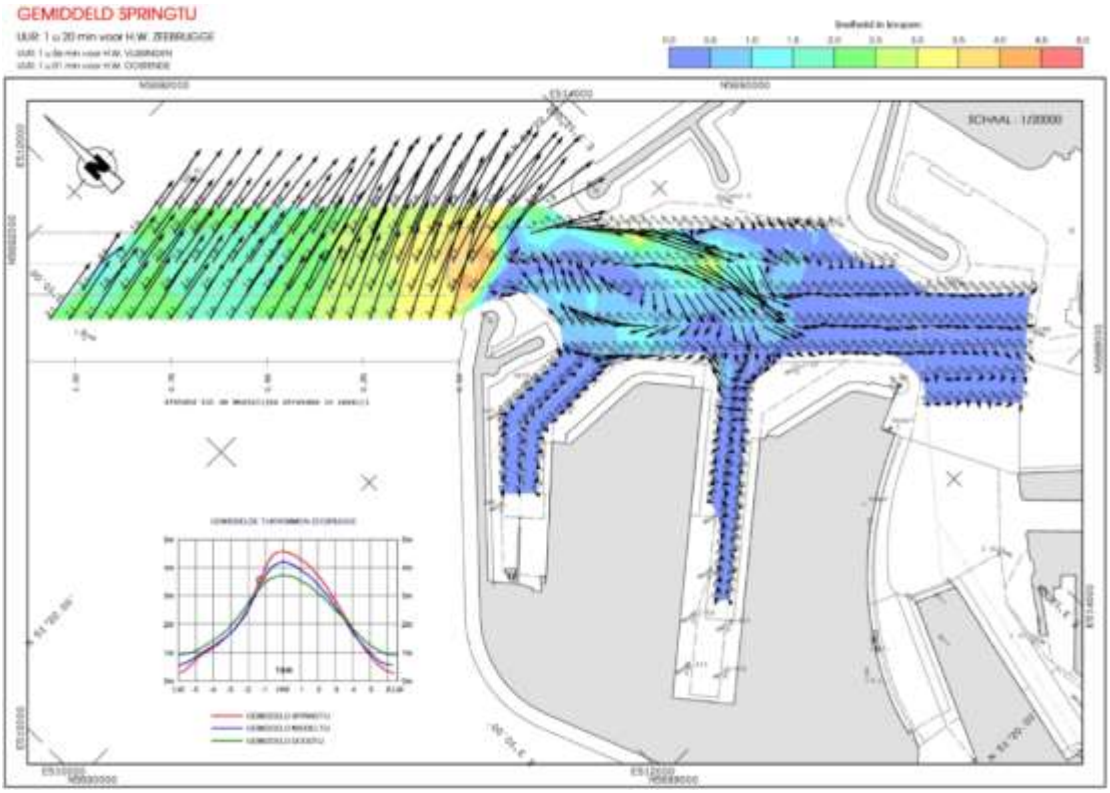

Figure 3: Velocity field of the harbour of Zeebrugge at 1 hour and 20 minutes before high water (IVA Maritieme Dienstverlening en Kust, 2011)

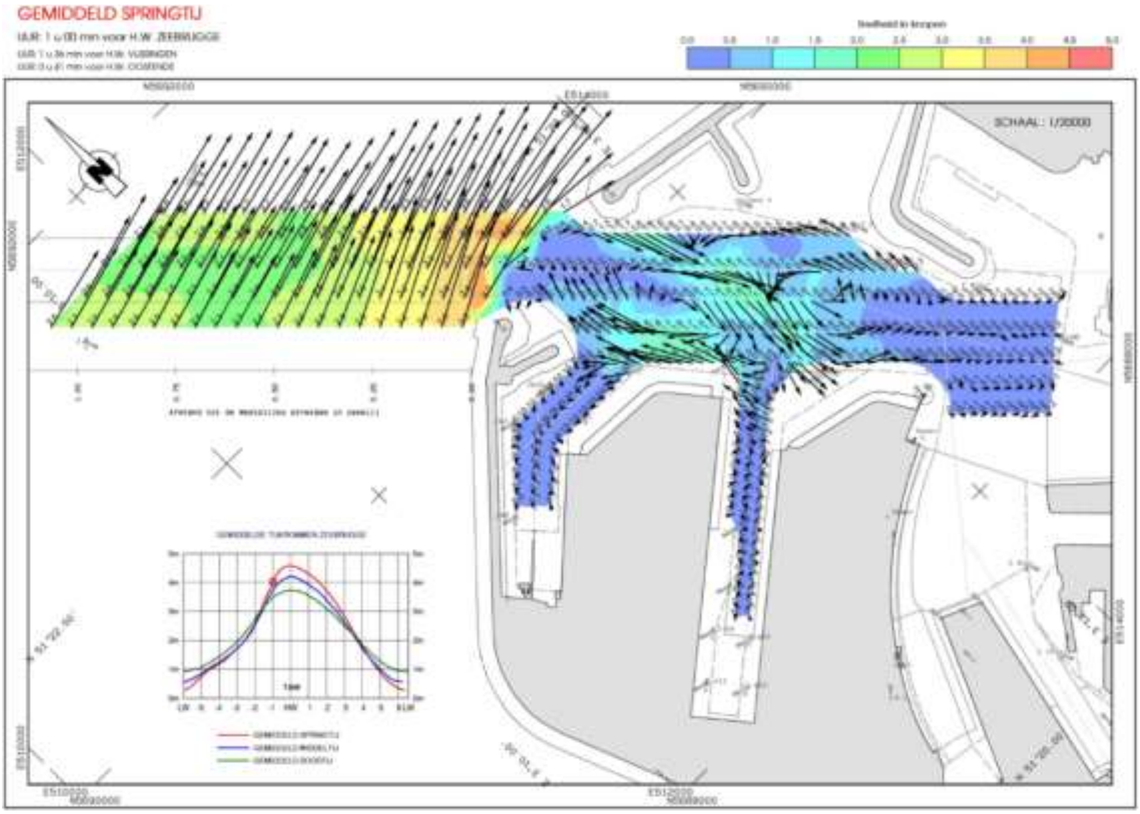

Figure 4: Velocity field of the harbour of Zeebrugge at 1 hour before high water (IVA Maritieme Dienstverlening en Kust, 2011)

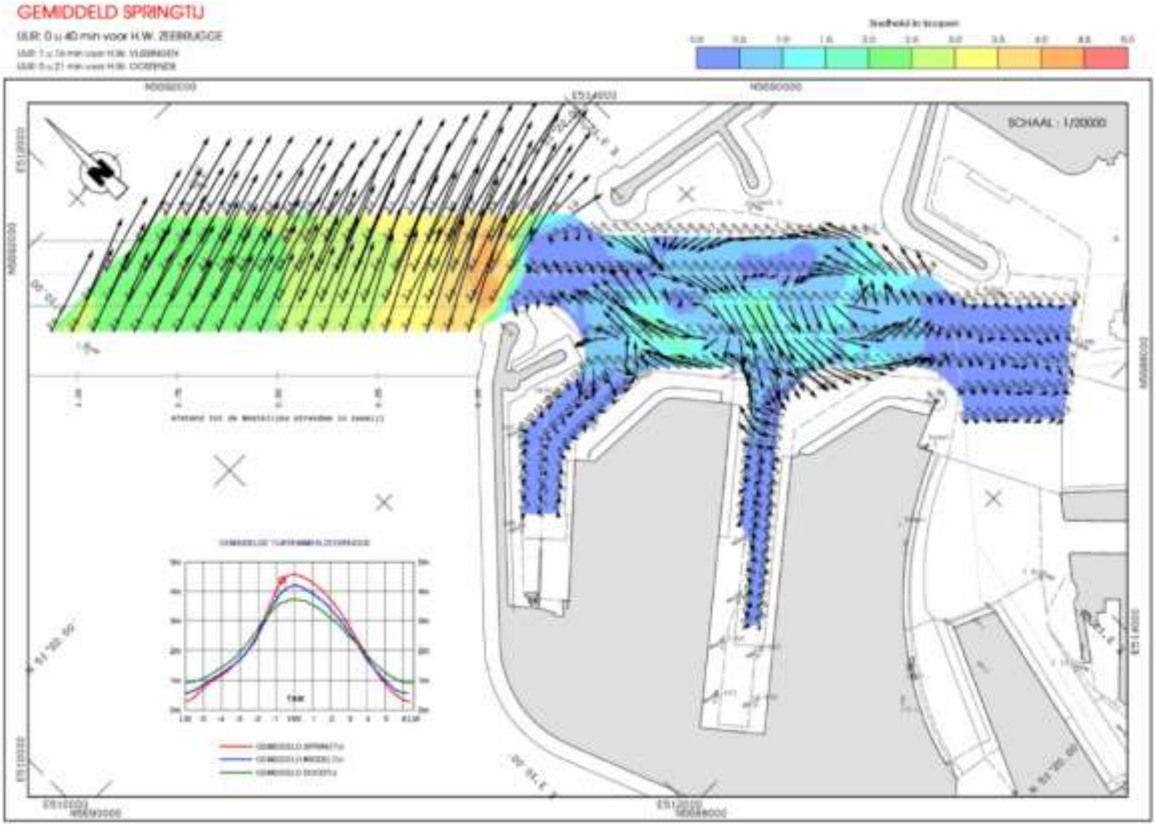

Figure 5: Velocity field of the harbour of Zeebrugge at 40 minutes before high water (IVA Maritieme Dienstverlening en Kust, 2011)

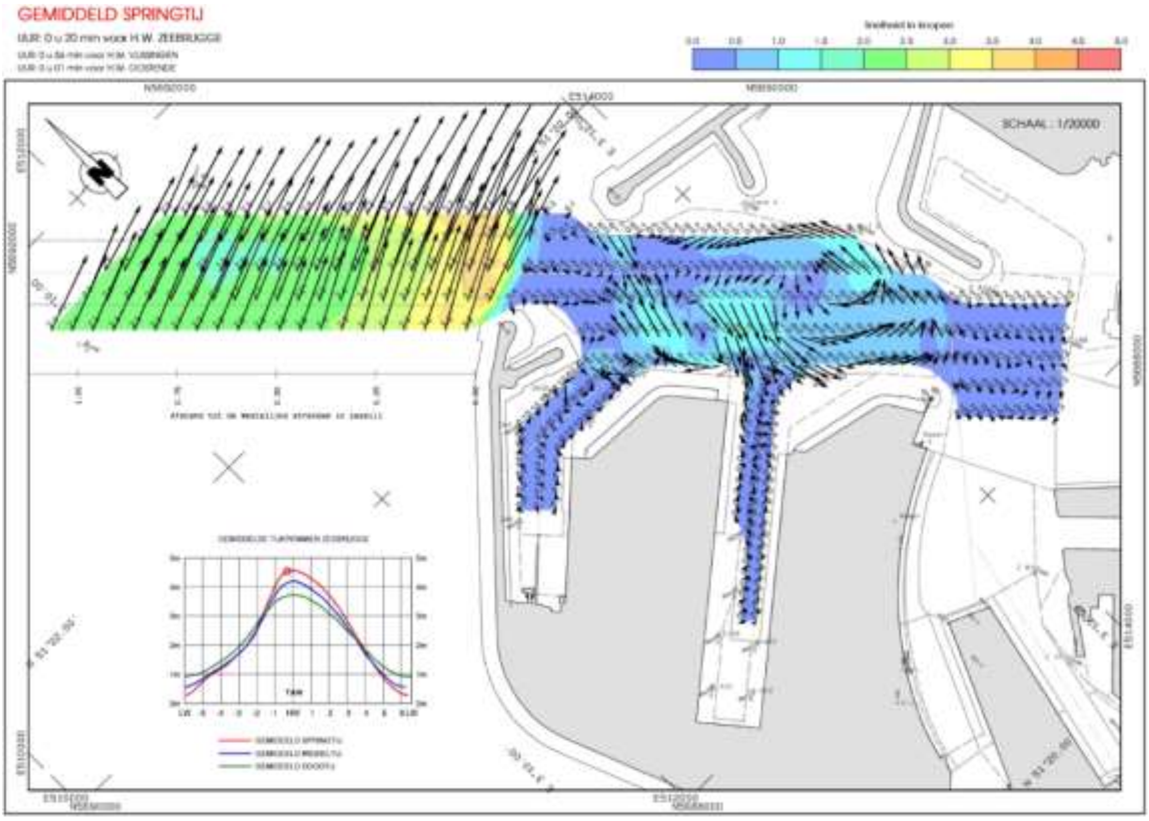

Figure 6: Velocity field of the harbour of Zeebrugge at 20 minutes before high water (IVA Maritieme Dienstverlening en Kust, 2011)

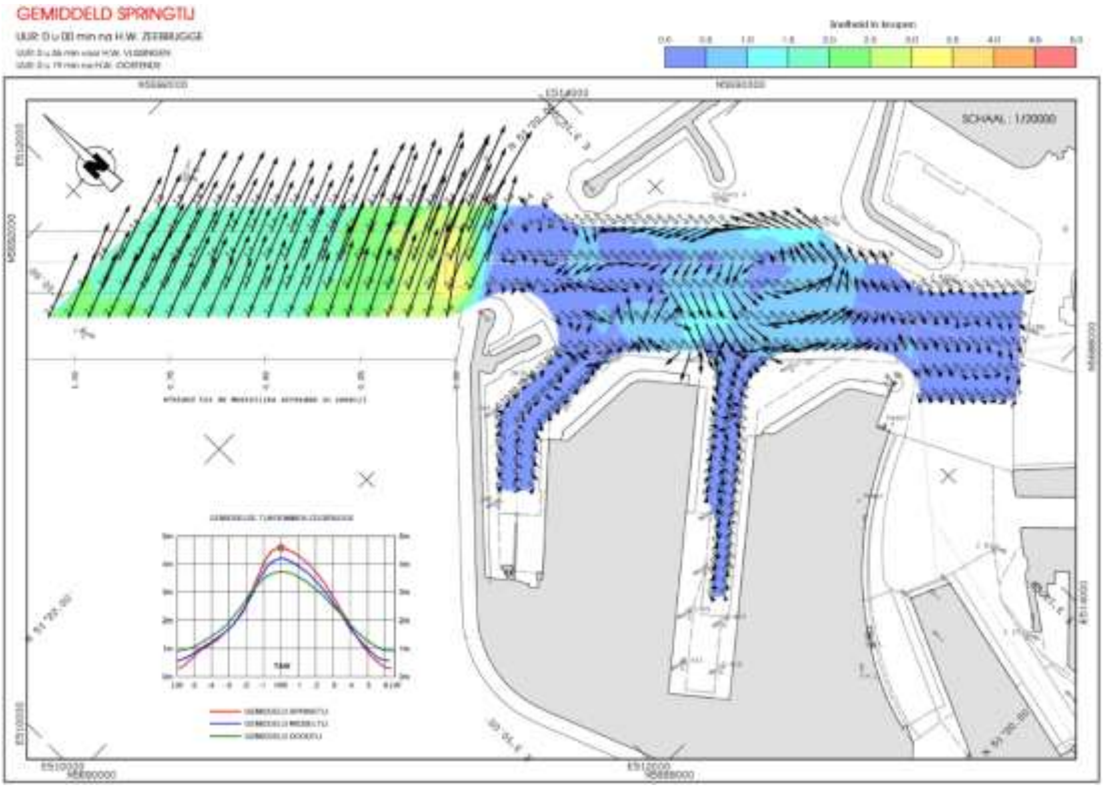

Figure 7: Velocity field of the harbour of Zeebrugge at high water (IVA Maritieme Dienstverlening en Kust, 2011)

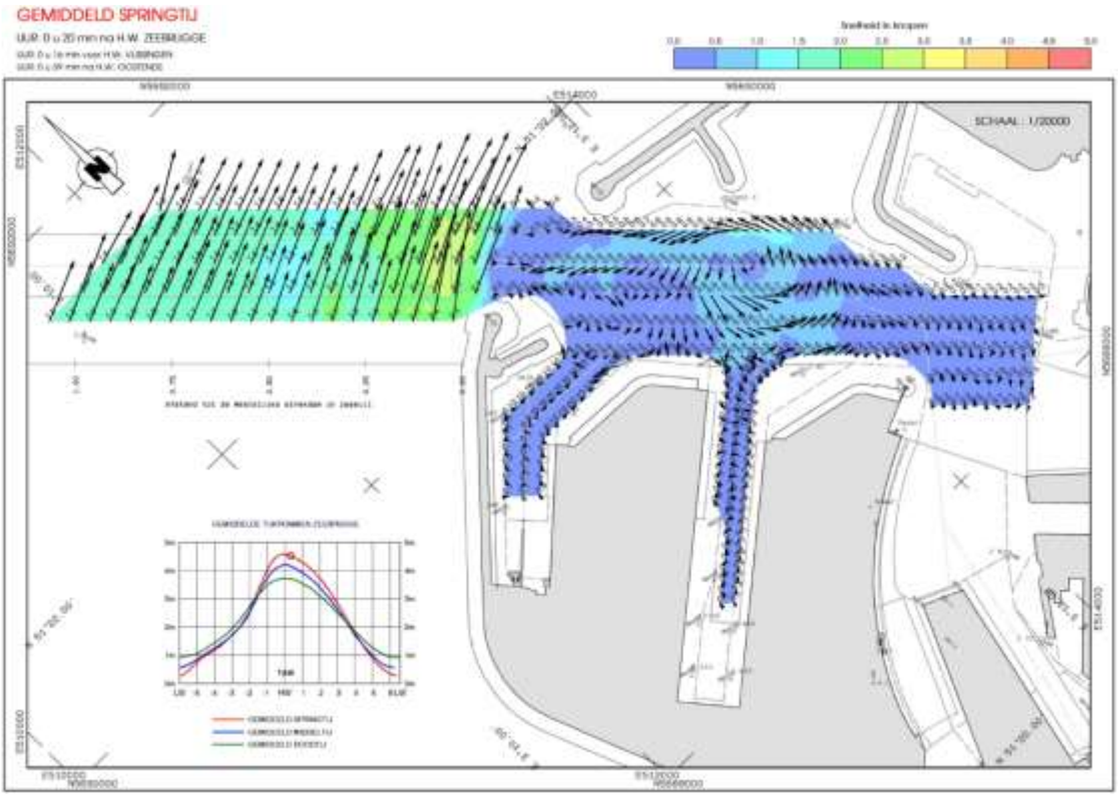

Figure 8: Velocity field of the harbour of Zeebrugge at 20 minutes after high water (IVA Maritieme Dienstverlening en Kust, 2011)

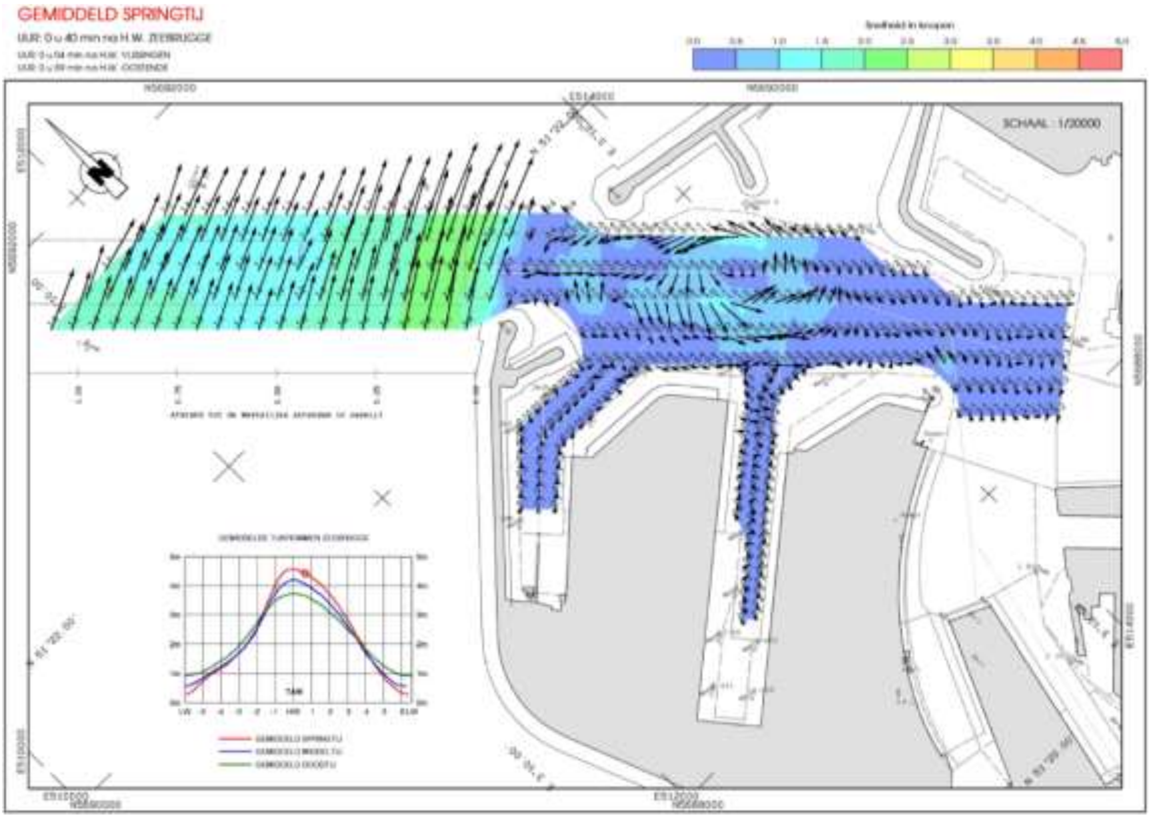

Figure 9: Velocity field of the harbour of Zeebrugge at 40 minutes after high water (IVA Maritieme Dienstverlening en Kust, 2011)

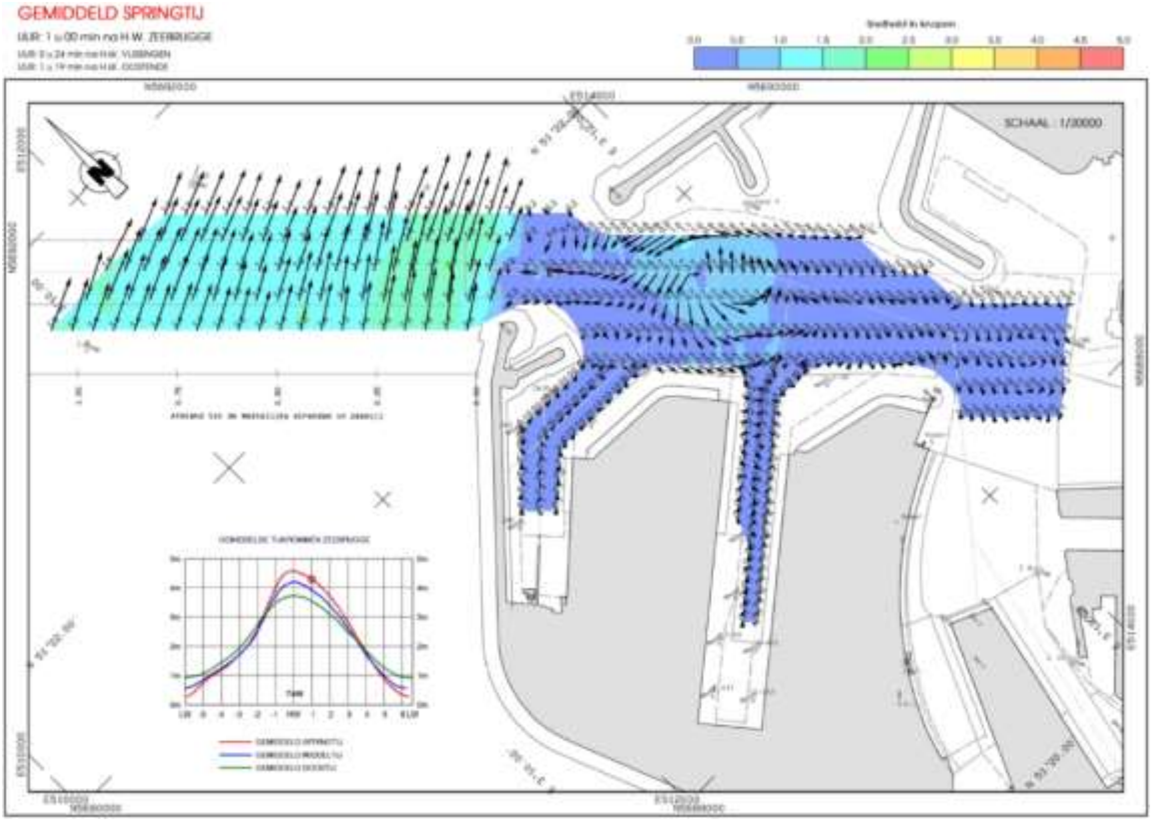

Figure 10: Velocity field of the harbour of Zeebrugge at 1 hour after high water (IVA Maritieme Dienstverlening en Kust, 2011)

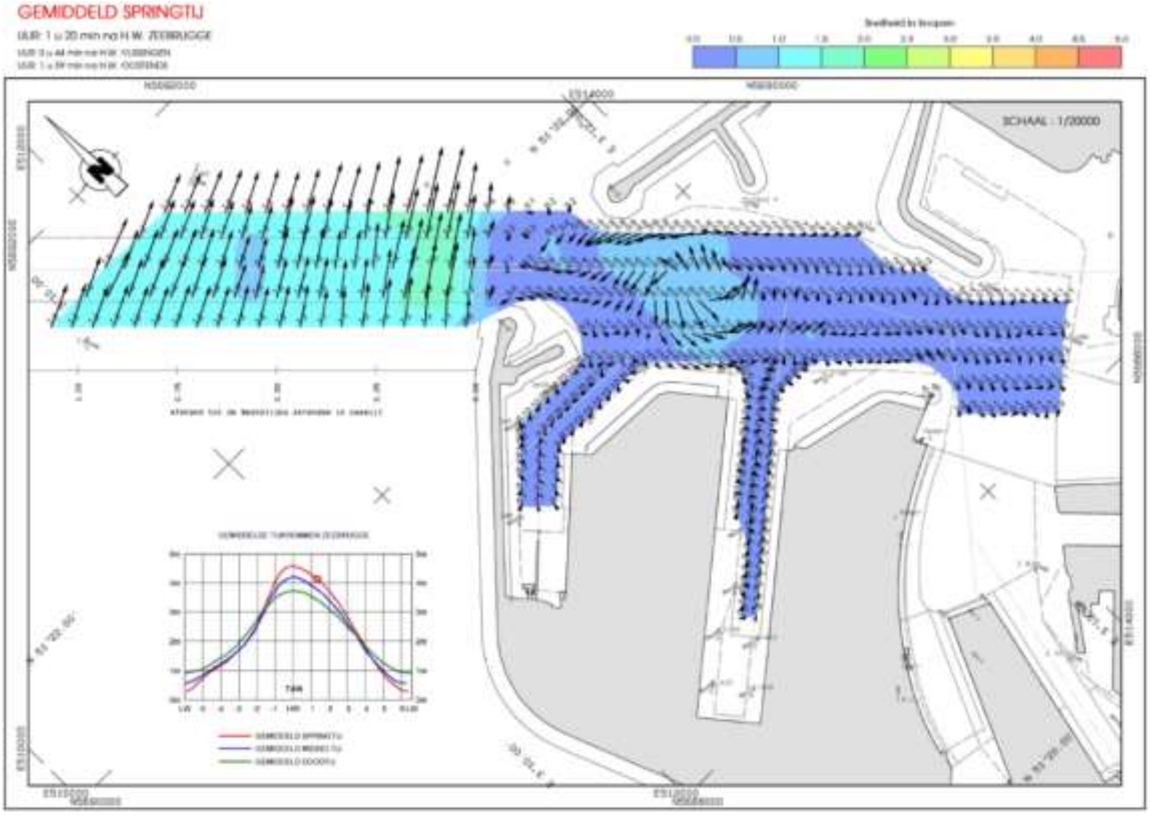

Figure 11: Velocity field of the harbour of Zeebrugge at 1 hour and 20 minutes after high water (IVA Maritieme Dienstverlening en Kust, 2011)

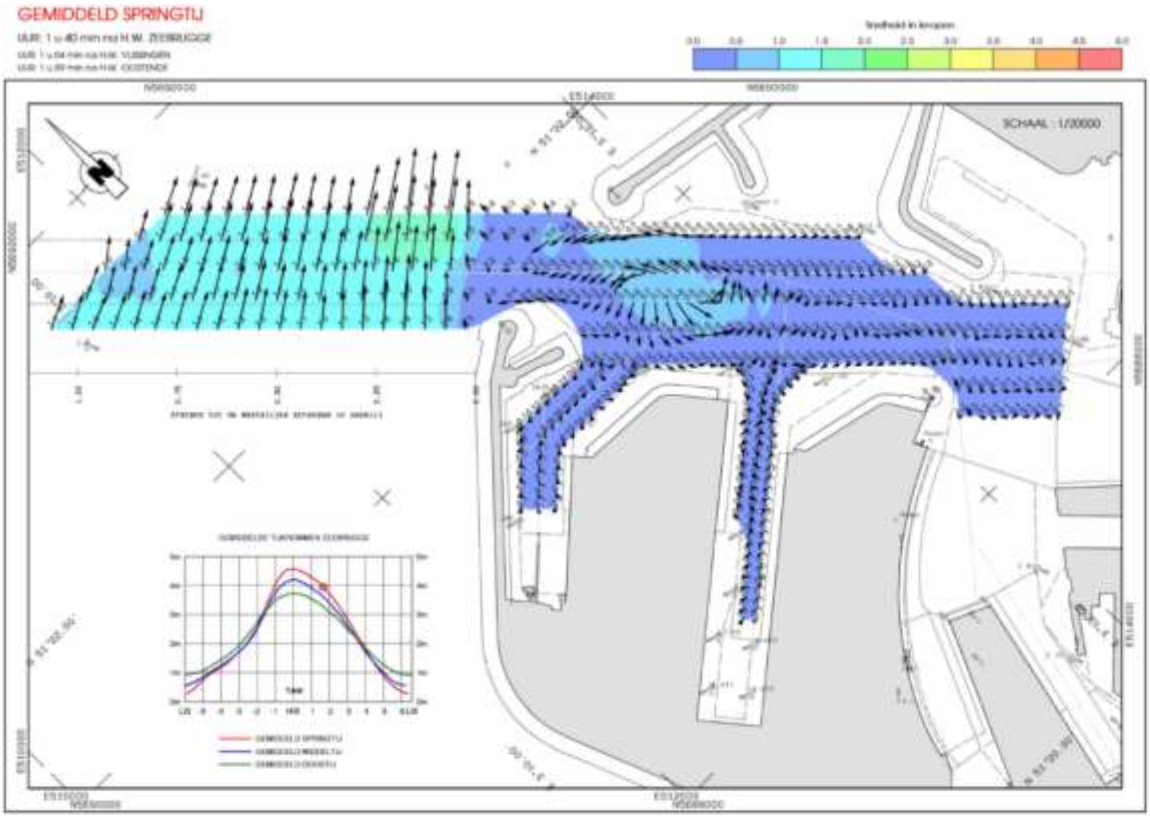

Figure 12: Velocity field of the harbour of Zeebrugge at 1 hour and 40 minutes after high water (IVA Maritieme Dienstverlening en Kust, 2011)

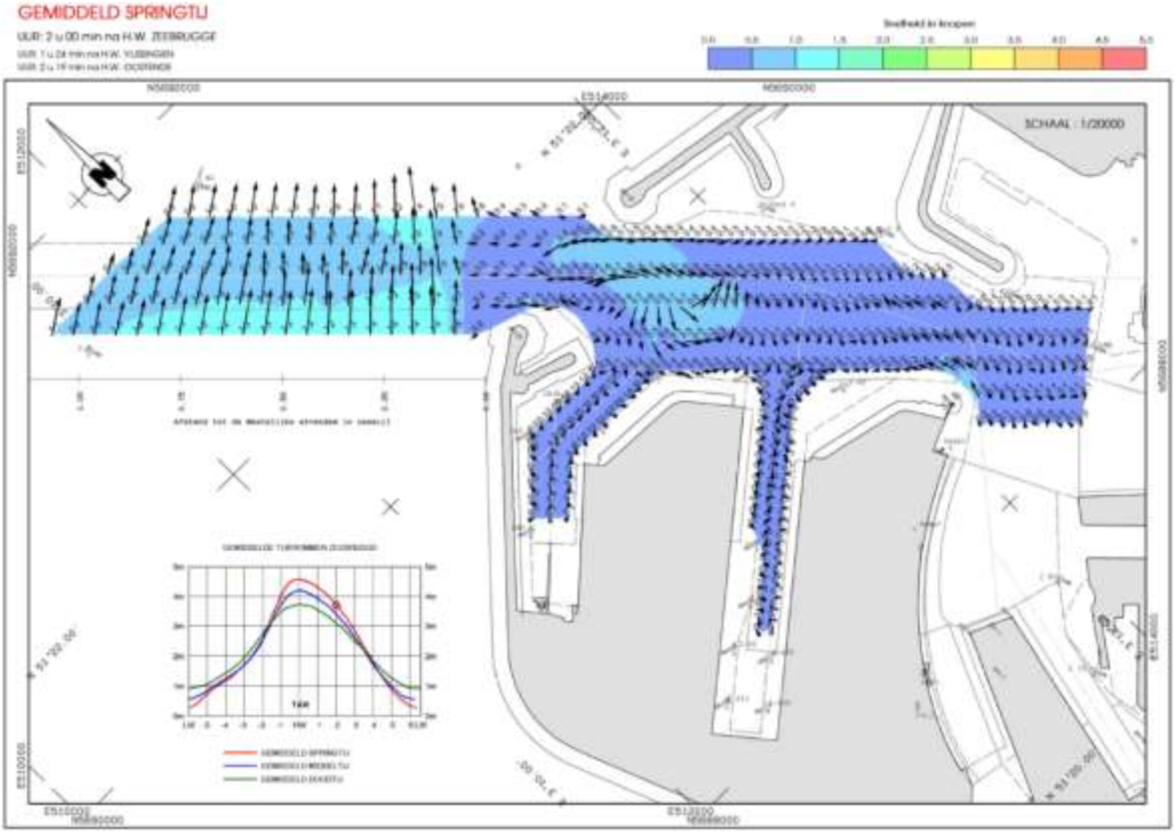

Figure 13: Velocity field of the harbour of Zeebrugge at 2 hours after high water (IVA Maritieme Dienstverlening en Kust, 2011)

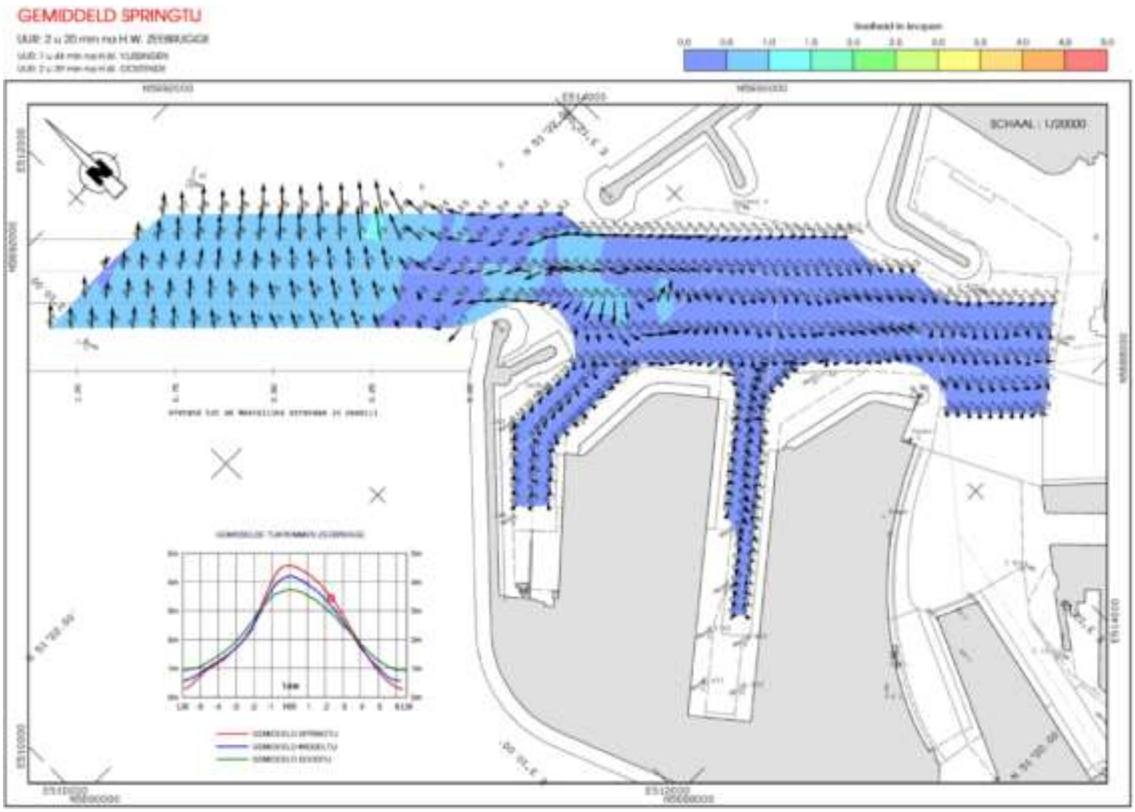

Figure 14: Velocity field of the harbour of Zeebrugge at 2 hours and 20 minutes after high water (IVA Maritieme Dienstverlening en Kust, 2011)

Appendix B: Location of the scenario roughness

In this appendix the exact location is shown of the applied roughness of the different scenarios.

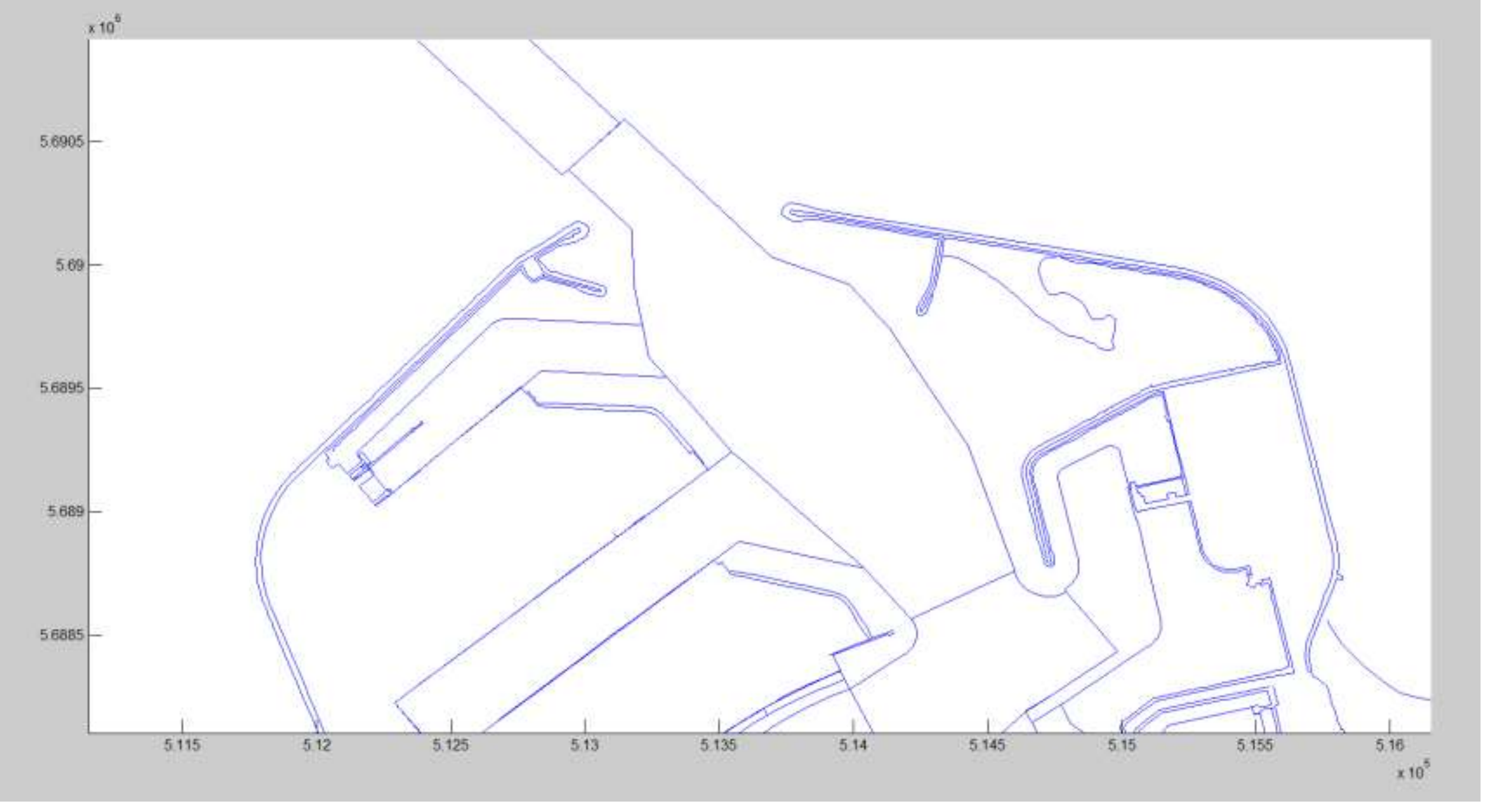

Scenario 1: No roughness

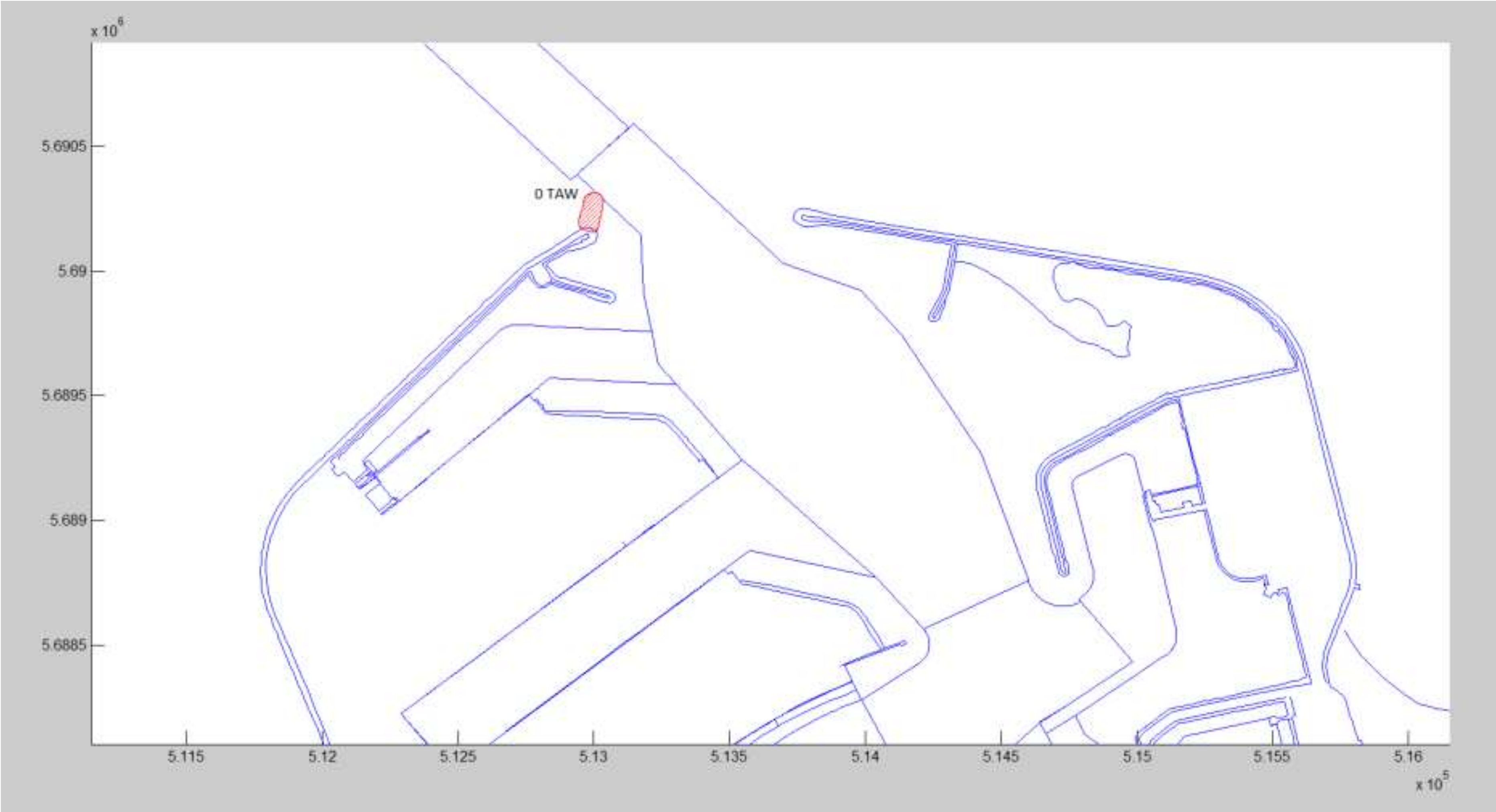

Scenario 2: Roughness on the west head, maximum height is 0 TAW

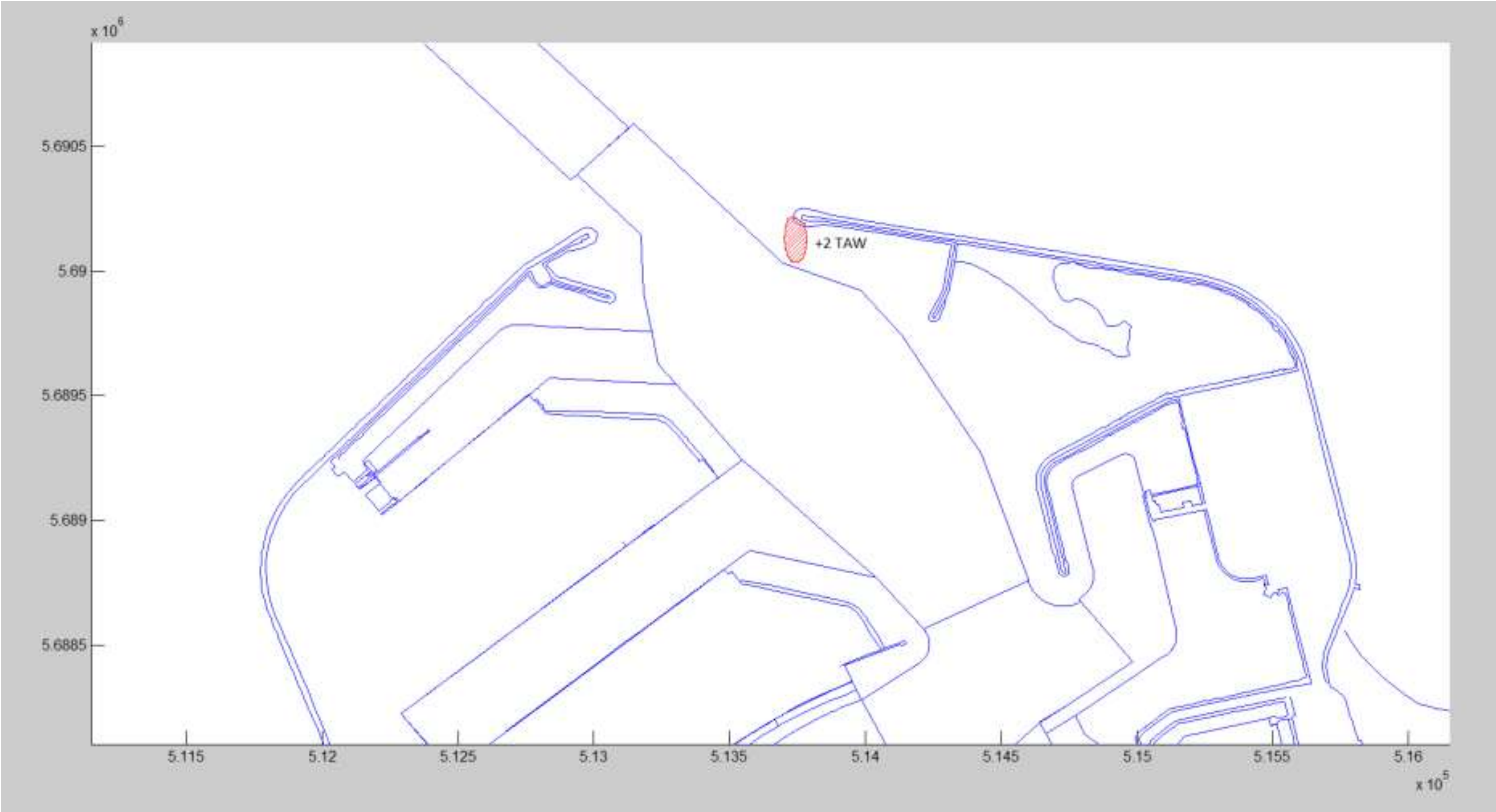

Scenario 3: Roughness on the east head, maximum height is +2 TAW

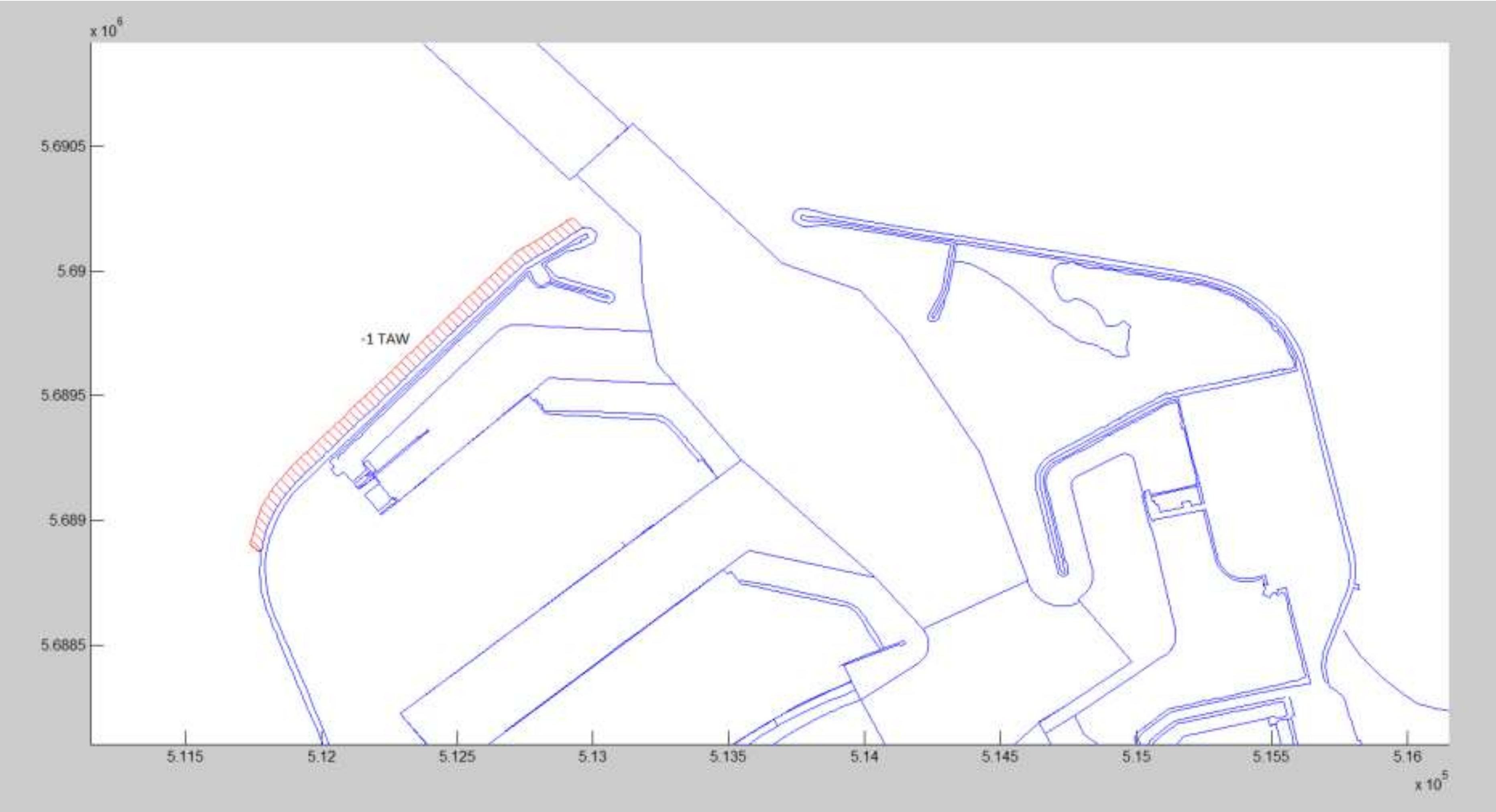

Scenario 4: Roughness on the west dam, height is -1 TAW

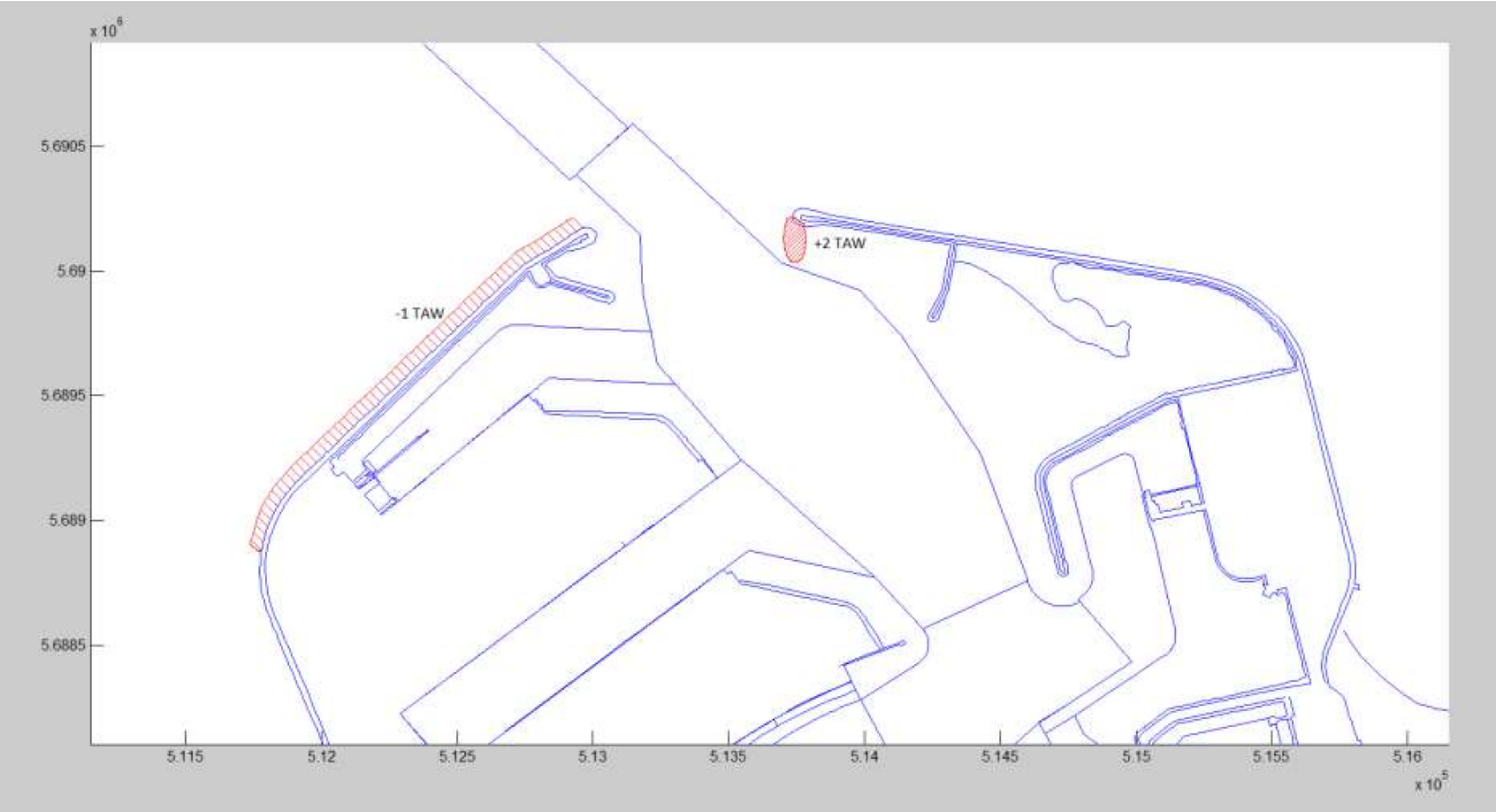

Scenario 5: Roughness on the west dam and on the east head, heights are -1 TAW en +2 TAW

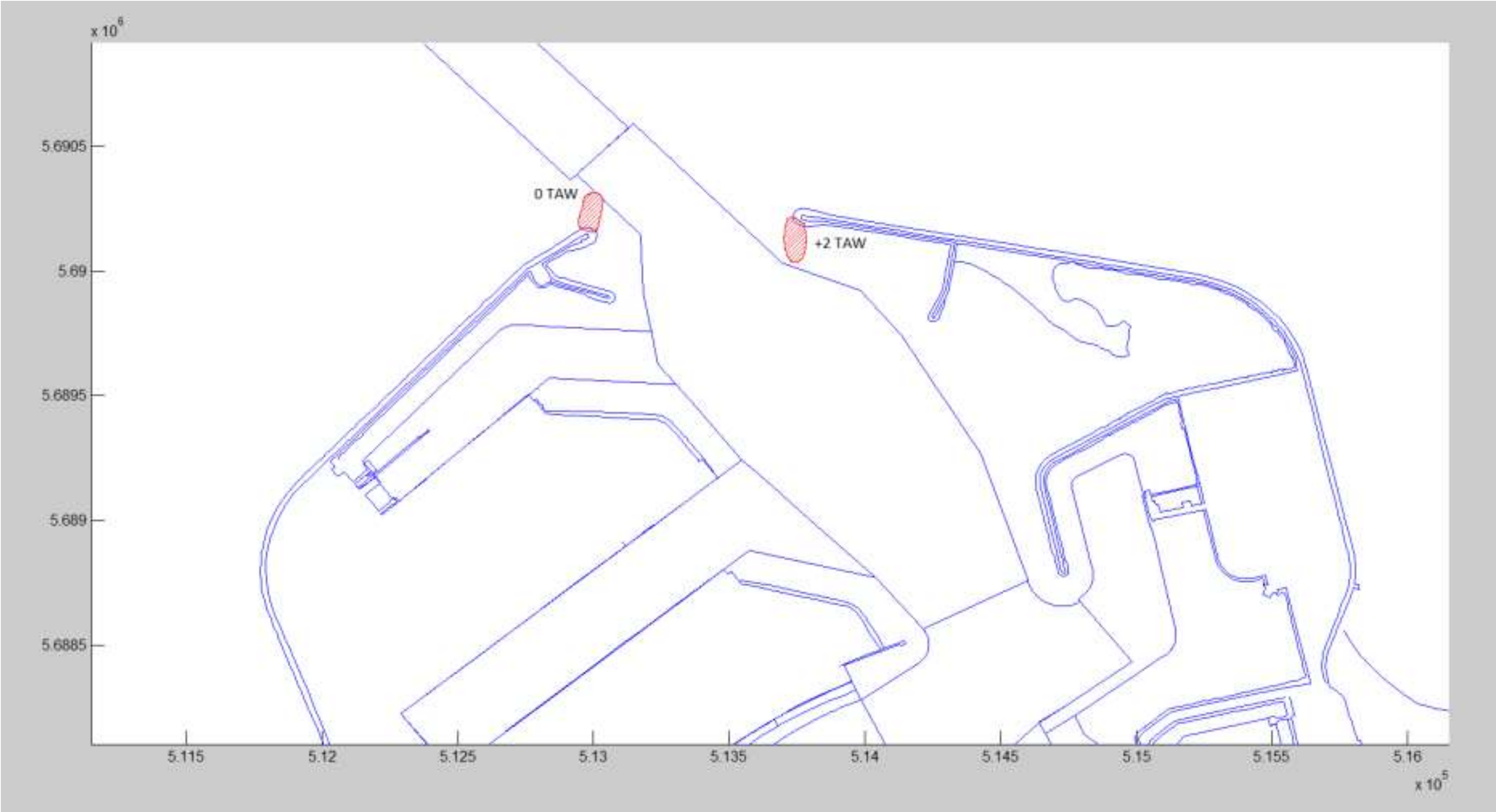

Scenario 6: Roughness on the east head and on the west head, heights are +2 TAW en 0 TAW

Appendix C: Vector fields of the different scenarios

In this appendix the velocity fields of the harbour entrance are shown at the same times as the natural data of appendix A.

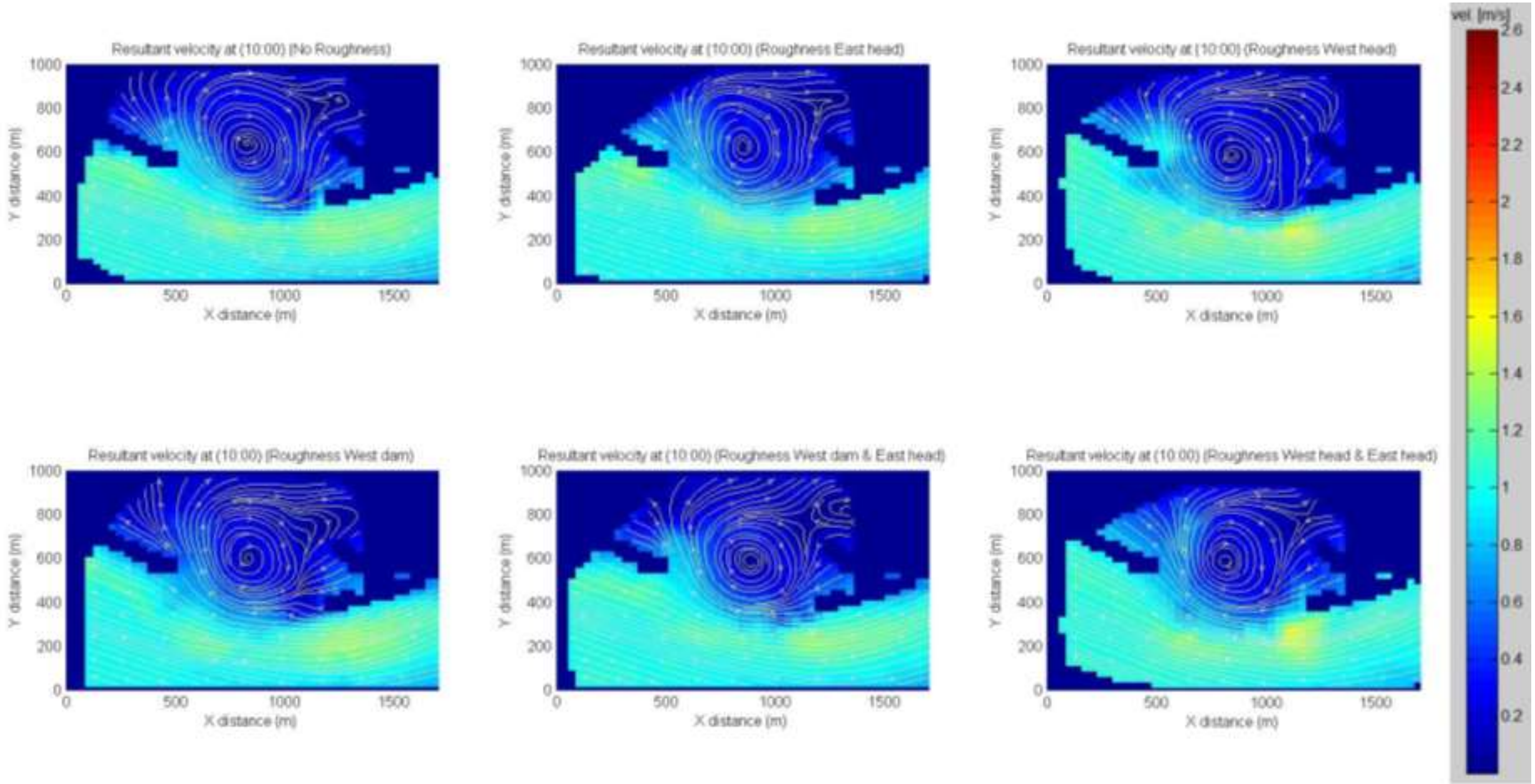

Figure 1: Velocity field of the physical model of Zeebrugge in with six different roughness scenarios at 2 hours before high water (from left to right scenario 1, 3, 2, 4, 5, 6)

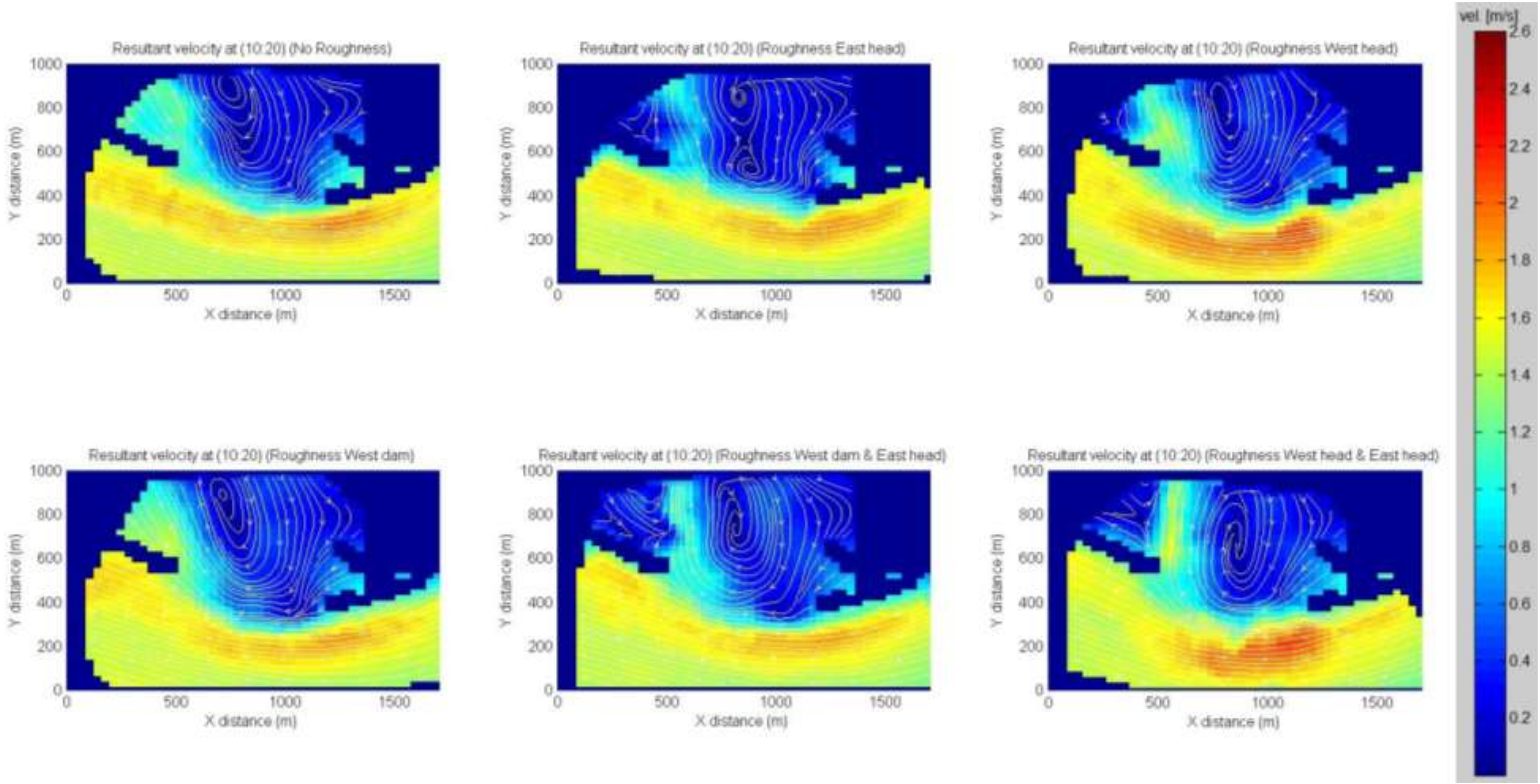

Figure 2: Velocity field of the physical model of Zeebrugge in with six different roughness scenarios at 1 hour and 40 minutes before high water (from left to right scenario 1, 3, 2, 4, 5, 6)

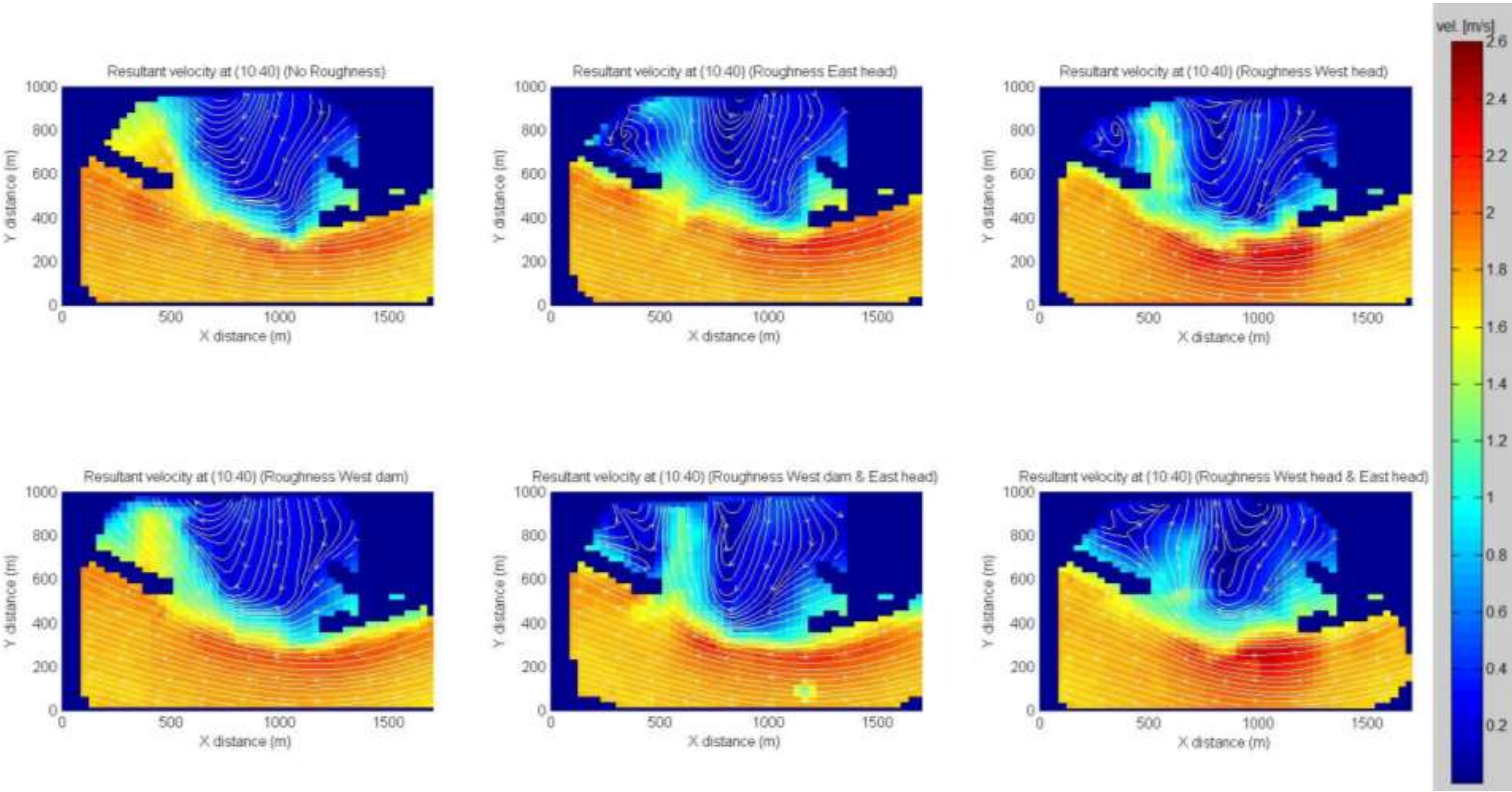

Figure 3: Velocity field of the physical model of Zeebrugge in with six different roughness scenarios at 1 hour and 20 minutes before high water (from left to right scenario 1, 3, 2, 4, 5, 6)

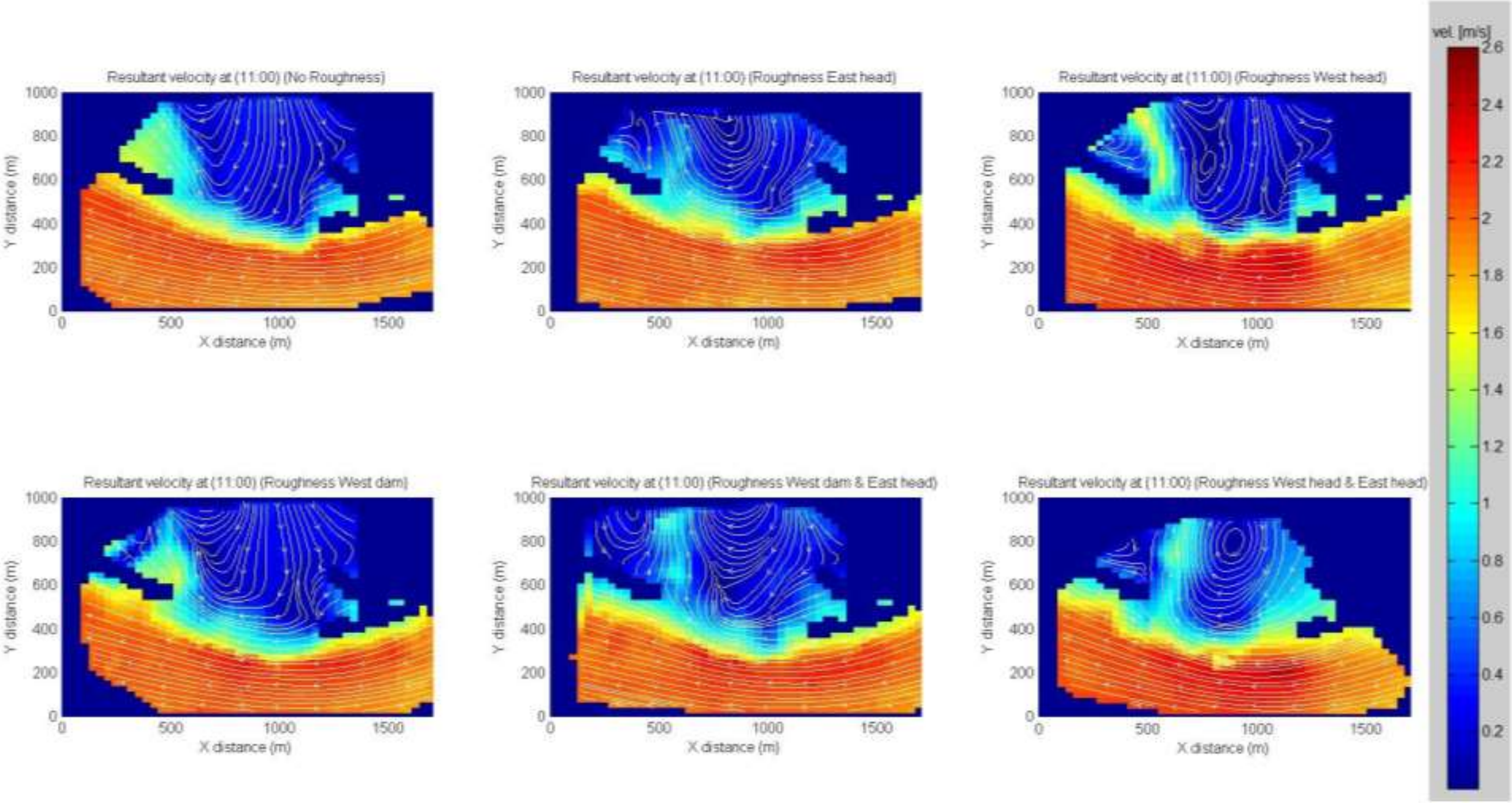

Figure 4: Velocity field of the physical model of Zeebrugge in with six different roughness scenarios at 1 hour before high water (from left to right scenario 1, 3, 2, 4, 5, 6)

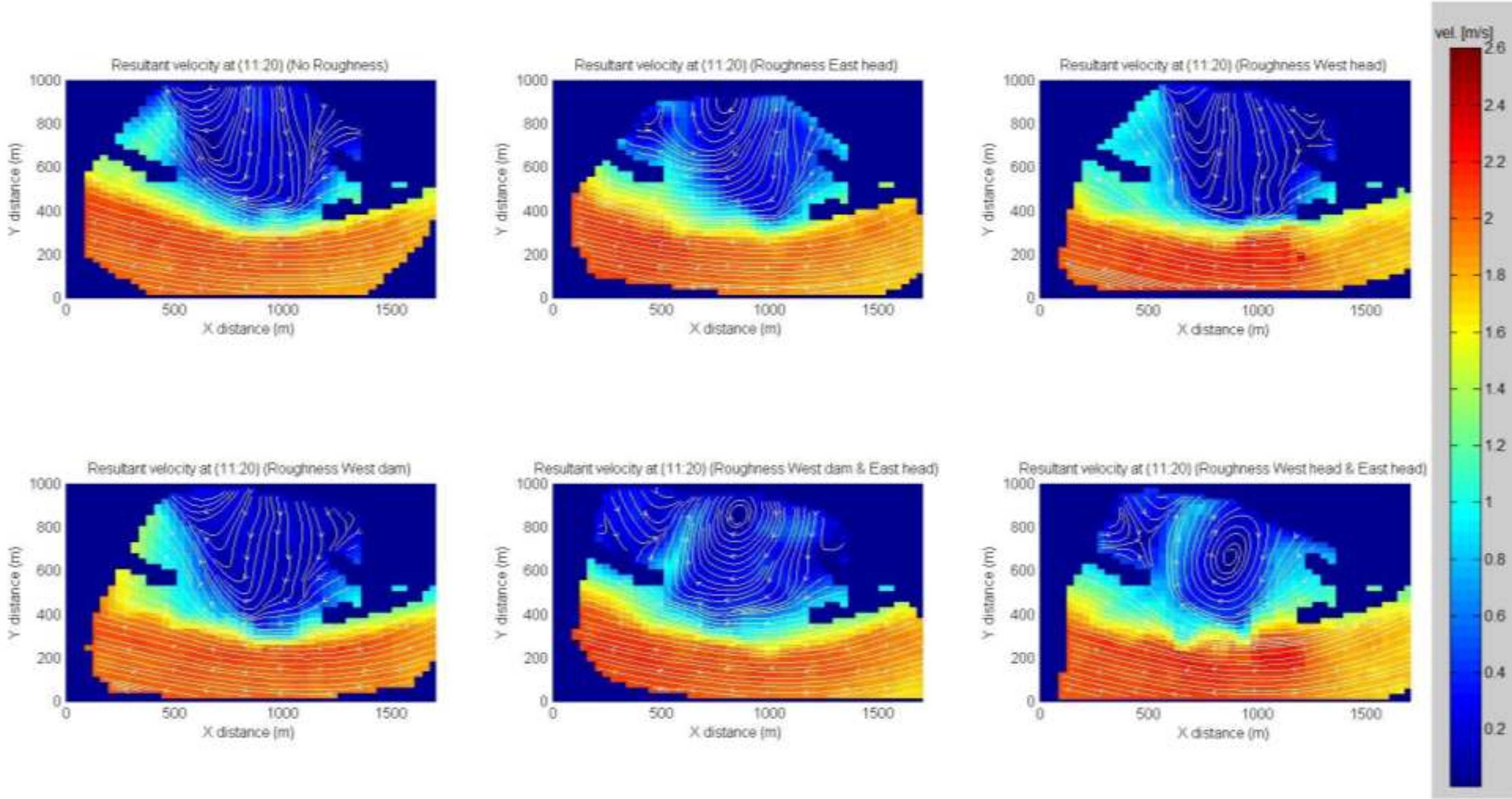

Figure 5: Velocity field of the physical model of Zeebrugge in with six different roughness scenarios at 40 minutes before high water (from left to right scenario 1, 3, 2, 4, 5, 6)

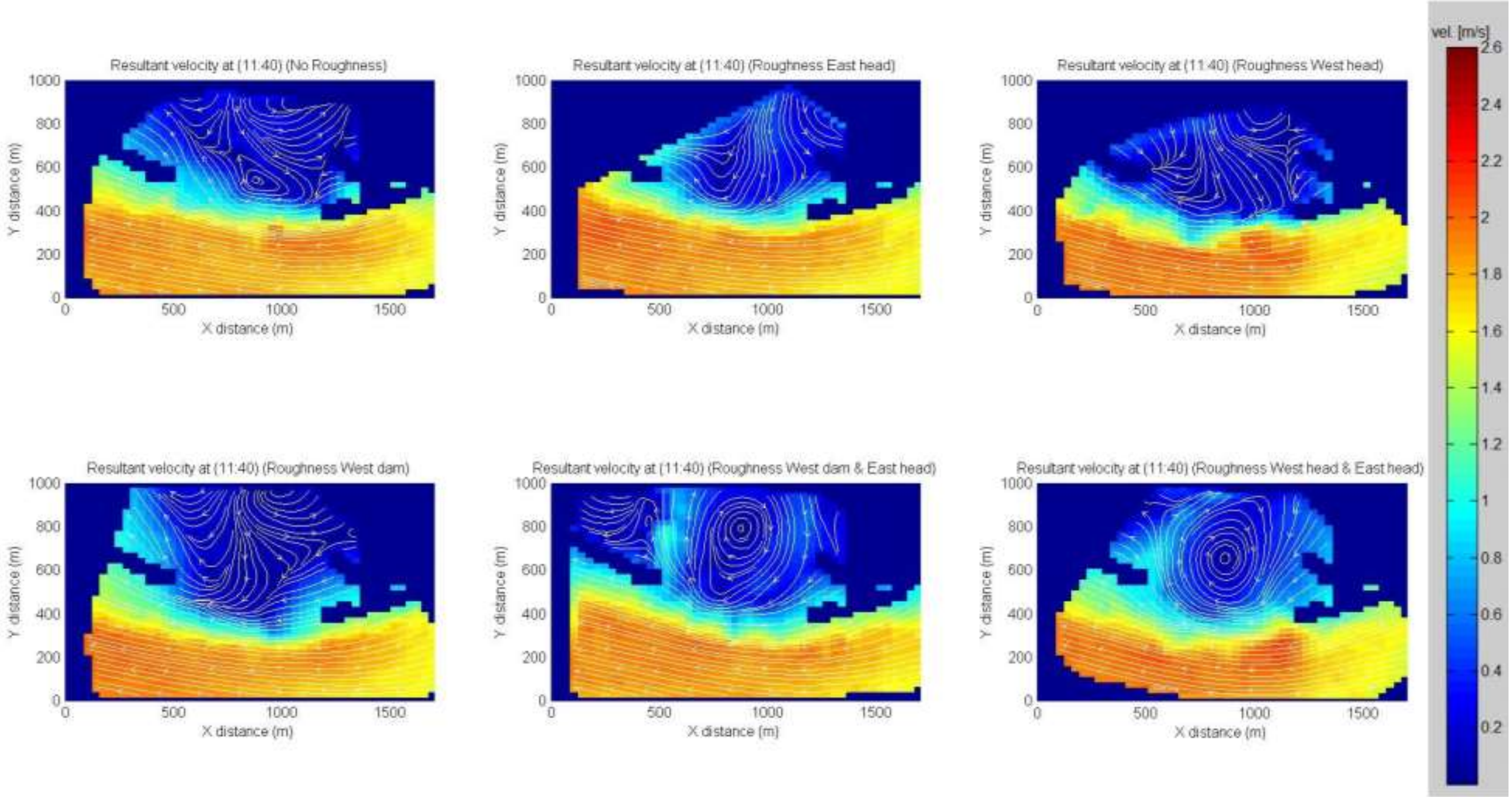

Figure 6: Velocity field of the physical model of Zeebrugge in with six different roughness scenarios at 20 minutes before high water (from left to right scenario 1, 3, 2, 4, 5, 6)

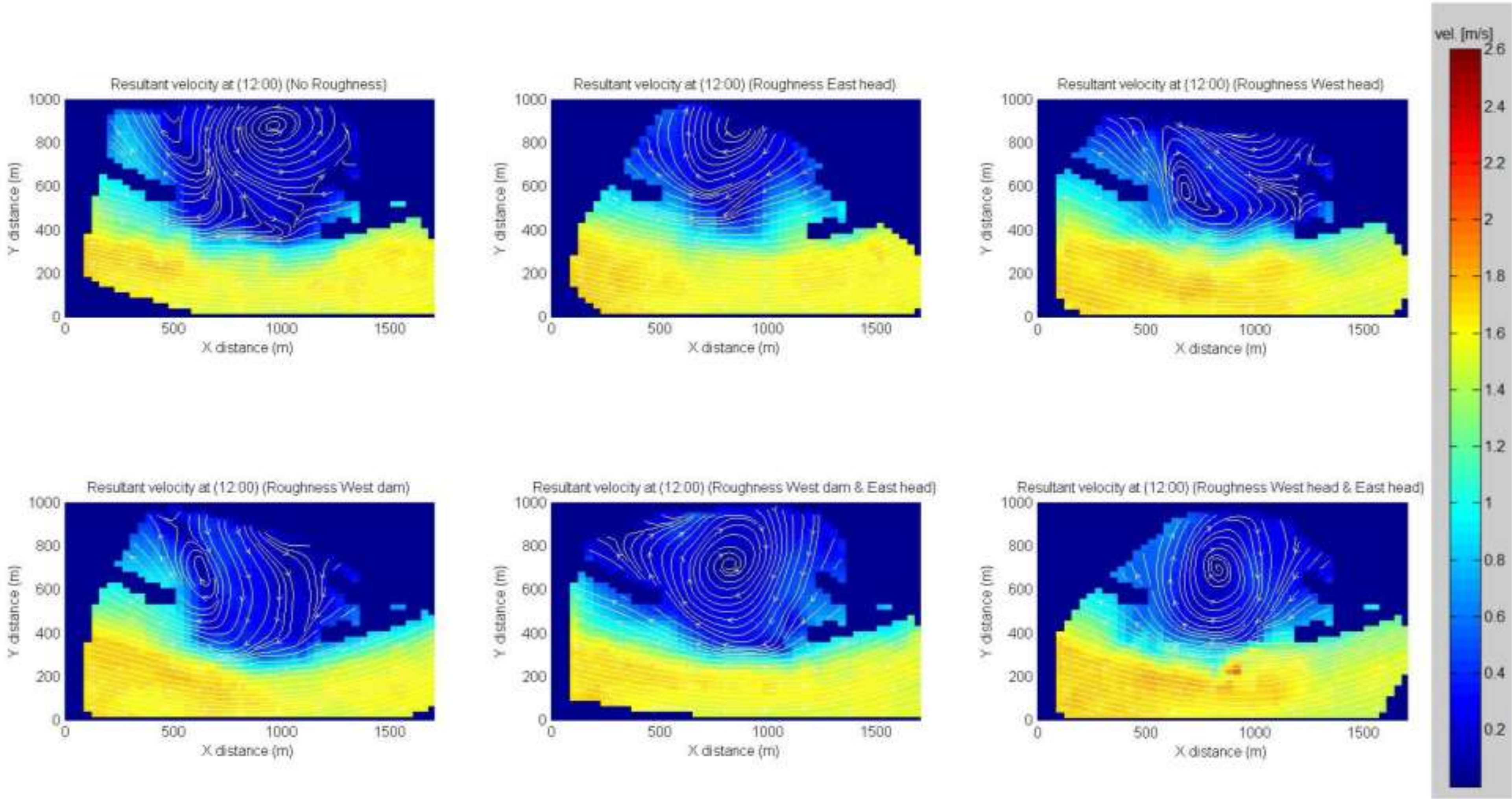

Figure 7: Velocity field of the physical model of Zeebrugge in with six different roughness scenarios at high water (from left to right scenario 1, 3, 2, 4, 5, 6)

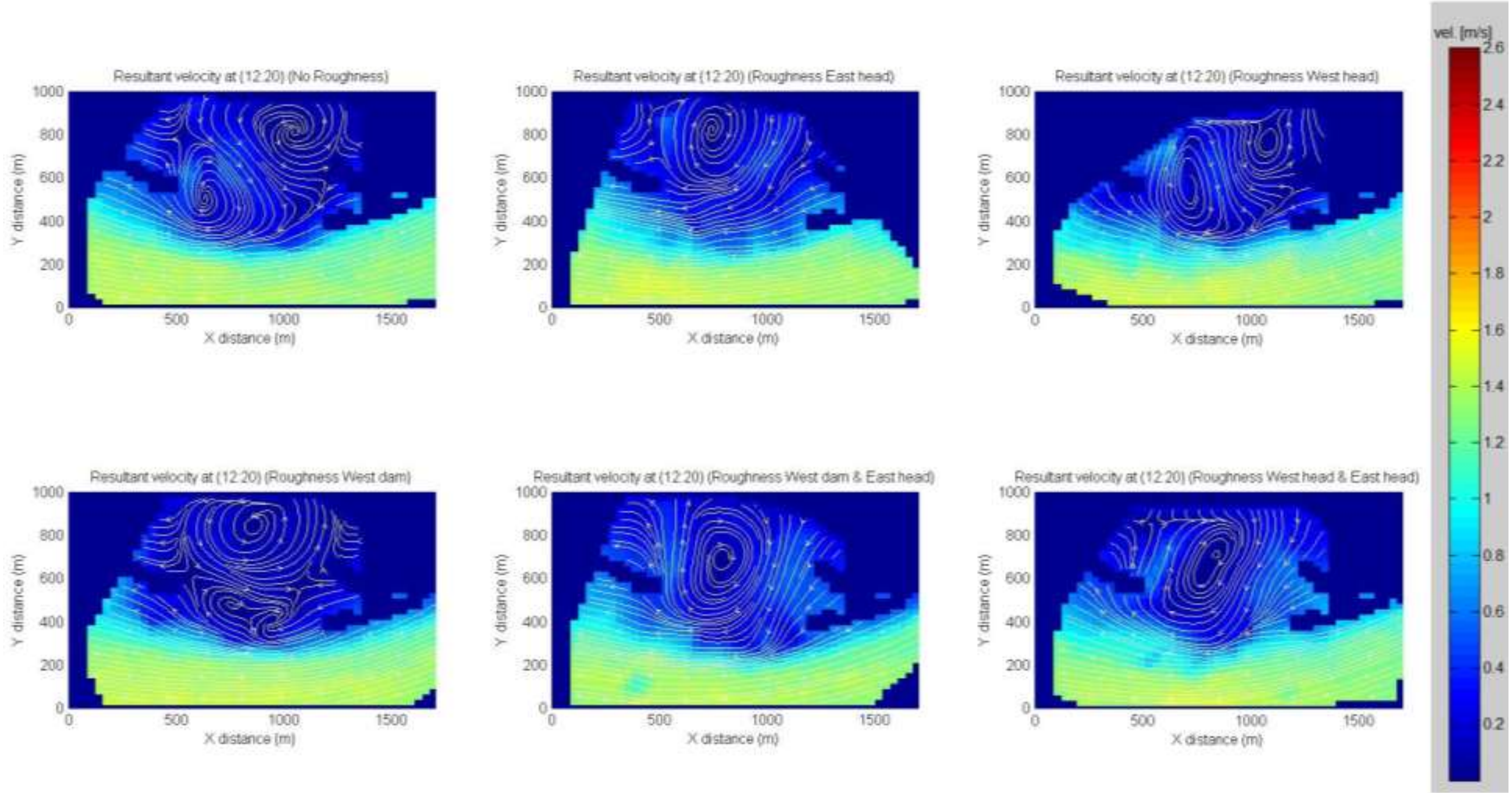

Figure 8: Velocity field of the physical model of Zeebrugge in with six different roughness scenarios at 20 minutes after high water (from left to right scenario 1, 3, 2, 4, 5, 6)

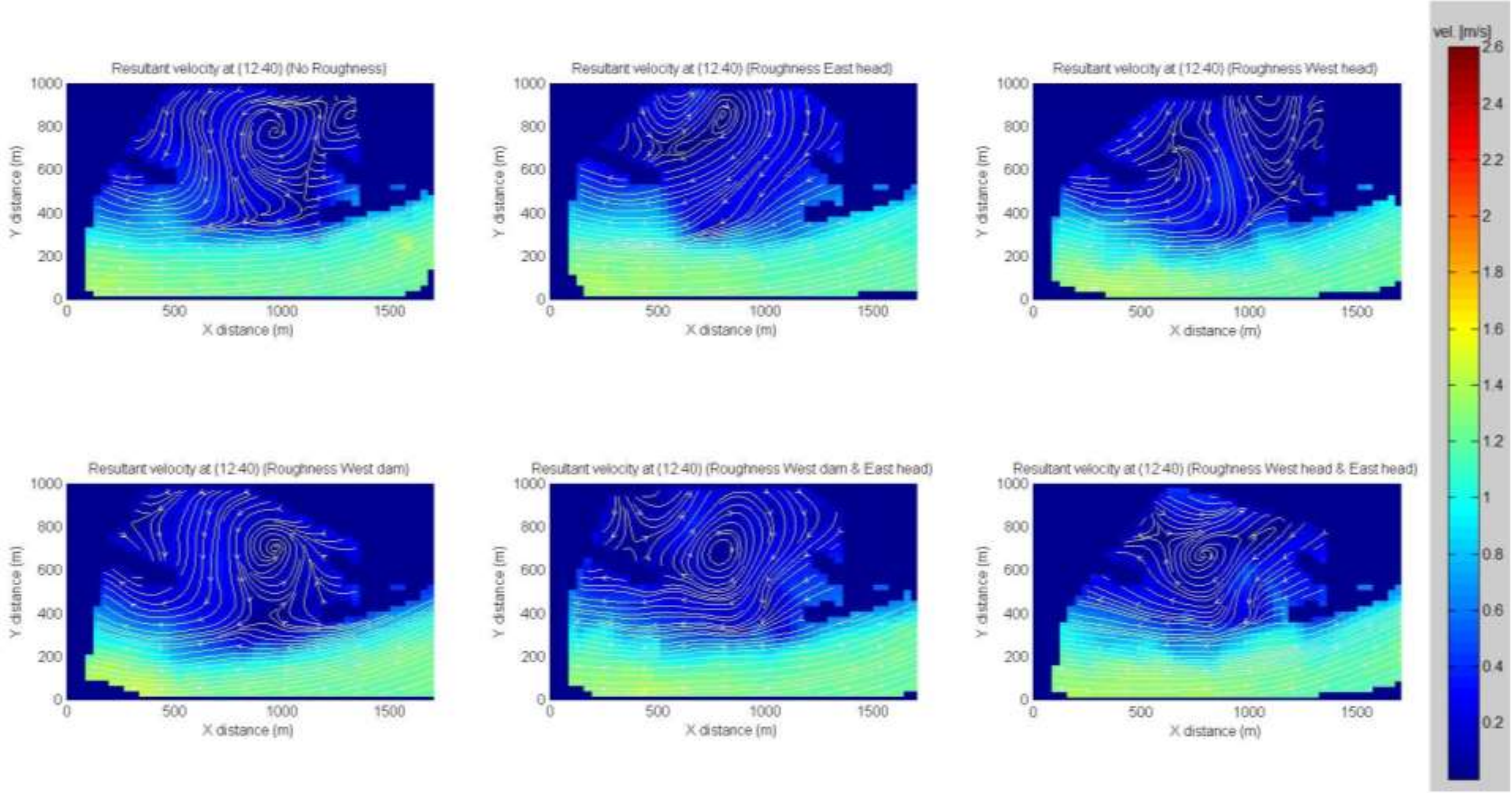

Figure 9: Velocity field of the physical model of Zeebrugge in with six different roughness scenarios at 40 minutes after high water (from left to right scenario 1, 3, 2, 4, 5, 6)

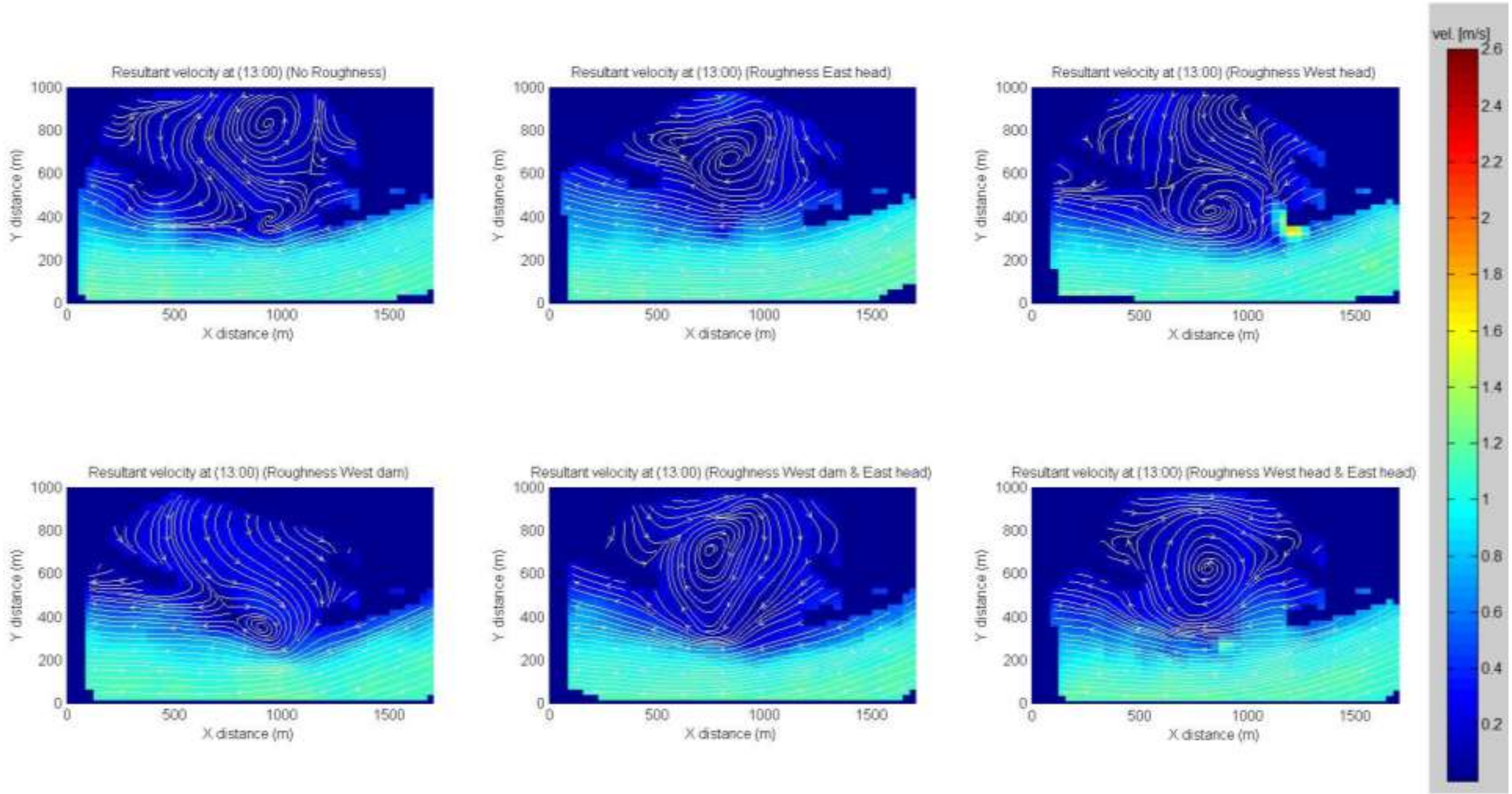

Figure 10: Velocity field of the physical model of Zeebrugge in with six different roughness scenarios at 1 hour after high water (from left to right scenario 1, 3, 2, 4, 5, 6)

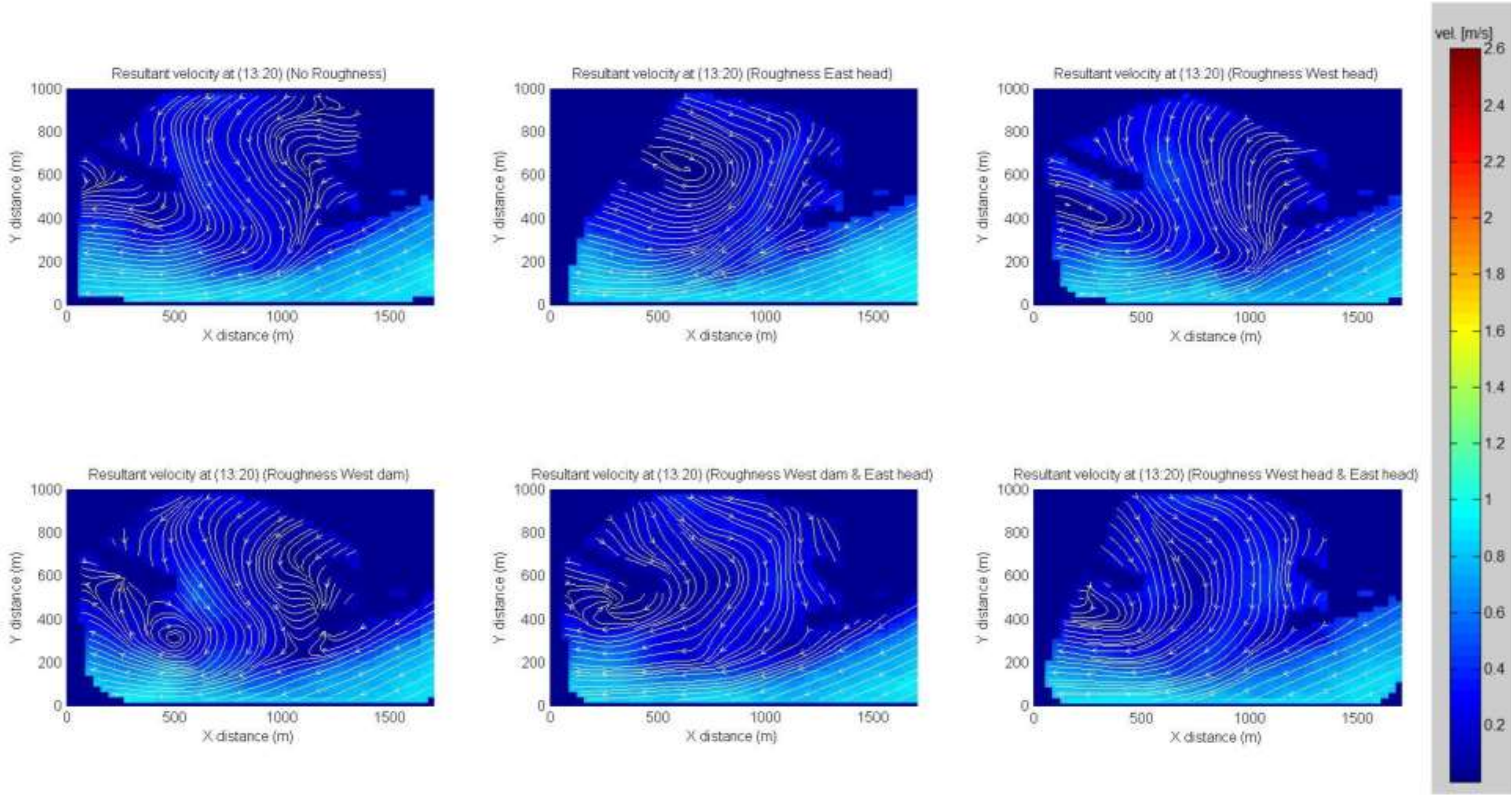

Figure 11: Velocity field of the physical model of Zeebrugge in with six different roughness scenarios at 1 hour and 20 minutes after high water (from left to right scenario 1, 3, 2, 4, 5, 6)

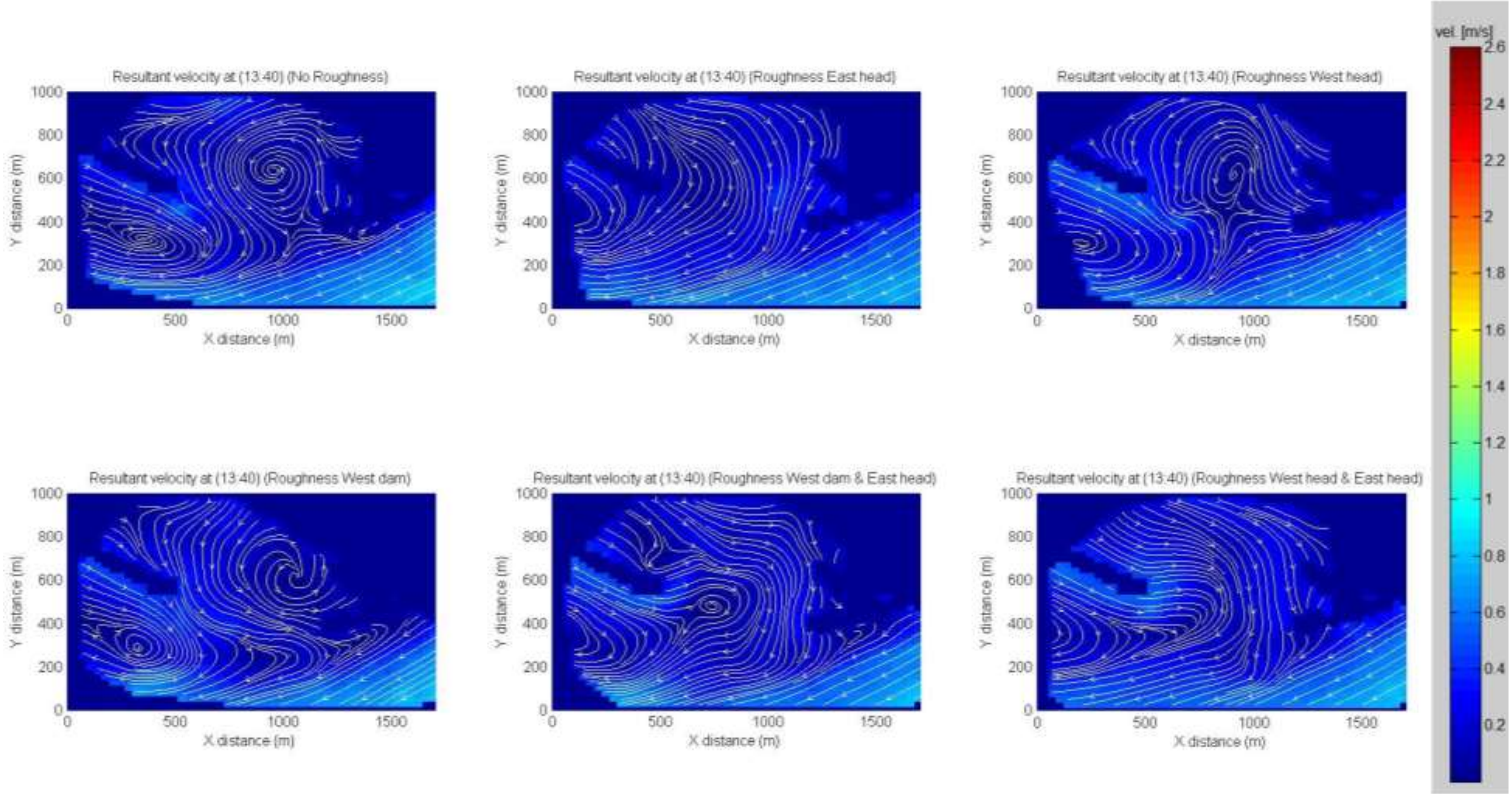

Figure 12: Velocity field of the physical model of Zeebrugge in with six different roughness scenarios at 1 hour and 40 minutes after high water (from left to right scenario 1, 3, 2, 4, 5, 6)

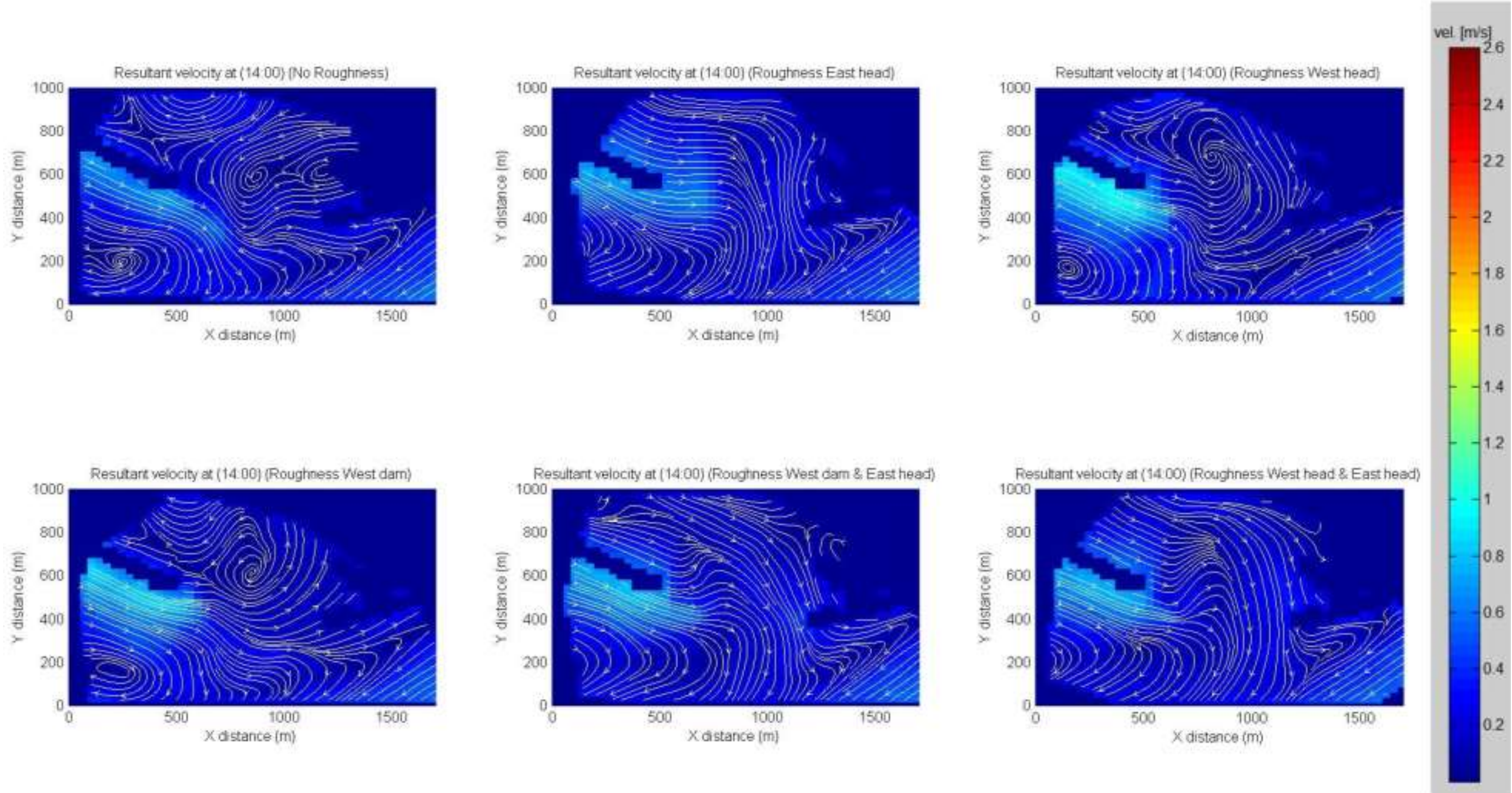

Figure 13: Velocity field of the physical model of Zeebrugge in with six different roughness scenarios at 2 hours after high water (from left to right scenario 1, 3, 2, 4, 5, 6)

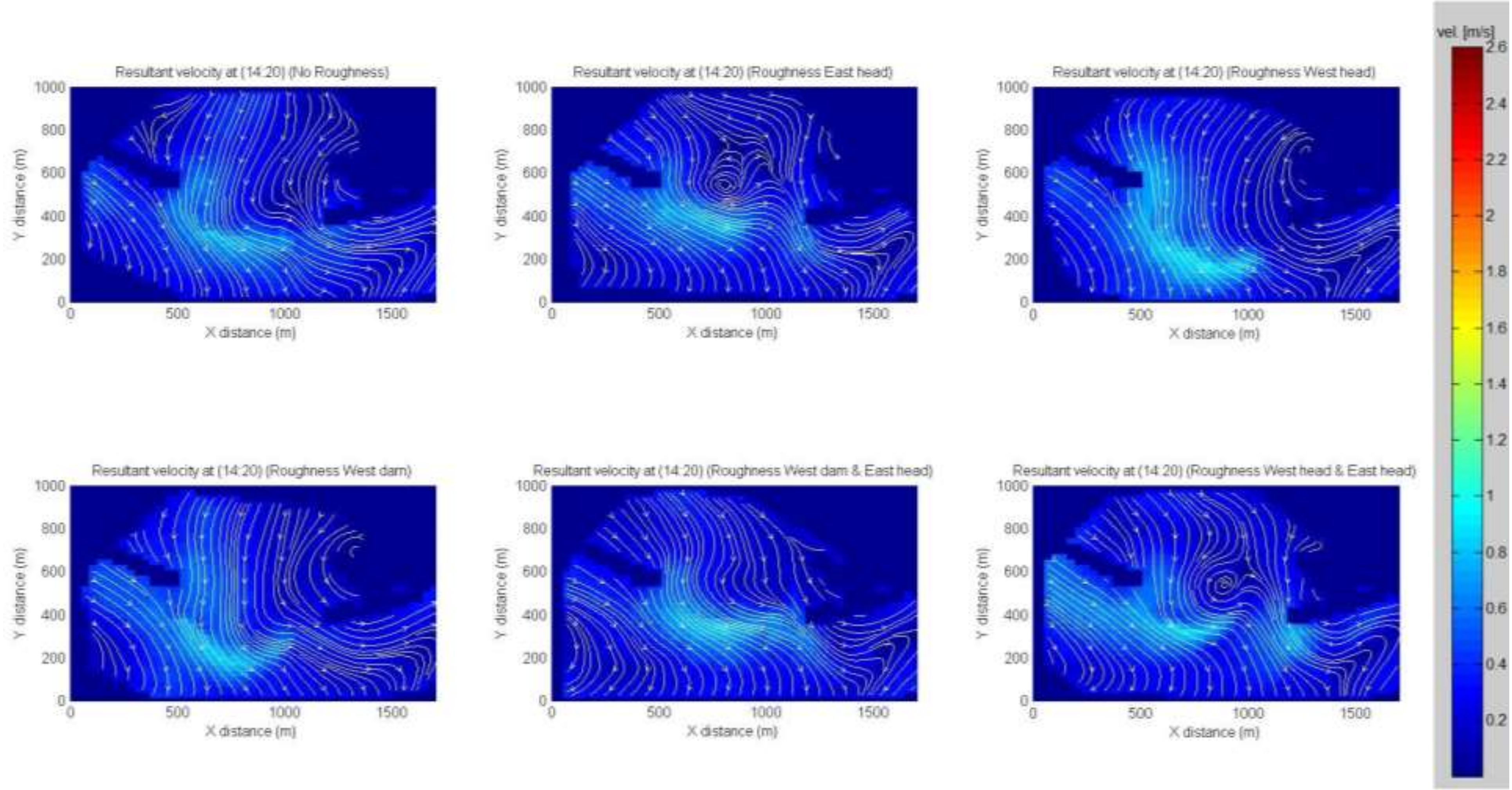

Figure 14: Velocity field of the physical model of Zeebrugge in with six different roughness scenarios at 2 hours and 20 minutes after high water (from left to right scenario 1, 3, 2, 4, 5, 6)

Appendix D: Close up vector fields of scenario 5 and 6

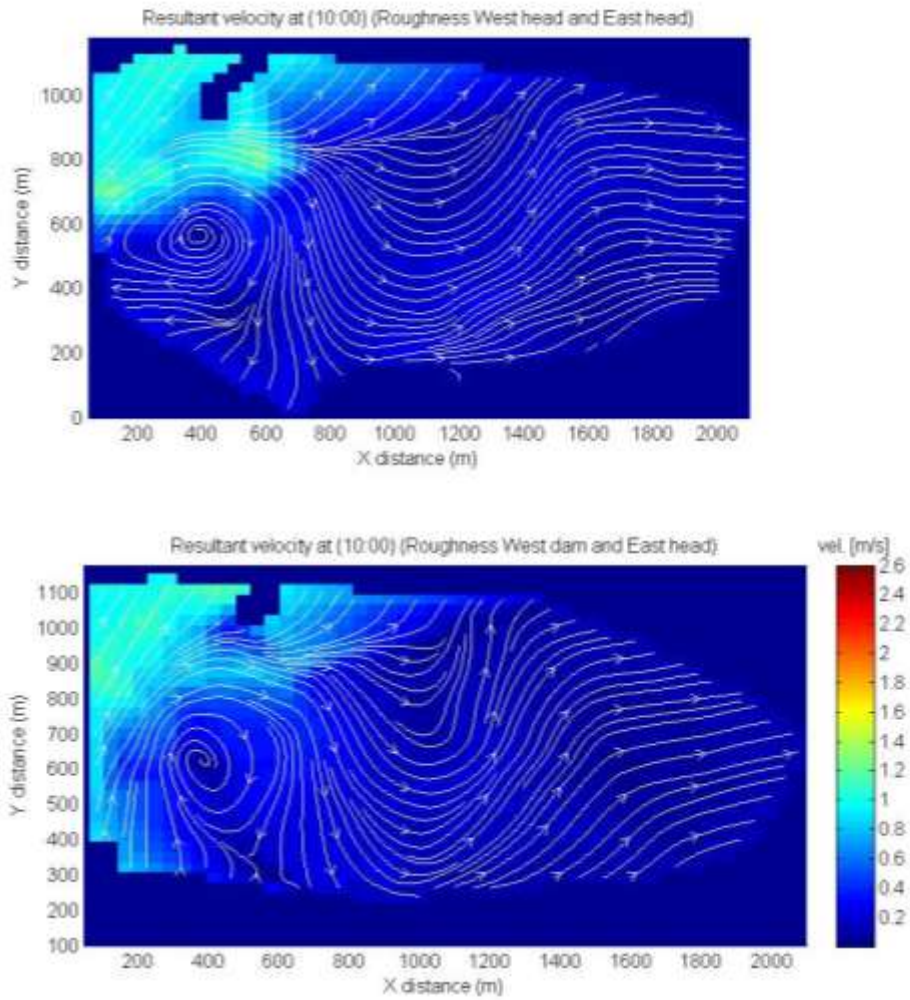

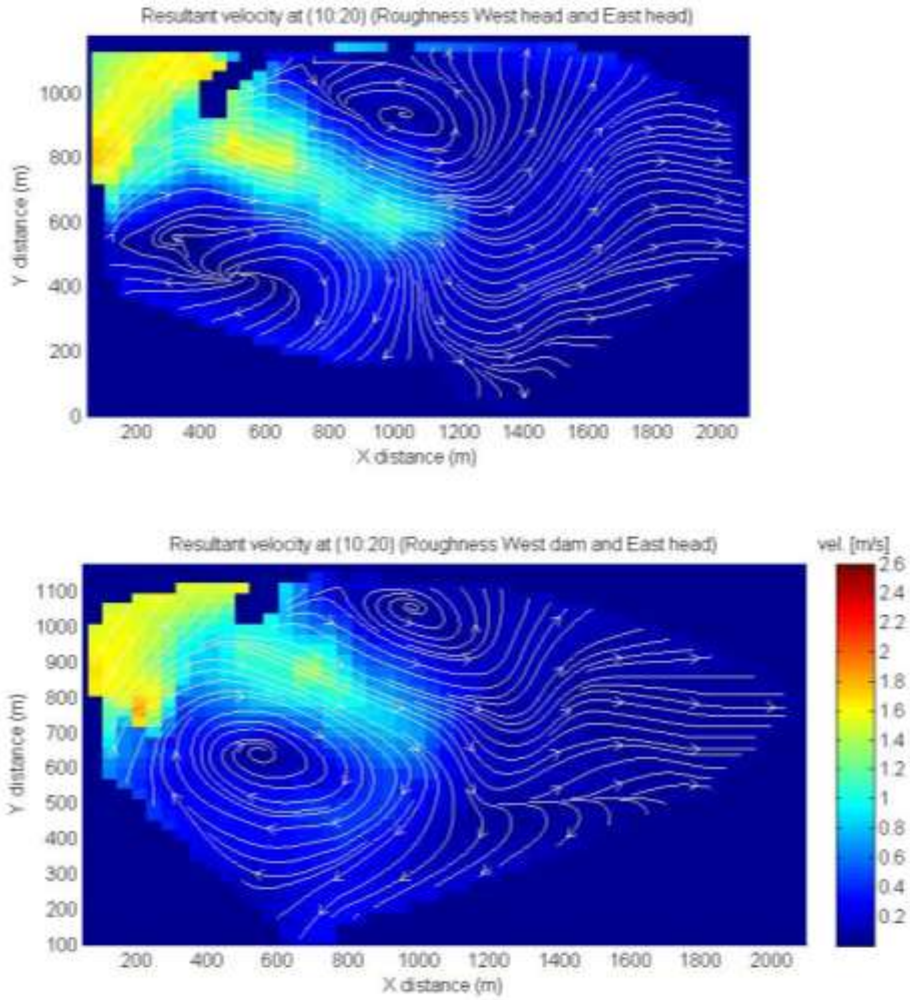

Figure 1: Velocity field of physical model of Zeebrugge with scenario 5 (bottom) and 6 (top) at 2 hours before high water

Figure 2: Velocity field of physical model of Zeebrugge with scenario 5 (bottom) and 6 (top) at 1 hour and 40 minutes before high water

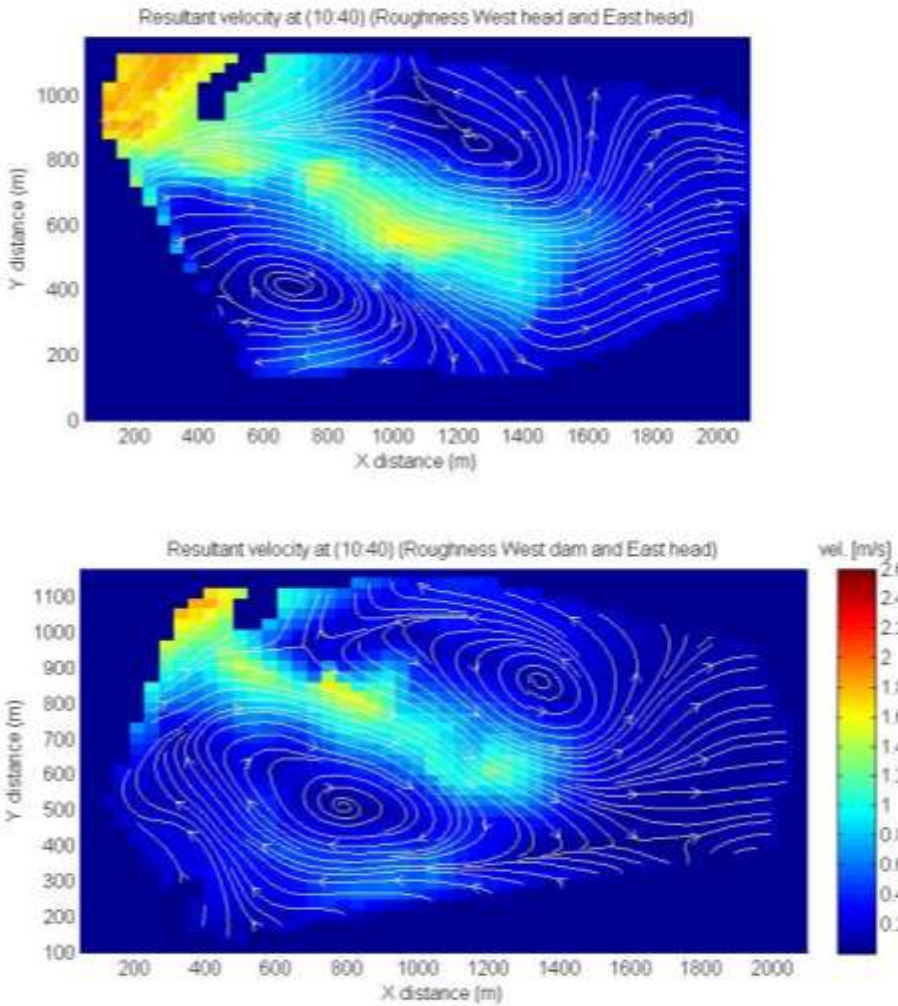

Figure 3: Velocity field of physical model of Zeebrugge with scenario 5 (bottom) and 6 (top) at 1 hour and 20 minutes before high water

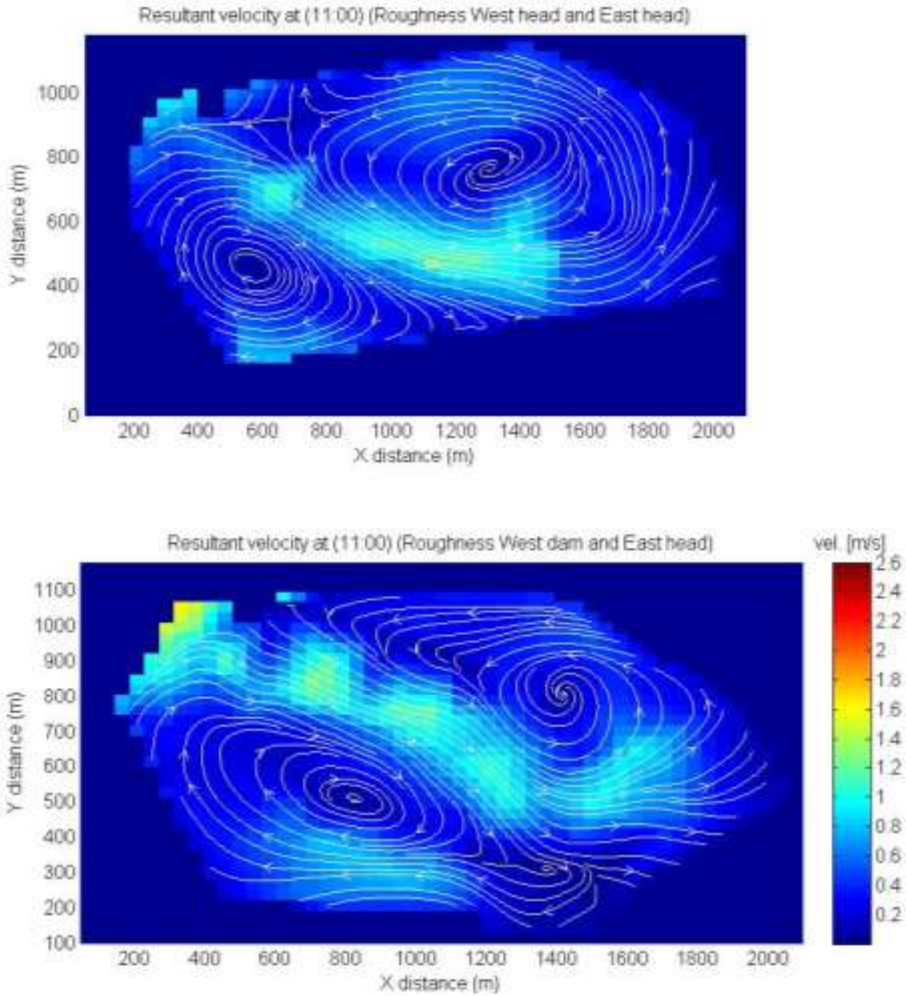

Figure 4: Velocity field of physical model of Zeebrugge with scenario 5 (bottom) and 6 (top) at 1 hour before high water

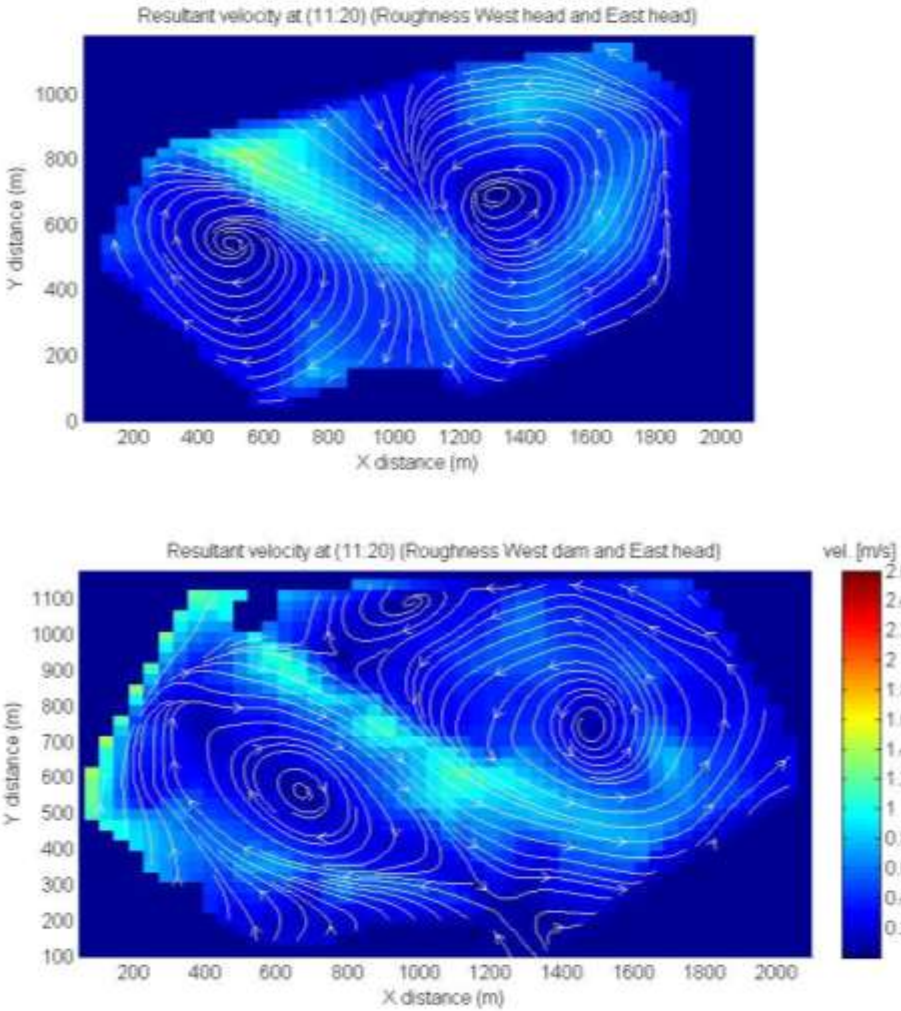

Figure 5: Velocity field of physical model of Zeebrugge with scenario 5 (bottom) and 6 (top) at 40 minutes before high water

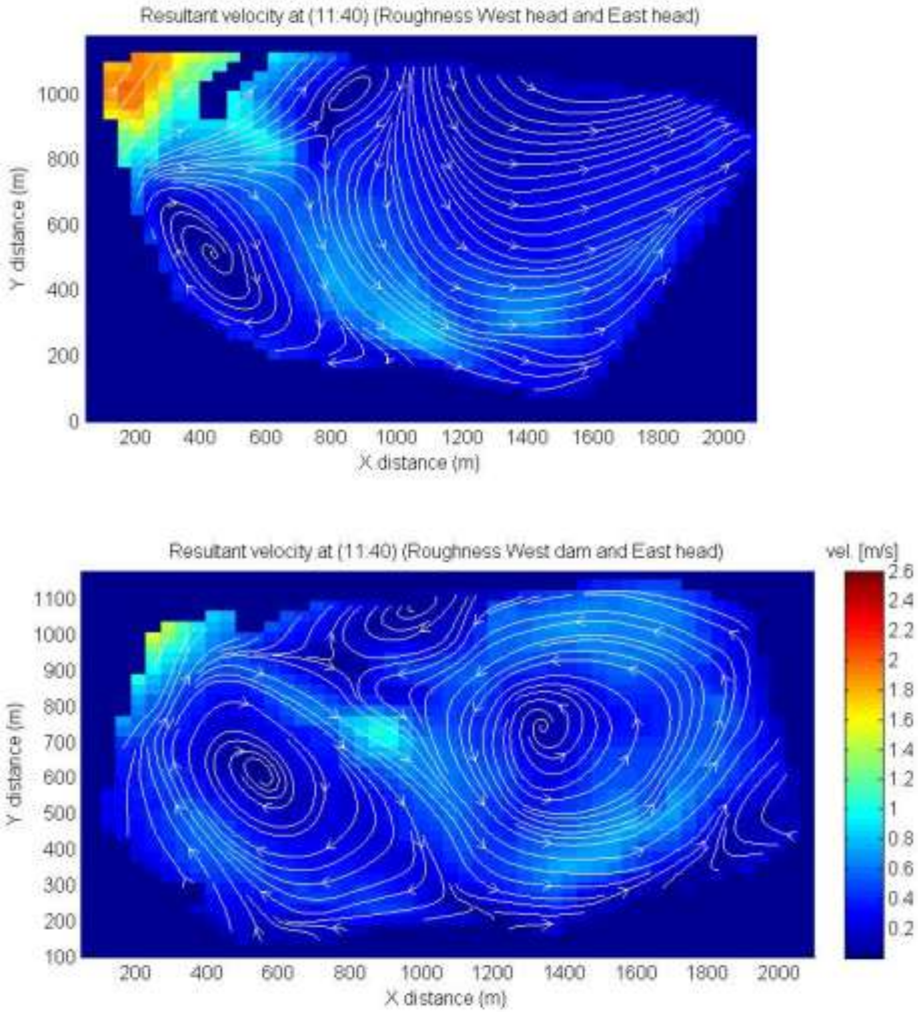

Figure 6: Velocity field of physical model of Zeebrugge with scenario 5 (bottom) and 6 (top) at 20 minutes before high water

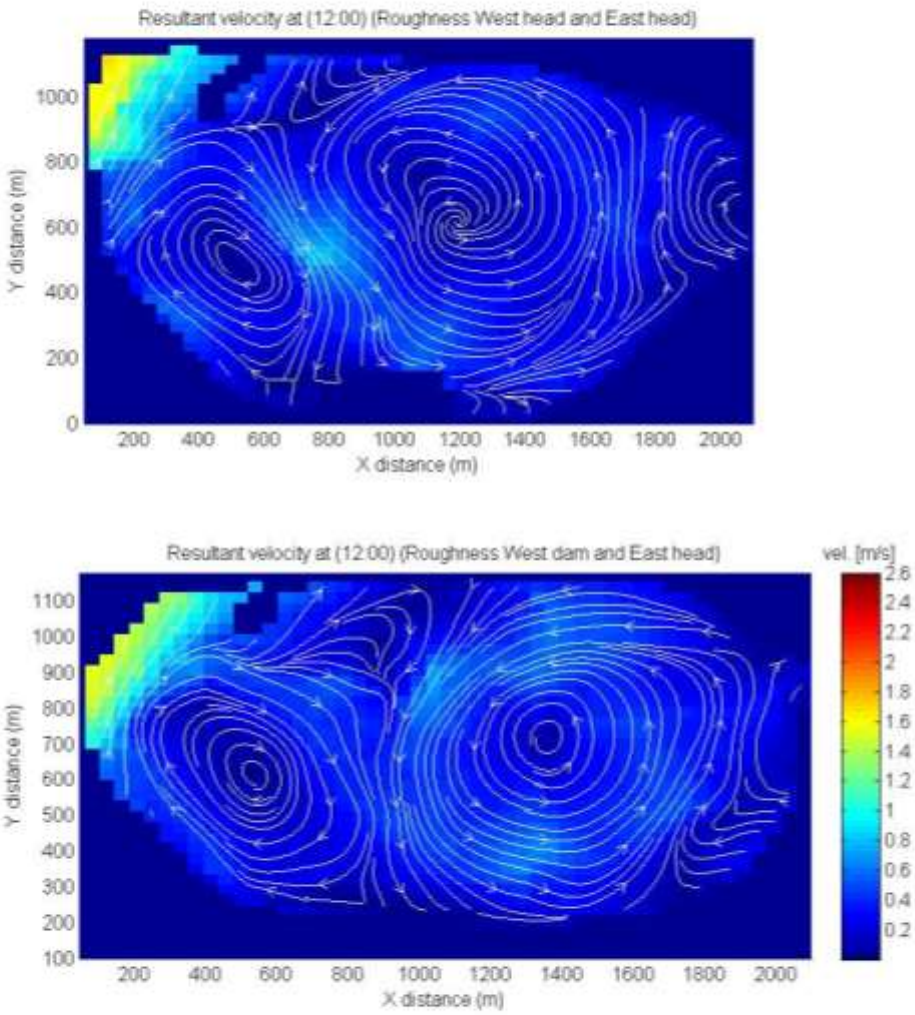

Figure 7: Velocity field of physical model of Zeebrugge with scenario 5 (bottom) and 6 (top) at high water

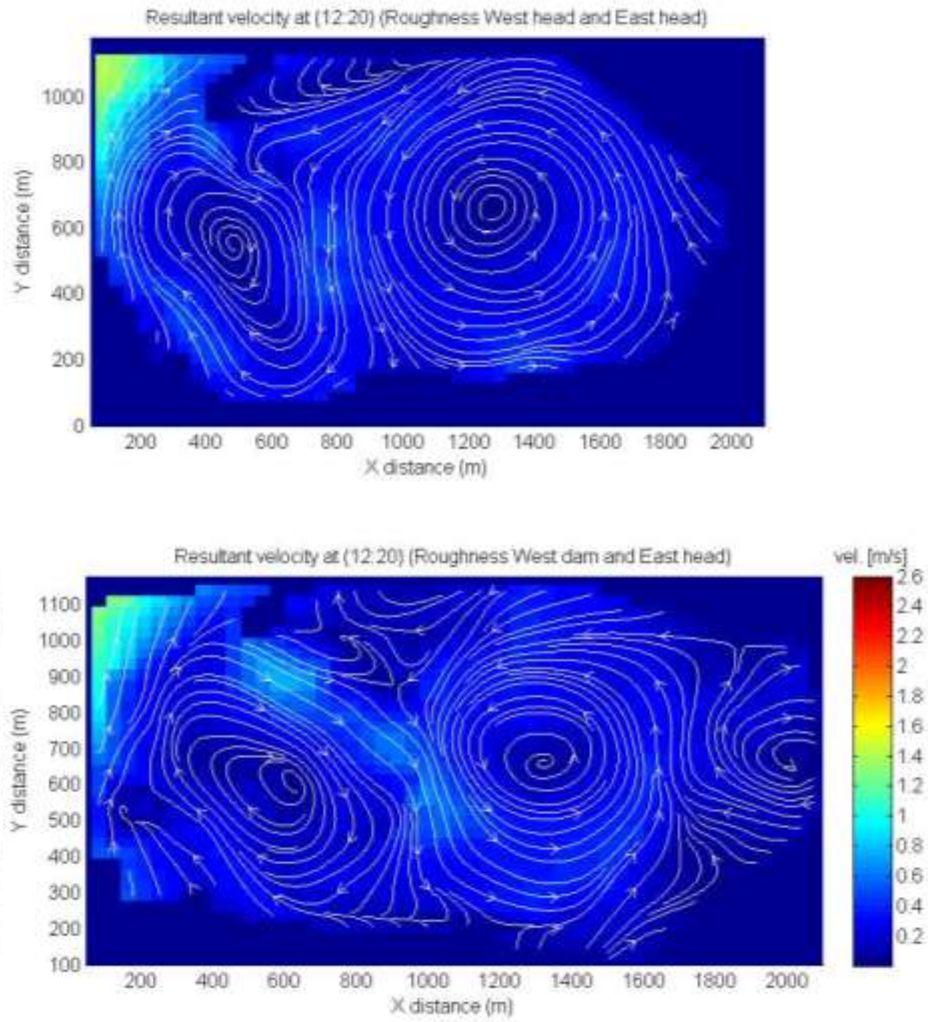

Figure 8: Velocity field of physical model of Zeebrugge with scenario 5 (bottom) and 6 (top) at 20 minutes after high water

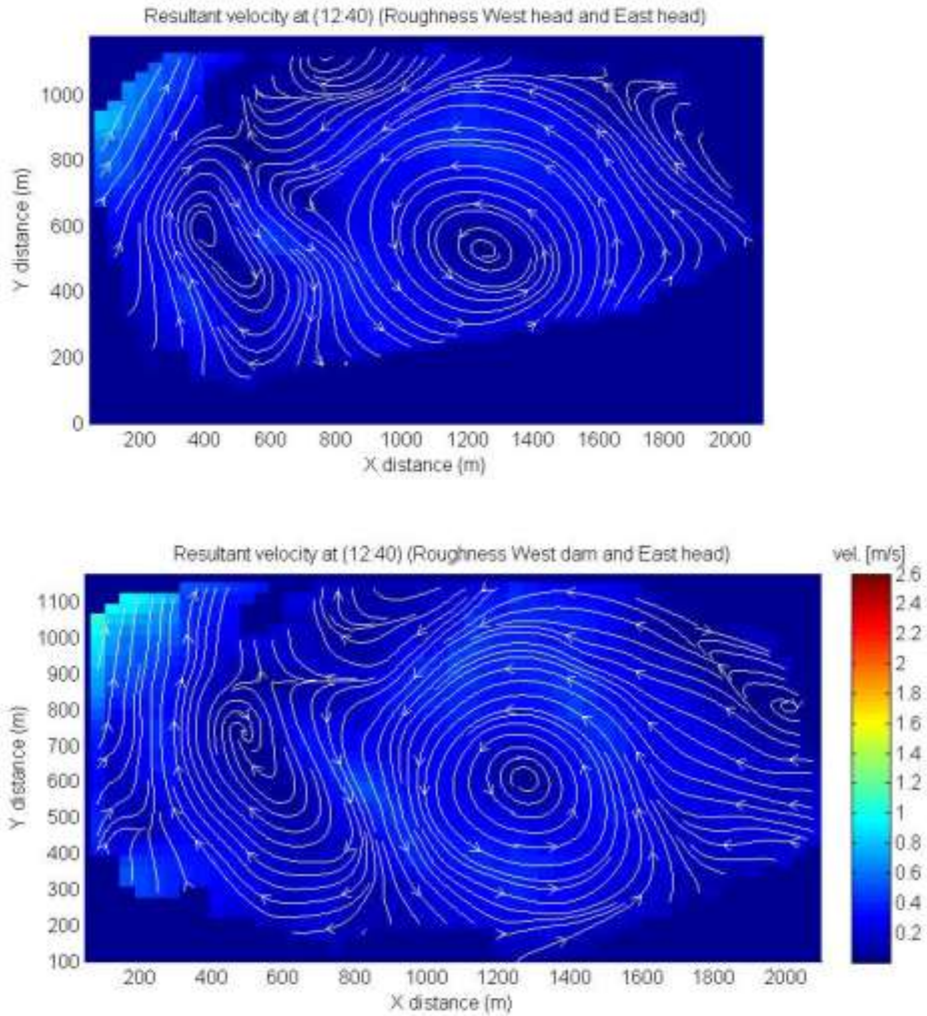

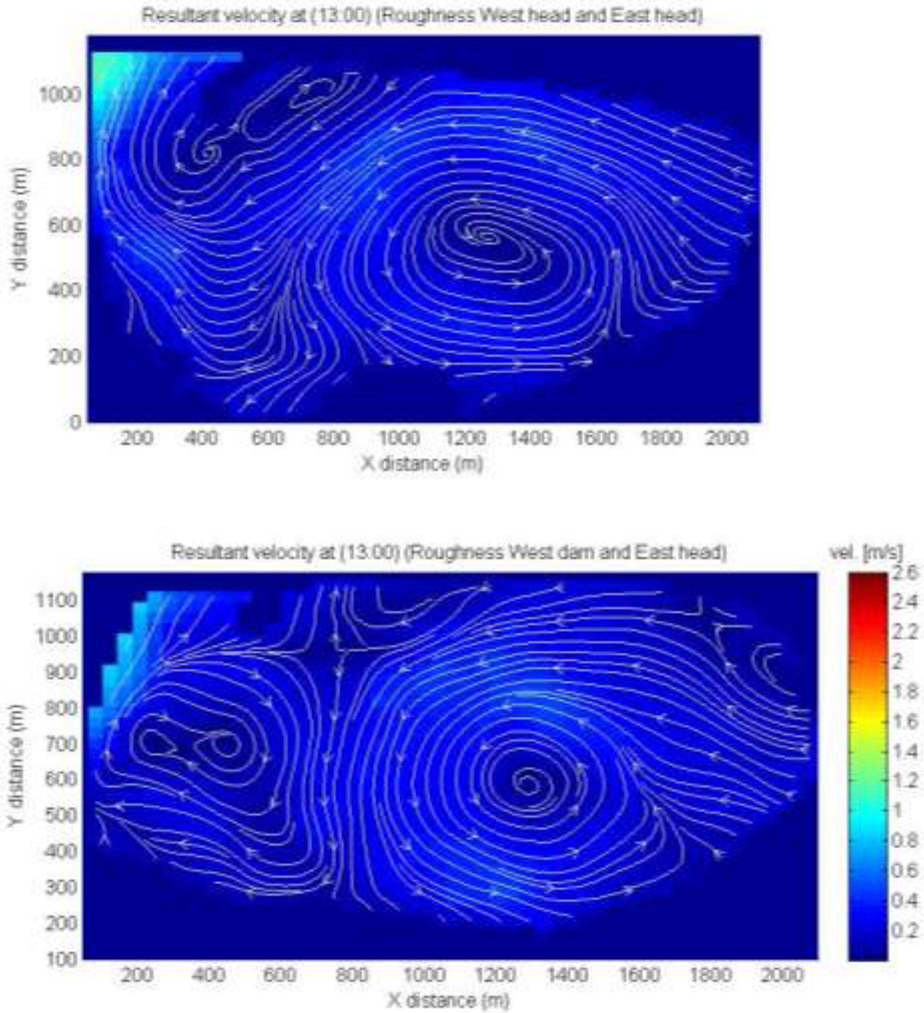

Figure 9: Velocity field of physical model of Zeebrugge with scenario 5 (bottom) and 6 (top) at 40 minutes after high water

Figure 10: Velocity field of physical model of Zeebrugge with scenario 5 (bottom) and 6 (top) at 1 hour after high water

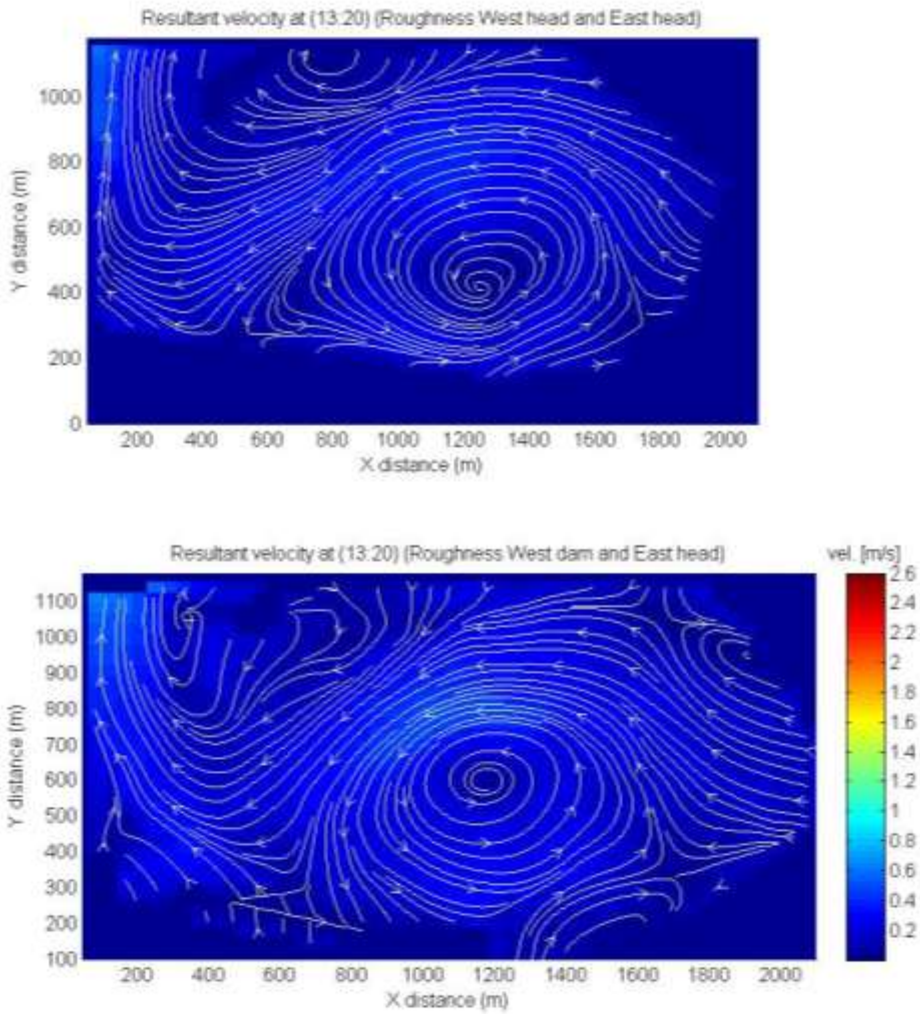

Figure 11: Velocity field of physical model of Zeebrugge with scenario 5 (bottom) and 6 (top) at 1 hour and 20 minutes after high water

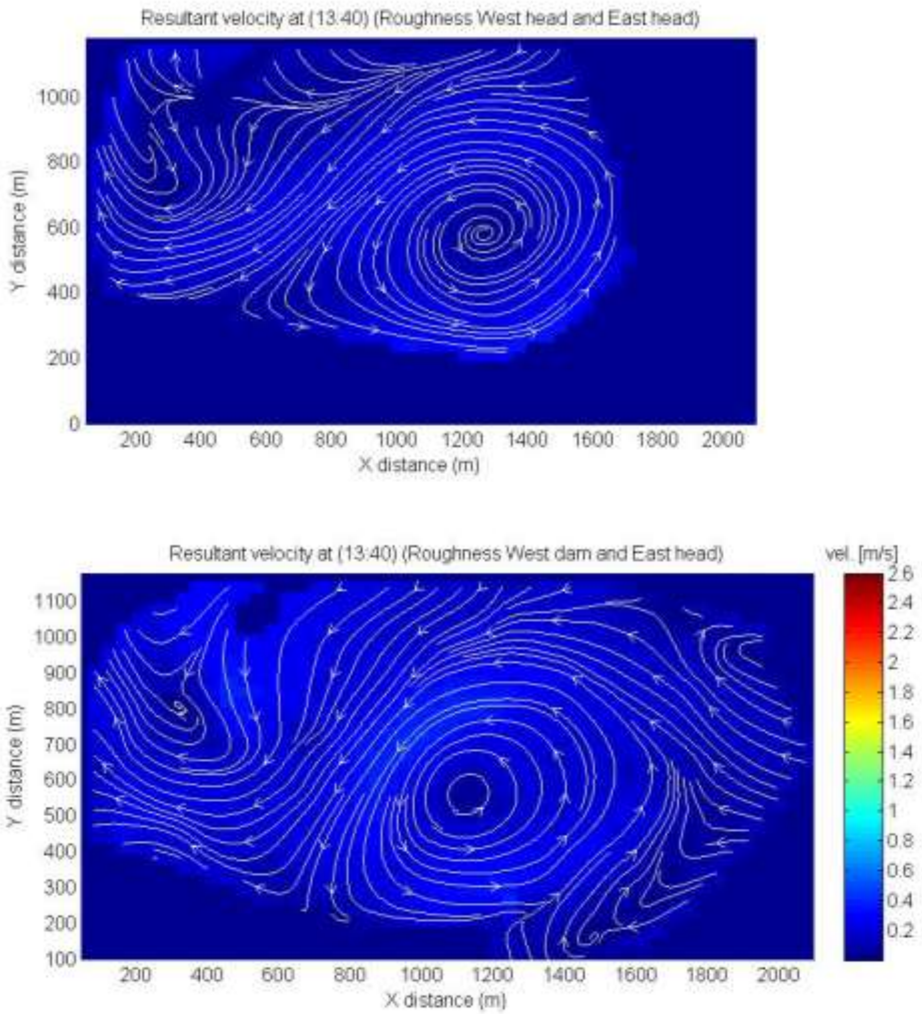

Figure 12: Velocity field of physical model of Zeebrugge with scenario 5 (bottom) and 6 (top) at 1 hour and 40 minutes after high water

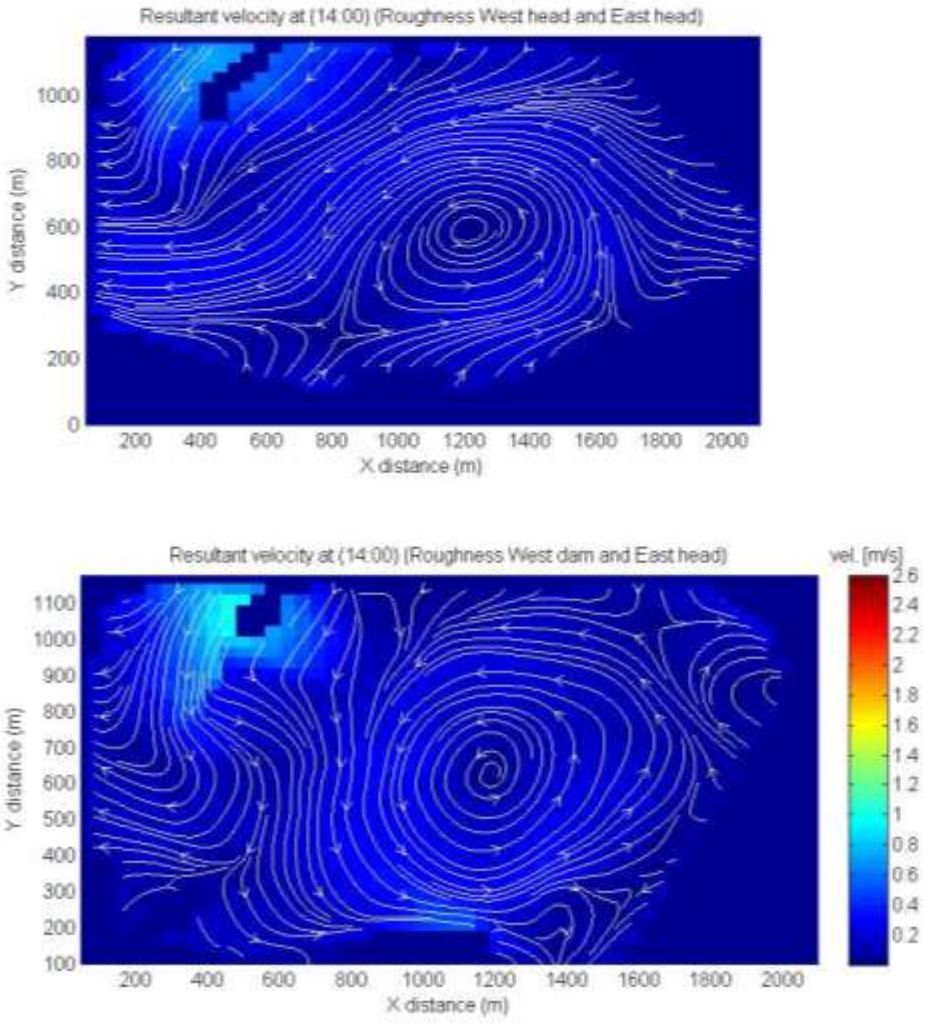

Figure 13: Velocity field of physical model of Zeebrugge with scenario 5 (bottom) and 6 (top) at 2 hours after high water

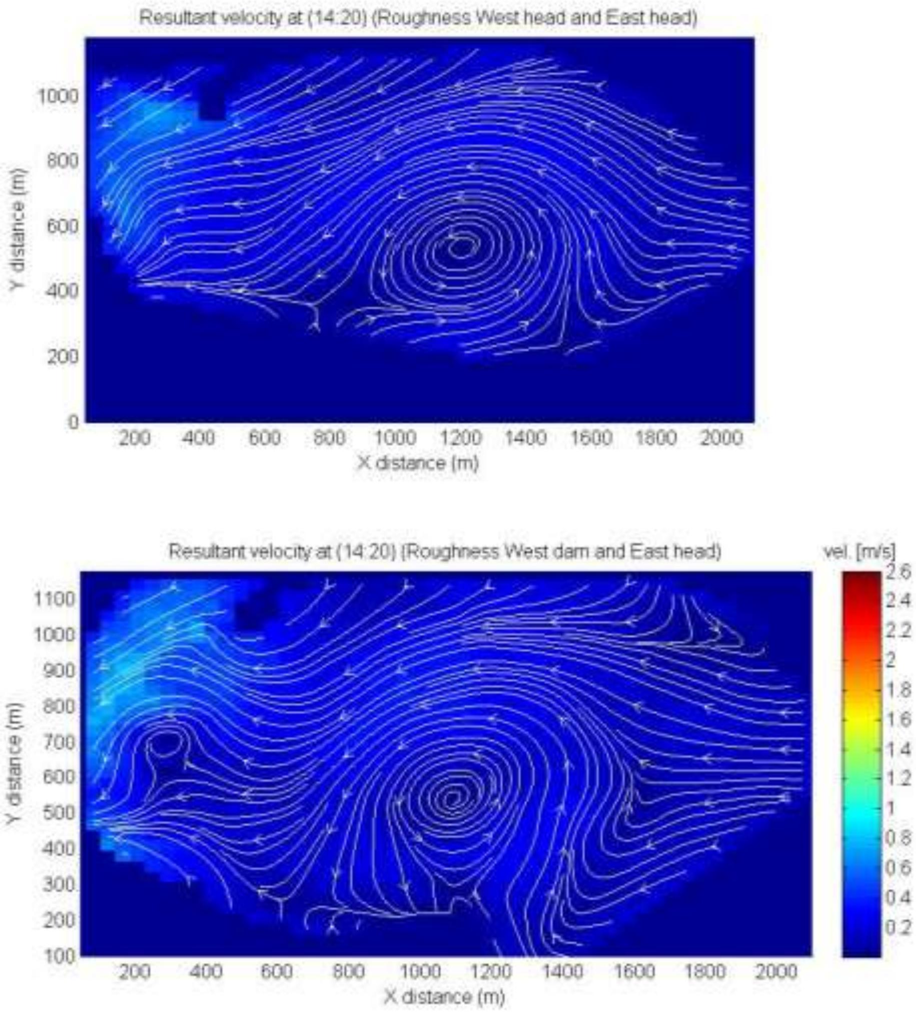

Figure 14: Velocity field of physical model of Zeebrugge with scenario 5 (bottom) and 6 (top) at 2 hours and 20 minutes after high water

Appendix E: EMS velocity and direction graphs

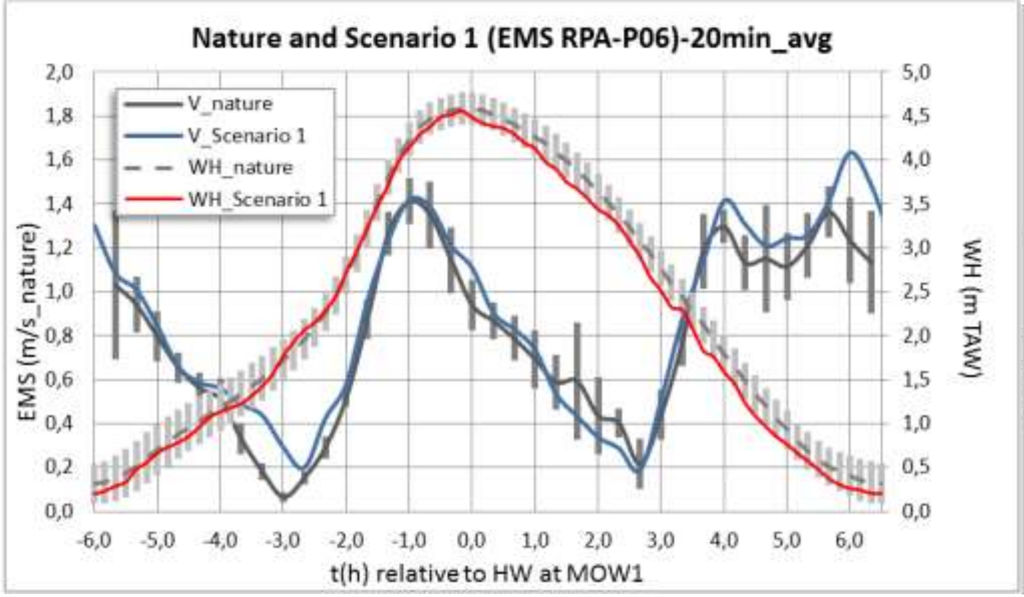

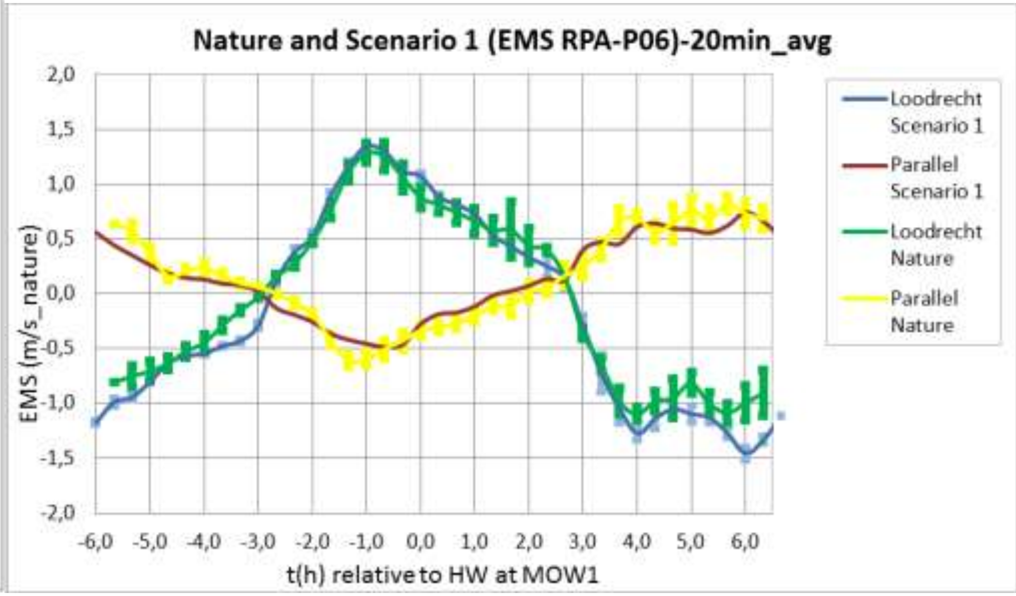

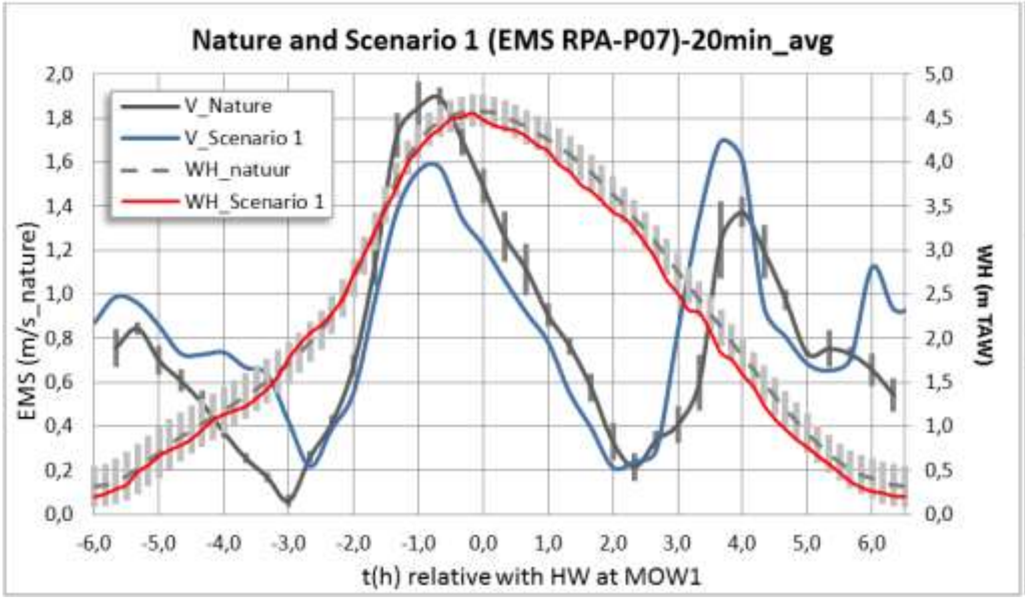

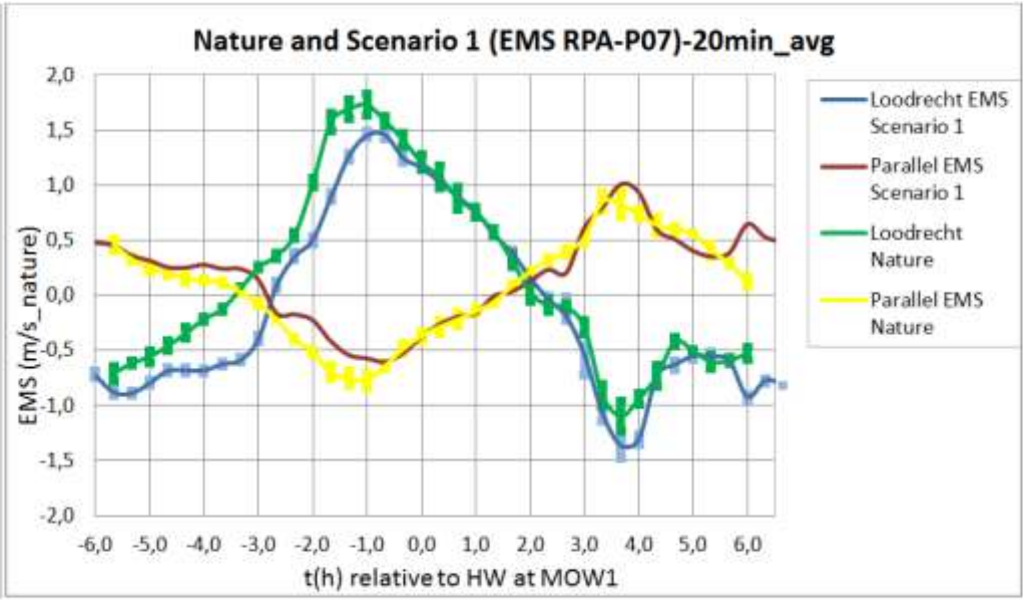

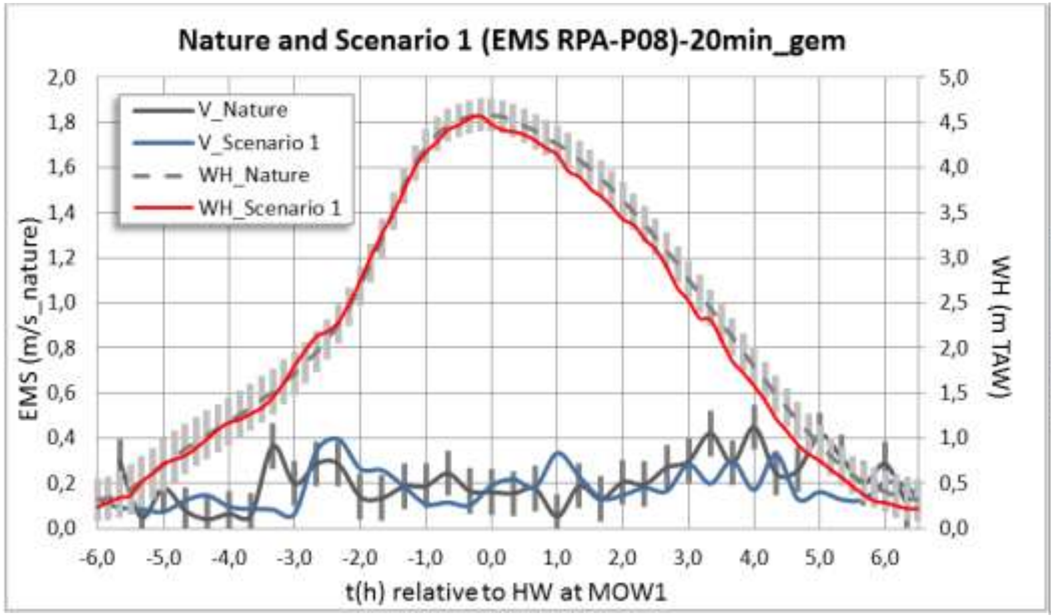
Nature and Scenario 1 (EMS RPA-P08)-20min_gem
V_Nature
V_Scenario 1
WH_Nature
WH_Scenario 1
EMS (m/s_nature)
WH (m TAW)
t(h) relative to HW at MOW1

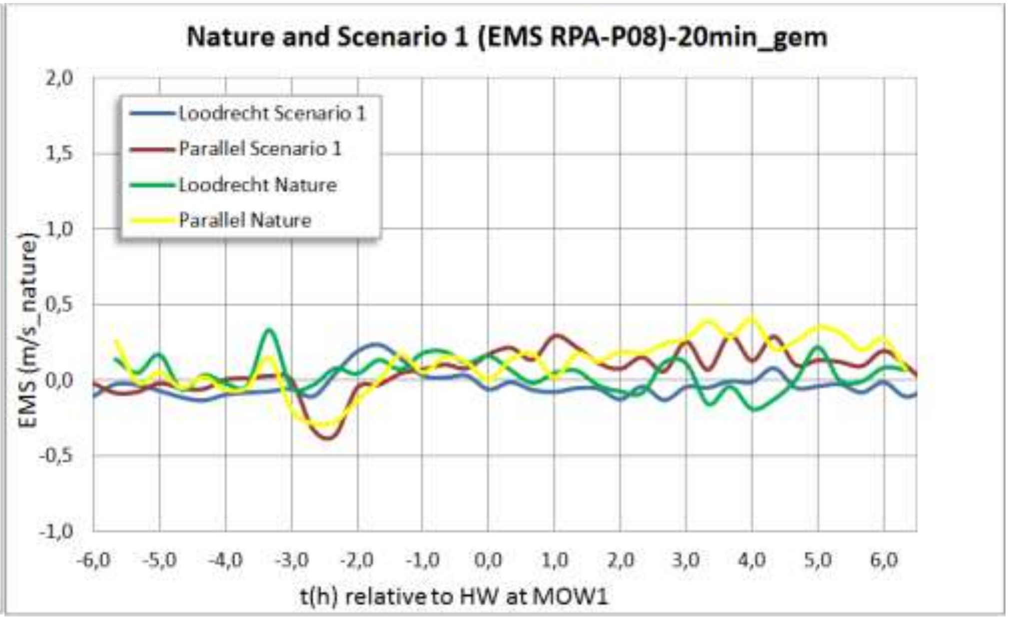
Nature and Scenario 1 (EMS RPA-P08)-20min_gem
Loodrecht Scenario 1
Parallel Scenario 1
Loodrecht Nature
Parallel Nature
EMS (m/s_nature)
t(h) relative to HW at MOW1

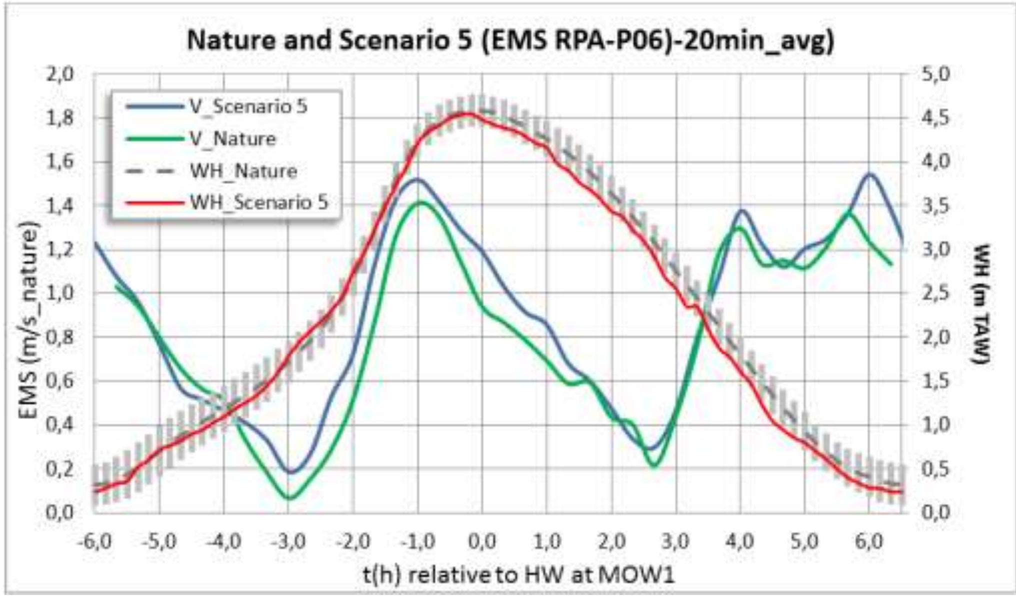
Nature and Scenario 5 (EMS RPA-P06)-20min_avg)
V_Scenario 5
V_Nature
WH_Nature
WH_Scenario 5
EMS (m/s_nature)
WH (m TAW)
t(h) relative to HW at MOW1

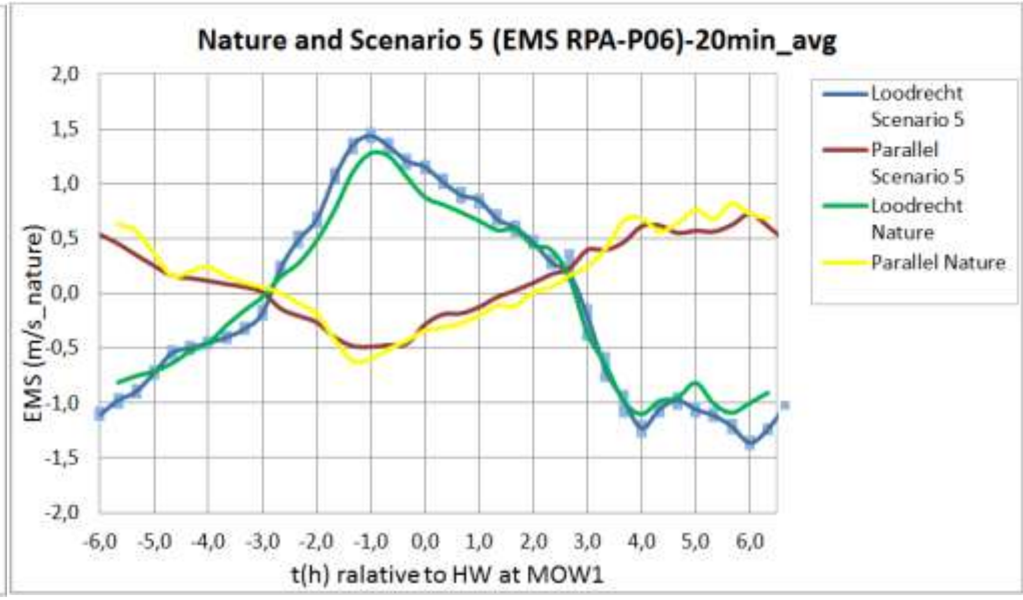
Nature and Scenario 5 (EMS RPA-P06)-20min_avg
Loodrecht Scenario 5
Parallel Scenario 5
Loodrecht Nature
Parallel Nature
EMS (m/s_nature)
t(h) ralative to HW at MOW1

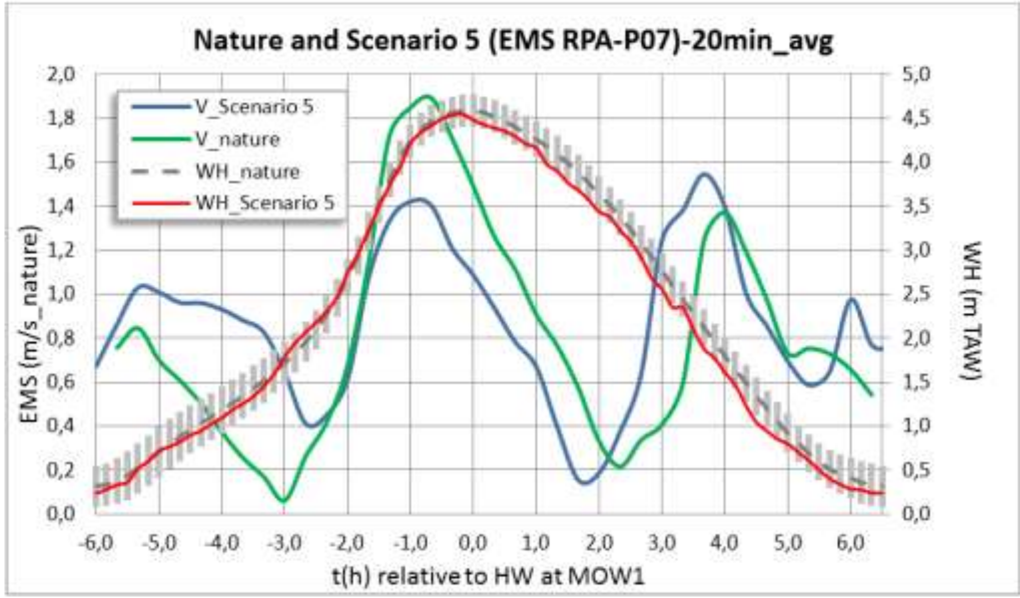
Nature and Scenario 5 (EMS RPA-P07)-20min_avg
V_Scenario 5
V_nature
WH_nature
WH_Scenario 5
EMS (m/s_nature)
WH (m TAW)
t(h) relative to HW at MOW1

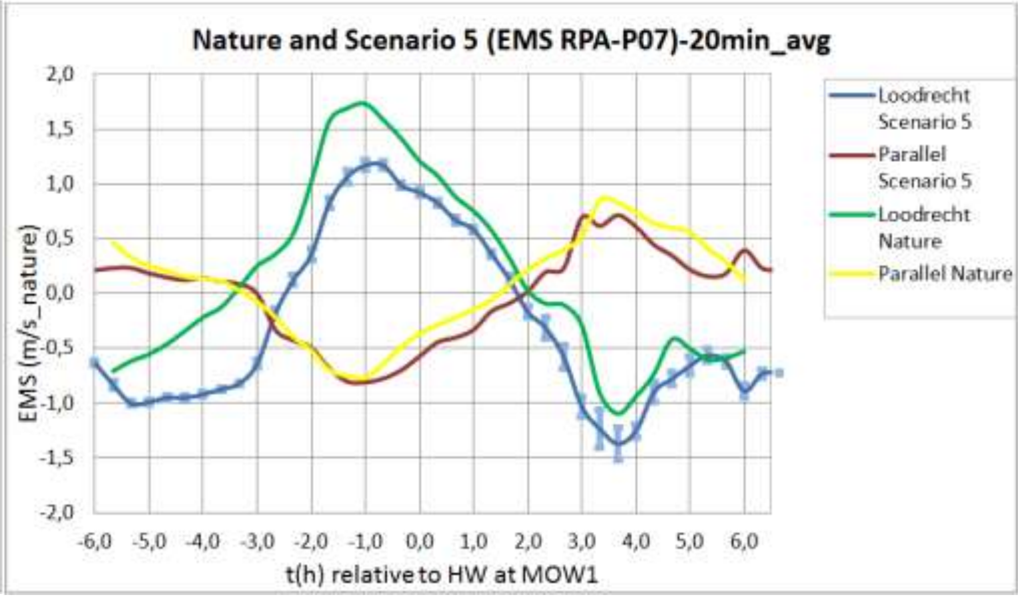
Nature and Scenario 5 (EMS RPA-P07)-20min_avg
Loodrecht Scenario 5
Parallel Scenario 5
Loodrecht Nature
Parallel Nature
EMS (m/s_nature)
t(h) relative to HW at MOW1

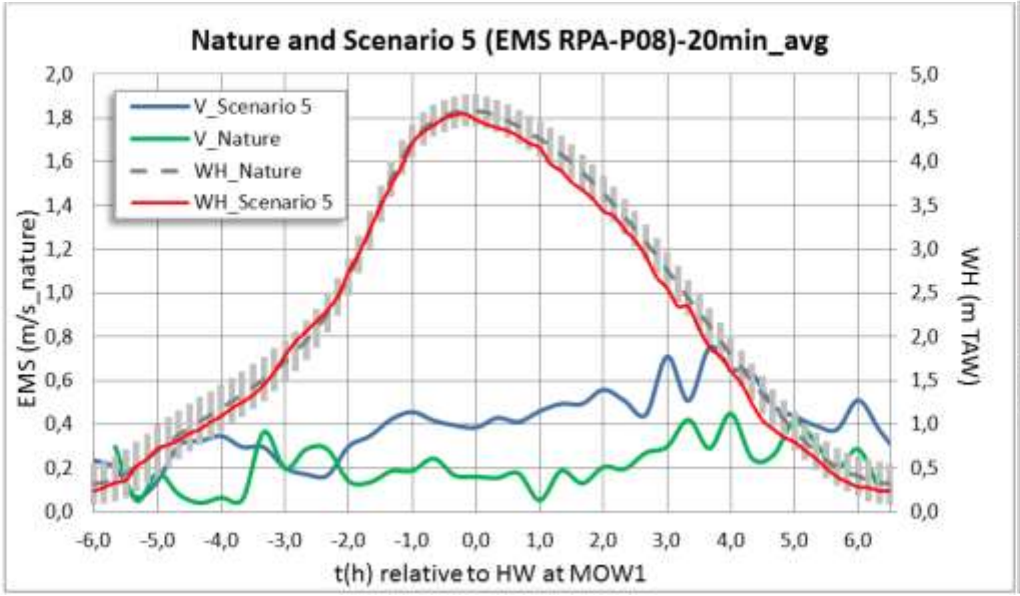
Nature and Scenario 5 (EMS RPA-P08)-20min_avg
V_Scenario 5
V_Nature
WH_Nature
WH_Scenario 5
EMS (m/s_nature)
WH (m TAW)
t(h) relative to HW at MOW1

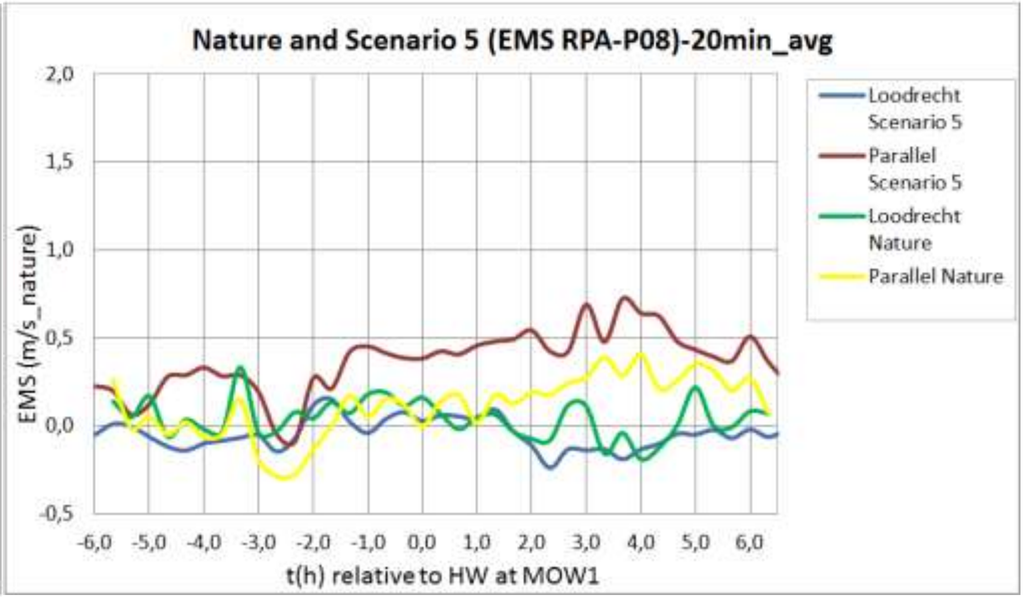
Nature and Scenario 5 (EMS RPA-P08)-20min_avg
Loodrecht Scenario 5
Parallel Scenario 5
Loodrecht Nature
Parallel Nature
EMS (m/s_nature)
t(h) relative to HW at MOW1

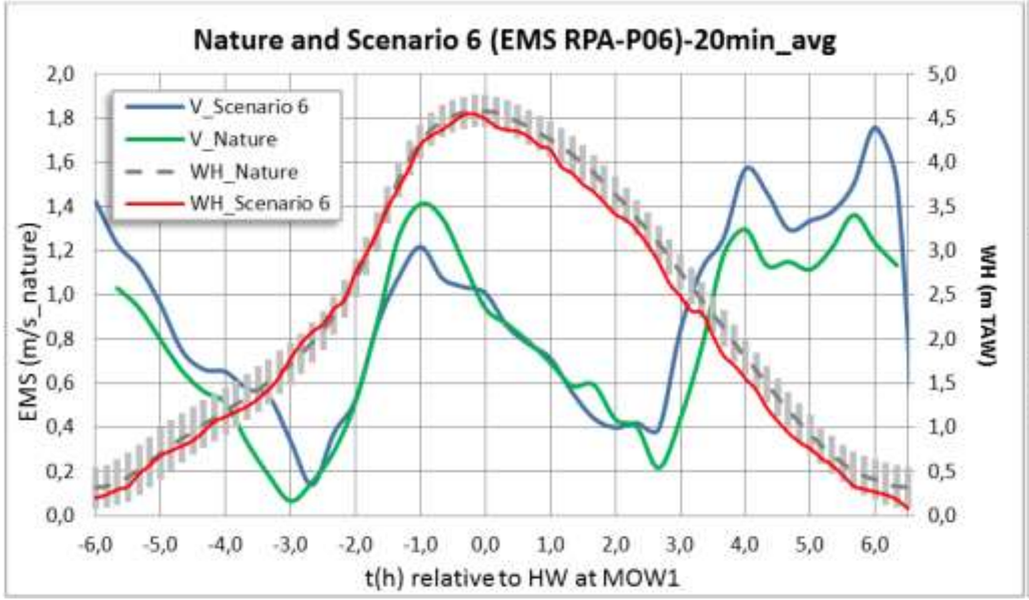
Nature and Scenario 6 (EMS RPA-P06)-20min_avg
V_Scenario 6
V_Nature
WH_Nature
WH_Scenario 6
EMS (m/s_nature)
WH (m TAW)
t(h) relative to HW at MOW1

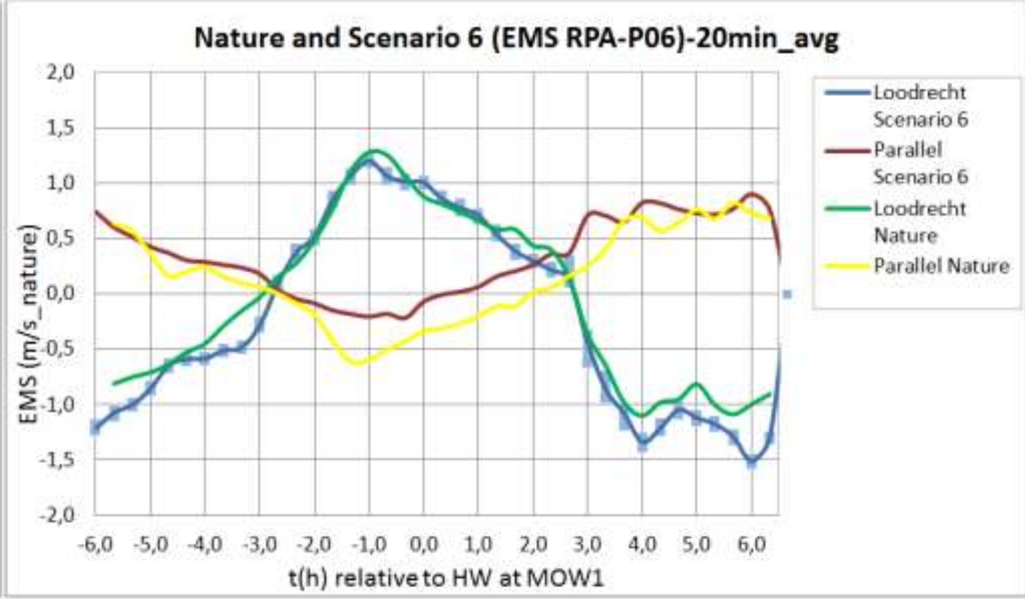
Nature and Scenario 6 (EMS RPA-P06)-20min_avg
Loodrecht Scenario 6
Parallel Scenario 6
Loodrecht Nature
Parallel Nature
EMS (m/s_nature)
t(h) relative to HW at MOW1

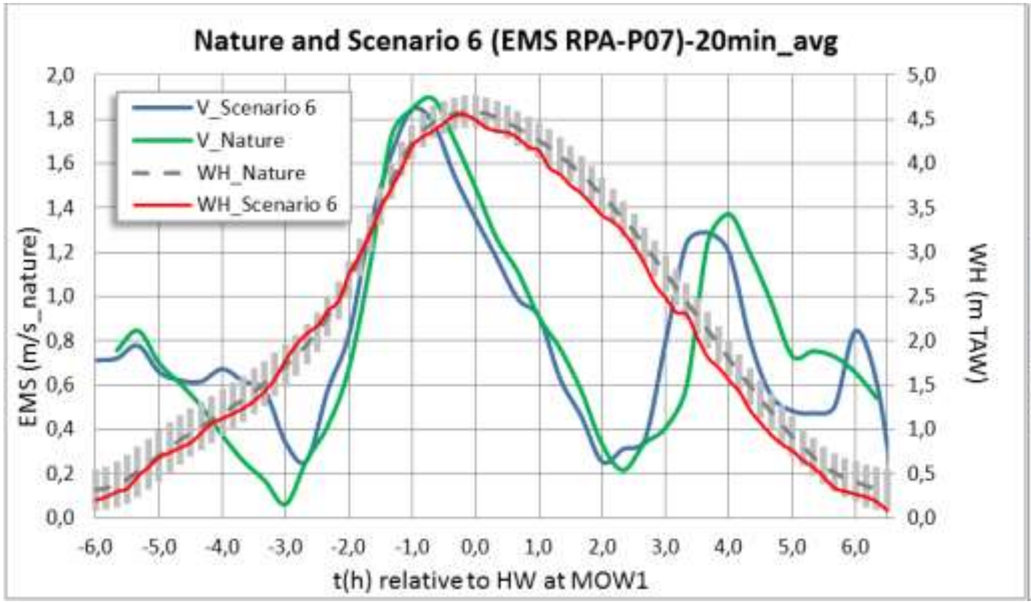
Nature and Scenario 6 (EMS RPA-P07)-20min_avg
V_Scenario 6
V_Nature
WH_Nature
WH_Scenario 6
EMS (m/s_nature)
WH (m TAW)
t(h) relative to HW at MOW1

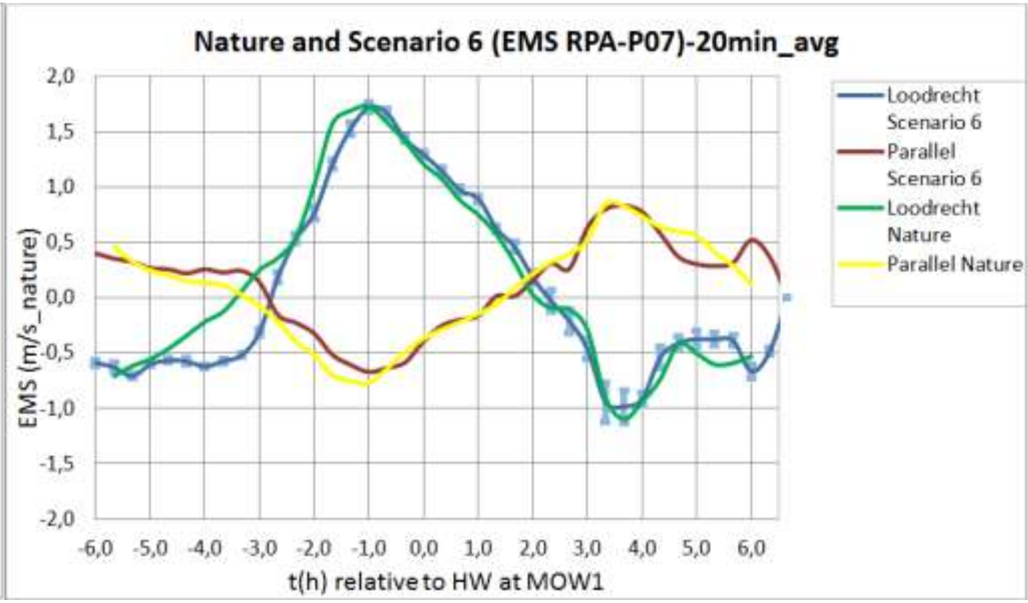
Nature and Scenario 6 (EMS RPA-P07)-20min_avg
Loodrecht Scenario 6
Parallel Scenario 6
Loodrecht Nature
Parallel Nature
EMS (m/s_nature)
t(h) relative to HW at MOW1

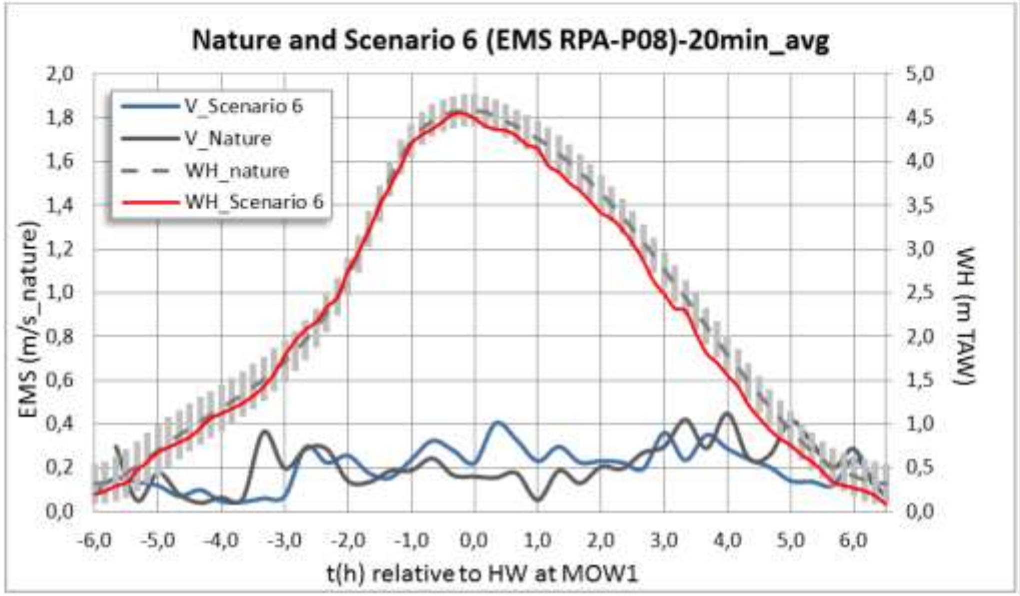
Nature and Scenario 6 (EMS RPA-P08)-20min_avg
V_Scenario 6
V_Nature
WH_nature
WH_Scenario 6
EMS (m/s_nature)
WH (m TAW)
t(h) relative to HW at MOW1

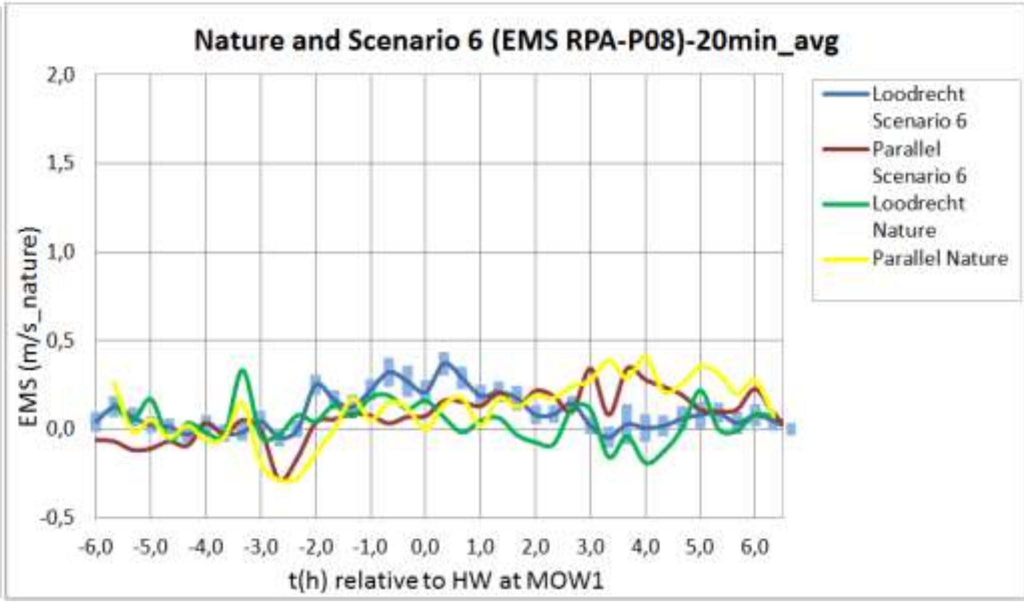
Nature and Scenario 6 (EMS RPA-P08)-20min_avg
Loodrecht Scenario 6
Parallel Scenario 6
Loodrecht Nature
Parallel Nature
EMS (m/s_nature)
t(h) relative to HW at MOW1